

NUCLEAR DATA AND MEASUREMENTS SERIES

ANL/NDM-32

Evaluated Fast Neutron Cross Sections of Uranium-238

by

W. Poenitz, E. Pennington, A.B. Smith, and R. Howerton

October 1977

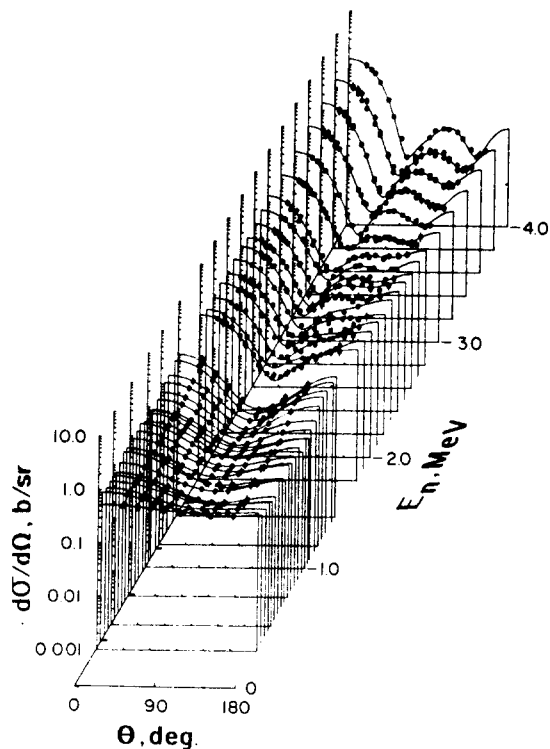
**ARGONNE NATIONAL LABORATORY,
ARGONNE, ILLINOIS 60439, U.S.A.**

NUCLEAR DATA AND MEASUREMENTS SERIES

ANL/NDM-32
EVALUATED FAST NEUTRON CROSS SECTIONS OF URANIUM-238

by
W. Poenitz, E. Pennington, and A. B. Smith
Argonne National Laboratory

and
R. Howerton
Lawrence Livermore Laboratory
October 1977



U of C AUA USERDA

ARGONNE NATIONAL LABORATORY,
ARGONNE, ILLINOIS 60439, U.S.A.

The facilities of Argonne National Laboratory are owned by the United States Government. Under the terms of a contract (W-31-109-Eng-38) between the U. S. Atomic Energy Commission, Argonne Universities Association and The University of Chicago, the University employs the staff and operates the Laboratory in accordance with policies and programs formulated, approved and reviewed by the Association.

MEMBERS OF ARGONNE UNIVERSITIES ASSOCIATION

The University of Arizona
Carnegie-Mellon University
Case Western Reserve University
The University of Chicago
University of Cincinnati
Illinois Institute of Technology
University of Illinois
Indiana University
Iowa State University
The University of Iowa

Kansas State University
The University of Kansas
Loyola University
Marquette University
Michigan State University
The University of Michigan
University of Minnesota
University of Missouri
Northwestern University
University of Notre Dame

The Ohio State University
Ohio University
The Pennsylvania State University
Purdue University
Saint Louis University
Southern Illinois University
The University of Texas at Austin
Washington University
Wayne State University
The University of Wisconsin

NOTICE

This report was prepared as an account of work sponsored by the United States Government. Neither the United States nor the United States Atomic Energy Commission, nor any of their employees, nor any of their contractors, subcontractors, or their employees, makes any warranty, express or implied, or assumes any legal liability or responsibility for the accuracy, completeness or usefulness of any information, apparatus, product or process disclosed, or represents that its use would not infringe privately-owned rights.

ANL/NDM-32
EVALUATED FAST NEUTRON CROSS SECTIONS OF URANIUM-238

by

W. Poenitz, E. Pennington, and A. B. Smith

Argonne National Laboratory

and

R. Howerton

Lawrence Livermore Laboratory

October 1977

In October 1977, the U.S. Energy Research and Development Agency (ERDA) was incorporated into the U.S. Department of Energy. The research and development functions of the former U.S. Atomic Energy Commission had previously been incorporated into ERDA in January 1975.

Applied Physics Division
Argonne National Laboratory
9700 South Cass Avenue
Argonne, Illinois 60439
USA

NUCLEAR DATA AND MEASUREMENTS SERIES

The Nuclear Data and Measurements Series presents results of studies in the field of microscopic nuclear data. The primary objective is the dissemination of information in the comprehensive form required for nuclear technology applications. This Series is devoted to: (a) measured microscopic nuclear parameters, (b) experimental techniques and facilities employed in measurements, (c) the analysis, correlation and interpretation of nuclear data, and (d) the evaluation of nuclear data. Contributions to this Series are reviewed to assure technical competence and, unless otherwise stated, the contents can be formally referenced. This Series does not supplant formal journal publication but it does provide the more extensive information required for technological applications (e.g., tabulated numerical data) in a timely manner.

TABLE OF CONTENTS

	<u>Page</u>
ABSTRACT	1
I. INTRODUCTION.	2
II. NEUTRON TOTAL CROSS SECTIONS.	4
III. NEUTRON ELASTIC SCATTERING.	8
IV. NEUTRON INELASTIC SCATTERING.	17
V. FISSION PROCESSES	39
VI. NEUTRON RADIATIVE CAPTURE	58
VII. (n;2n') and (n;3n') PROCESSES	78
VIII. PHOTON PRODUCTION PROCESSES	82
IX. SOME INTEGRAL TESTS	84
X. SUMMARY COMMENT	97

REFERENCES, TABLES, AND FIGURES FOLLOW RELEVANT SECTIONS

EVALUATED FAST NEUTRON CROSS SECTIONS
OF URANIUM-238*

by

W. Poenitz, E. Pennington and A. Smith
Argonne National Laboratory

and

R. Howerton
Lawrence Livermore Laboratory

ABSTRACT

An evaluated fast neutron data file of ^{238}U is presented in the ENDF/B format. The incident energy range extends from 0.045 to 20.0 MeV. The content consists of: (1) neutron total cross sections, (2) fission cross sections, neutron emission spectra and associated properties, (4) neutron radiative-capture cross sections, (5) (n;2n') and (n;3n') processes, and (6) photon-production cross sections and spectra. The methodology of the file derivation is outlined. File content is graphically illustrated and uncertainty estimates are given. Comparisons with comparable portions of ENDF/B-IV are made and some large differences are noted. Some results of integral "benchmark" tests using this file are outlined. Many of the components of this file are those explicitly submitted for ENDF/B, Version V.

**This work supported by the U.S. Department of Energy.*

I. INTRODUCTION

The explicit objective of this evaluation is the provision of fast neutron and photon-production components of the ENDF/B-V ^{238}U evaluated nuclear data file.[I-1] The scope is all significant neutron cross sections, reaction processes, and emission spectra throughout the incident energy range 0.045 to 20.0 MeV and all photon production processes. The content consists of the reaction types: (1) neutron total cross sections, (2) neutron elastic scattering cross sections and angular distributions, (3) neutron inelastic scattering cross sections, angular distributions and emission spectra, (4) fission cross sections, emission spectra, and fission properties (5) neutron radiative capture cross sections, (6) $(n;2n')$ and $(n;3n')$ cross sections and emission spectra, and (7) photon-production cross sections and associated spectra. The scope does not include the resolved and unresolved resonance region below 0.045 MeV. Some particle-emission processes are energetically possible but greatly inhibited by the coulomb barrier. Quantitative estimates indicated that these cross sections are very small and thus these processes were ignored. In the course of the evaluation, some integral "benchmark" tests were carried out for guidance. Where relevant to the evaluation, these integral results are outlined. Indications of the uncertainties associated with the various file components is given where meaningful estimates can be made. The results of the present evaluation are compared with those of ENDF/B-IV and regions of both agreement and discrepancy are noted.

This report generally constitutes the documentation for the ^{238}U evaluated nuclear data file submitted for ENDF/B-V. Exceptions are prompt and delayed fission neutron properties which, as provided here in, are not necessarily identical to those of ENDF/B-V. These fission-neutron properties were necessary for the testing of the file. Also, the file does not explicitly identify $(n;n',f)$, $(n;2n',f)$, etc., fission cross sections as these were felt to be largely speculative and not essential for most file applications. With these provisos, this evaluated file is a subset of the complete ENDF/B-V file, formulated under the auspices of E. Pennington et al.[I-2].

Subsequent portions of this report are devoted to: neutron total cross sections (II), neutron elastic scattering (III), neutron inelastic scattering (IV), fission processes (V), neutron radiative capture (VI), $(n;2n')$ and $(n;3n')$ processes (VII), photon-production processes (VIII), and the results of some of the integral testing (IX).

REFERENCES--SECTION I

- I-1. Brookhaven National Laboratory Report, ENDF-102, (1975), Editors D. Garber, C. Dunford and S. Pearlstein.
- I-2. E. Pennington, W. Poenitz, and A. Smith, Trans. Am. Nucl. Soc. 26, 591 (1977).

II. NEUTRON TOTAL CROSS SECTIONS

This portion of the file compliments the resolved and unresolved resonance values of Ref. II-1 at the lower energy extremity and extends upward to 20.0 MeV. All evaluated results are given as pointwise data. An experimental data base, consisting of the values given in Refs. II-2 to II-20, was assembled. From this large base, data sets were subjectively selected in various energy ranges as indicated by consistency between various measured sets to within several standard deviations. Some data sets were rejected in part or total as being inconsistent with the body of information. At lower energies, there was not a large multiplicity of experimental results. The selected data were combined to form a master set extending over the full energy range of interest. Weighted averages of experimental values were then constructed from the master set using energy-averaging increments varying from 20 keV at the lower extreme to 400 keV at the maximum energy of 20.0 MeV. The resulting energy-averaged cross sections were then plotted on a large scale and slightly adjusted (e.g., by $\sim 1\%$) in order to give a smooth energy dependence. This smoothing procedure removed the small fluctuations observed in some of the higher resolution experiments (e.g., those of Ref. II-2). Such fluctuations are not generally observed and were judged of insufficient importance in most applications to warrant the additional complexity requisite to their inclusion in the file. The final evaluated result is compared with the corresponding evaluated total neutron cross sections of ^{238}U as given in ENDF/B-IV in Fig. II-1. The two evaluations are very similar. The major area of difference is in the region 400-800 keV where the present evaluation is several percent lower than that of

ENDF/B-IV. This difference is probably real as it is well supported by a number of very consistent measurements. The uncertainty in the present evaluated cross sections from 300 keV to 10 MeV is estimated to be less than 3%. This uncertainty estimate may increase by up to a factor of two going to 20 MeV and below 300 keV where the data base is not as well defined. Despite these uncertainties, it appears that the total neutron cross sections of ^{238}U from ~ 300 keV to 20 MeV are among the best known of such cross sections. This is fortunate as the precise total cross section makes possible reasonable determinations of partial cross sections (e.g., total-inelastic-scattering cross sections) by means of differences and provide a good basis for quantitatively verifying models essential to the evaluation of some of the partial cross sections.

This evaluation was completed in mid-1976. In early 1977 it was suggested that there might be large uncertainties in the total cross sections at the lower-energy extreme. Therefore, the NNCSC data base was independently reviewed in May 1977. This review did not indicate any substantive modifications to the evaluation. Further measurements were made explicitly to test the file over the range ~ 0.1 to 4.0 MeV. None of these newer results differed from the present evaluation by more than the uncertainty estimates and generally by a great deal less. They did indicate 1.5 to 3% lower cross sections in the region 0.1 to 0.3 MeV. This is a small difference and the inclusion of the new results in a re-evaluation would lead to even smaller changes in the evaluation and thus a re-evaluation was not carried out.

REFERENCES -- SECTION II

- II-1. E. Pennington, W. Poenitz and A. Smith, Trans. Am. Nucl. Soc. 16, 591 (1977).
- II-2. D. Kopsch et al., Karlsruhe Laboratory Report, KFK-1199 (1973).
- II-3. J. Whalen, private communication (1973).
- II-4. C. Uttley, Paris Conference on Nuclear Data (1972), data values obtained from the NNDC.
- II-5. R. Schwartz et al., National Bureau of Standards Report, NBS-138 (1974).
- II-6. J. Hayes et al., Nucl. Sci. Eng. 50, 543 (1973).
- II-7. C. Hibdon and A. Langsdorf, data obtained from NNDC.
- II-8. R. Tabony (1974), data obtained from NNDC.
- II-9. D. Foster and D. Glasgow, Phys. Rev. C3, 576 (1971).
- II-10. A. Smith, private communication (1973).
- II-11. N. Nereson and S. Darden, Phys. Rev. 89, 775 (1953).
- II-12. J. Leroy et al., J. Phys. et Rad. 24, 826 (1963).
- II-13. J. Coon et al., Phys. Rev. 98, 1369 (1955).
- II-14. P. Bowen et al., Nucl. Phys. 22, 640 (1961).
- II-15. R. Day and R. Henkel, Phys. Rev. 92, 358 (1953).
- II-16. J. Vervier and A. Martegani, Nucl. Phys. 6, 260 (1958).
- II-17. J. Cabe et al., CEA Report, CEA-5-4524 (1973).
- II-18. R. Batchelor and J. Towle, Nucl. Phys. 65, 236 (1965).
- II-19. Mubarandaniand et al., Nucl. Instr. & Methods 115, 35 (1974).
- II-20. Konov et al., Proc. of the 1973 Kiev Conf.

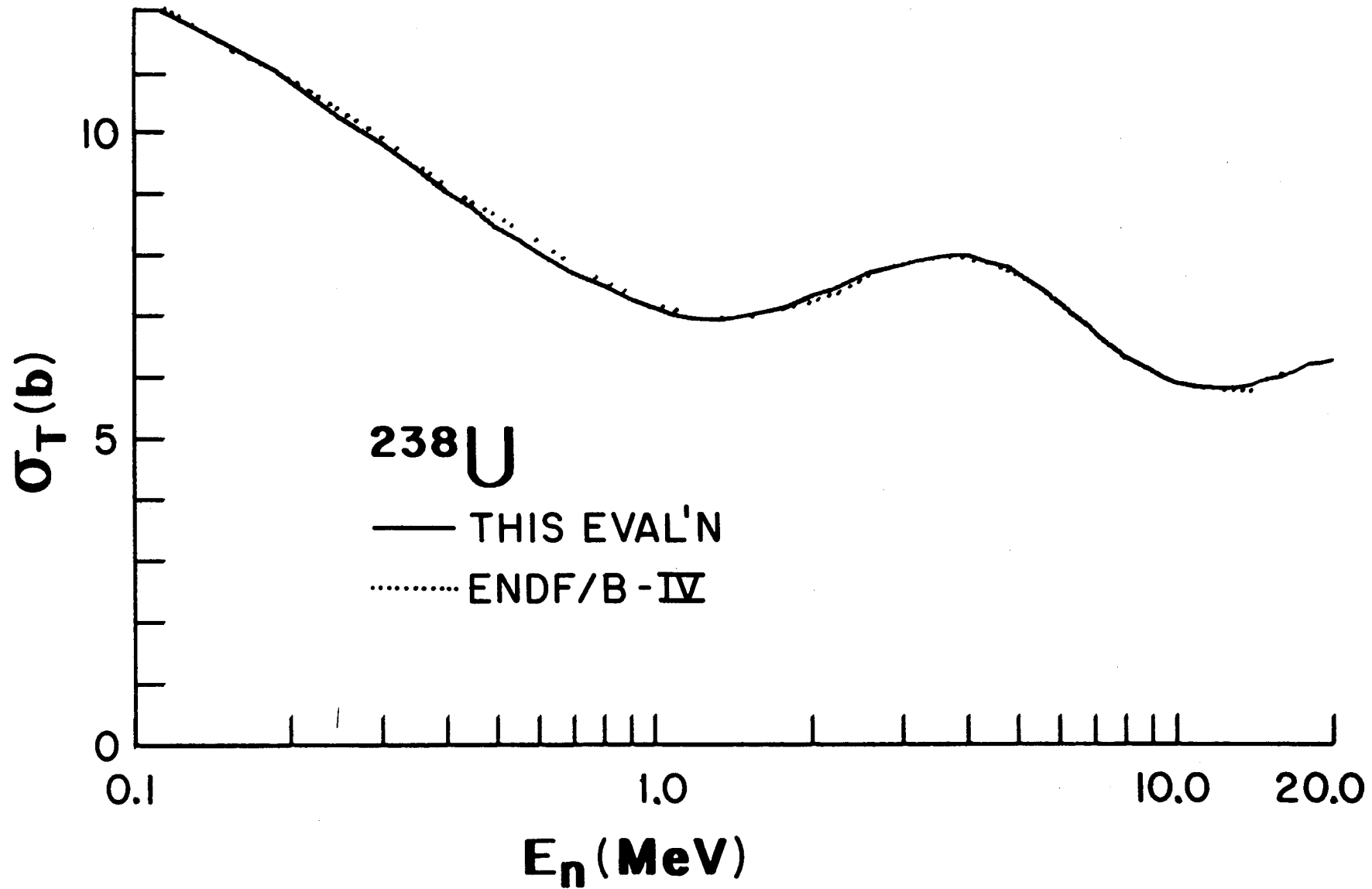


Fig. II-1. Comparison of the Present Evaluated Neutron Total Cross Sections of ^{238}U (—) with those Given in ENDF/B-IV (.....).

III. NEUTRON ELASTIC SCATTERING

The elastic scattering evaluation is based upon experimental information from the inelastic threshold at ~ 45 keV to 1.8 MeV. The evaluation uses the experimental results of Langsdorf et al. [III-1] at the inelastic threshold. This total-scattering result should be equivalent to elastic scattering at this energy. The remainder of the experimental data, given in Refs. III-2 to III-13, were least-square fitted with Legendre polynomial series. The results from the fitting procedures were corrected for inelastic-neutron scattering contributions, where present, and the corrected Legendre-expansion coefficients expressed as a function of energy. The results of Refs. III-2, III-4, III-6, III-9 and III-11 were given preference as they were generally the more cases there were no inelastic perturbations). A smooth energy dependence of the Legendre coefficients was determined by fitting procedures and values at selected energies used to construct the evaluated elastic scattering cross sections. The latter were verified by comparisons with measured distributions judged to be the most reliable. In these test cases the evaluated distributions generally agreed with the measured values to within experimental uncertainties.

The model of Ref. III-13 was used to calculate elastic neutron scattering distributions from 1.8-20.0 MeV. This model is discussed in detail in Ref. III-13 and was shown therein to be very descriptive of both neutron-total cross sections and differential elastic neutron distributions. In many ways, the model is similar to that of LaGrange [III-14]. In this high-energy region it was assumed that the compound-elastic scattering was negligible. This assumption was verified by comparing calculated distributions with the

measured 2.5-MeV elastic scattering cross sections recently reported by Haouat et al. [III-11] and by Marcella et al. [III-12]. Furthermore, the model is very descriptive of the lower energy results of Smith [III-4], Barnard et al. [III-2], and Guenther et al. [III-13] as further discussed in Ref. III-13. Some of these comparisons of measured and calculated values are shown in Fig. III-1. Additional comparisons between model-calculated values and the measured results of Refs. III-6, III-7, III-9, III-10 and III-15, III-21 are shown in Figs. III-2 and III-3. In all of these latter comparisons the measured values contained some contributions due to inelastic-neutron-scattering processes. These were estimated from the reported experimental resolutions and appropriate corrections were made to the model-calculated results before comparing with the experiments. Generally, the experimental evidence supports the model-calculated values up to energies of more than 14-MeV. This model provides a quantitative mechanism for interpolating between measured values and extrapolating in angle to obtain the angle-integrated cross sections. Below energies of approximately 1.0 MeV the various partial non-elastic cross sections are reasonably well known. Therefore, the evaluation treats the elastic-scattering magnitude in this low-energy region as a free parameter, adjusted later to assure the internal consistency of the file. At energies above ~ 1.0 MeV the elastic scattering cross section sets the value of the non-elastic cross section.

The relative evaluated angular distributions are expressed as f_{ℓ} coefficients. This format has a shortcoming at energies above 15-MeV since ℓ is limited to a maximum of 20. This limit is only marginally sufficient for high-fidelity representations but a slight truncation of the parameters will have little effect for most applications. Final tests assured that the

evaluated file was consistent with Wick's Limit [III-22]. The uncertainty in the evaluated elastic scattering cross section was estimated to be less than $\lesssim 7\%$ from ~ 0.3 to 15.0 MeV somewhat larger at higher energies. Any subsequent adjustments of file content either to assure internal consistency or to modify partial cross sections were kept well within this uncertainty.

The above elastic scattering cross sections and the better-known total cross sections place stringent limitations on the non-elastic cross sections (i.e., other portions of the file). The implication is an uncertainty of $\lesssim 200$ mb associated with the non-elastic cross section over the large majority of the energy range. Since fission is known to relatively good precision and is not large, and radiative capture is small, the sum of the total inelastic scattering and $(n;2n')$ and $(n;3n')$ cross sections is relatively well defined. In particular, large changes in the total inelastic scattering cross section in the MeV region cannot be accepted. This is discussed further in Ref. III-13.

The present evaluated elastic scattering cross sections are compared with those of ENDF/B-IV in Fig. III-4. The same figure compares non-elastic cross sections implied by the respective total and elastic scattering cross sections. The present evaluation is very much different from ENDF/B-IV; in some areas by amounts that are well beyond acceptable uncertainties in microscopic cross section values. These differences imply large changes in the inelastic-scattering cross sections from those given in ENDF/B-IV. This conclusion cannot be avoided with any reasonable interpretation of the uncertainties in the microscopic total and elastic-scattering cross sections.

REFERENCES -- SECTION III

- III-1. A. Langsdorf et al., Argonne National Laboratory Report, ANL-5567 (rev.) (1961).
- III-2. E. Barnard et al., Nucl. Phys. 80, 46 (1966).
- III-3. I. Korzh et al., Ukain. Fiz. Zhurn, 6, 626 (1974).
- III-4. A. Smith, Nucl. Phys. 47, 633 (1963).
- III-5. R. Allen et al., Phys. Rev. 104, 731 (1956).
- III-6. P. Guenther et al., Argonne National Laboratory Report, ANL/NDM-16 (1975).
- III-7. L. Cranberg and J. Levin, Phys. Rev. 109, 2063 (1958).
- III-8. W. Gilboy and J. Towle, Nucl. Phys. 42, 86 (1963).
- III-9. H. Knitter et al., Zeits. Phys. 224, 358 (1971)
- III-10. R. Batchelor and J. Towle, Nucl. Phys. 65, 236 (1965).
- III-11. G. Haouat et al., NEANDC Report, NEANDC(E) 180L (1977); see also Proc. Inter. Conf. on Interaction of Neutrons with Nuclei, CONF-769715 (1976).
- III-12. T. Marcella et al., Proc. Inter. Conf. on Interactions of Neutrons with Nuclei, CONF-760715 (1976).
- III-13. A. Smith et al., Argonne National Laboratory Report, ANL/NDM-22 (1976); also to be published in Nucl. Sci. Eng.
- III-14. Ch. LaGrange, Proc. of EANDC Topical Discussion on "Critique of Nuclear Models and their Validity in the Evaluation of Nuclear Data," NEANDC Report, NEANDC(J) 38L (1975).
- III-15. M. Walt and J. Beyster, Los Alamos Scientific Laboratory Report, LA-2061 (1956).
- III-16. S. Buccino et al., Zeits. Phys. 196, 103 (1966).
- III-17. W. Kinney and F. Perey, Oak Ridge National Laboratory Report, ORNL-4804 (1973).
- III-18. B. Ya Guzhovskii, Atom. Energy 11, 395 (1961).

- III-19. J. Coon et al., Phys. Rev. 111, 250 (1958).
- III-20. L. Rosen and L. Stewart, Los Alamos Scientific Laboratory Report, LA-2111 (1957).
- III-21. J. Kammerdiener, Lawrence Livermore Laboratory Report, UCRL-51232 (1972).
- III-22. See A. Lane and R. Thomas, Rev. Mod. Phys. 30, 257, p. 293 (1958).

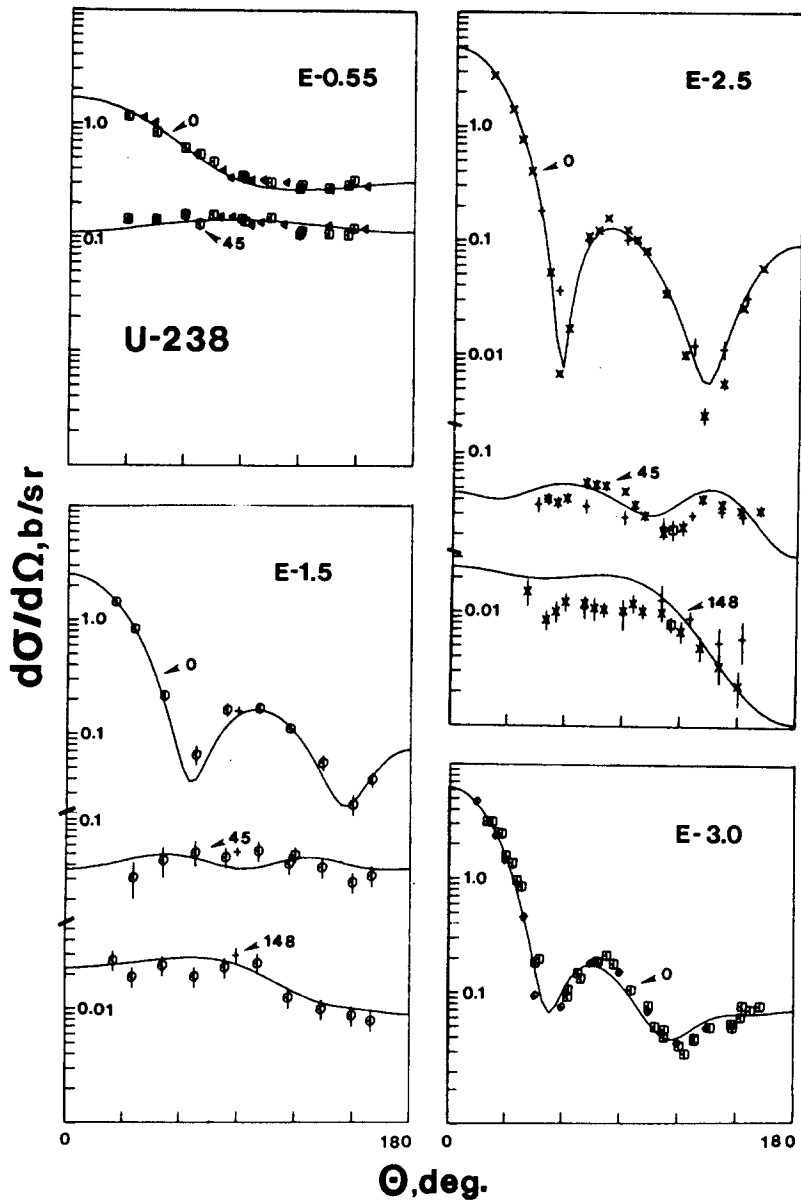


Fig. III-1. Measured and Evaluated Elastic and Inelastic Neutron Scattering Cross Sections of ^{238}U . The curves represent the present evaluation and data points the results of measurements as cited in the text. The 0.55, 1.5 and 2.5 MeV measurements fully resolve the elastic and inelastic components. The 3.0 MeV distribution includes the first inelastic component ($E_x = 45$ keV).

Fig. III-2. Illustrative Comparisons of Evaluated and Measured Elastic Scattering Cross Sections as Described in the Text. The measured values are noted by data points, the evaluation by curves. Again, corrections have been made for the inelastic content of the measured values.

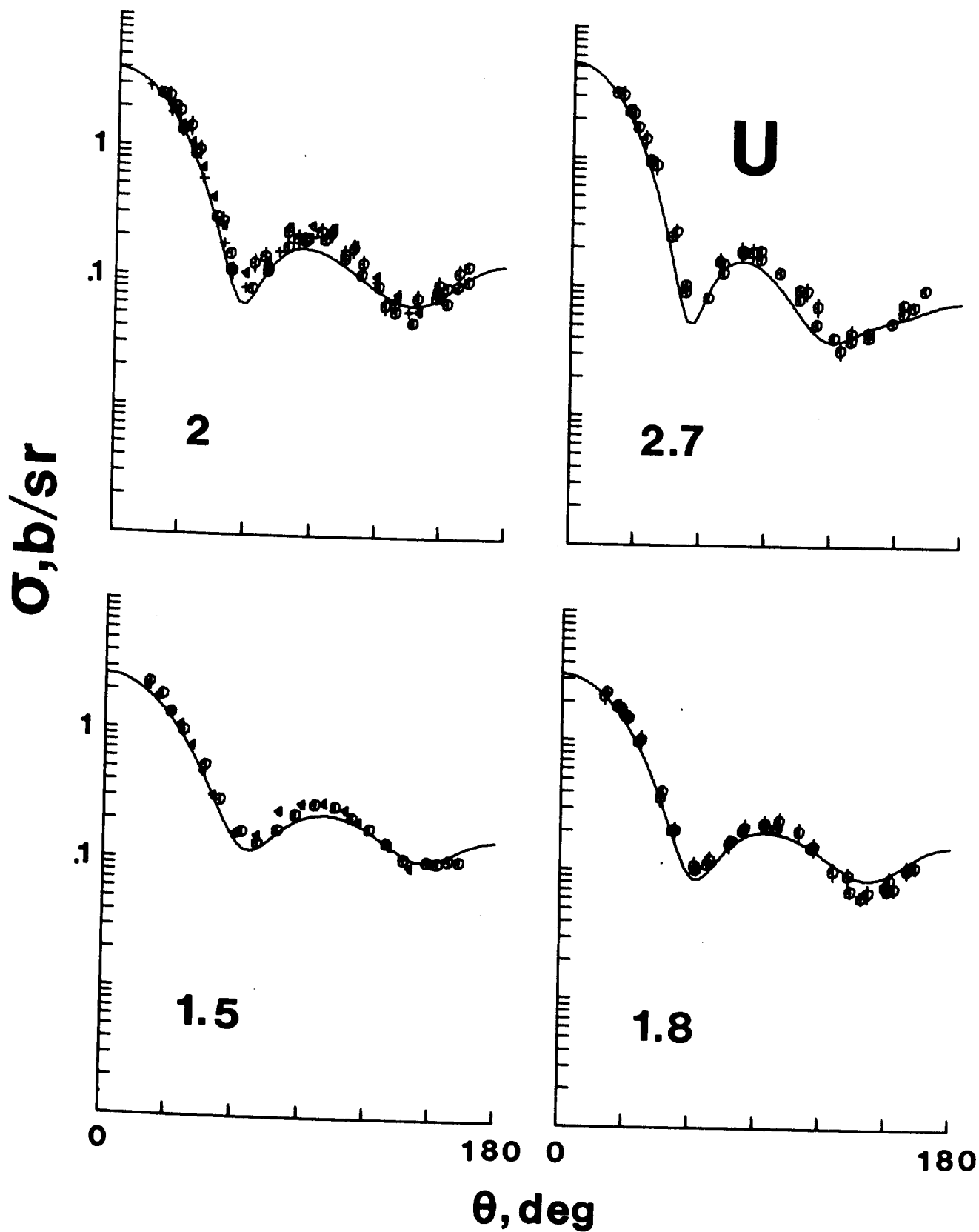
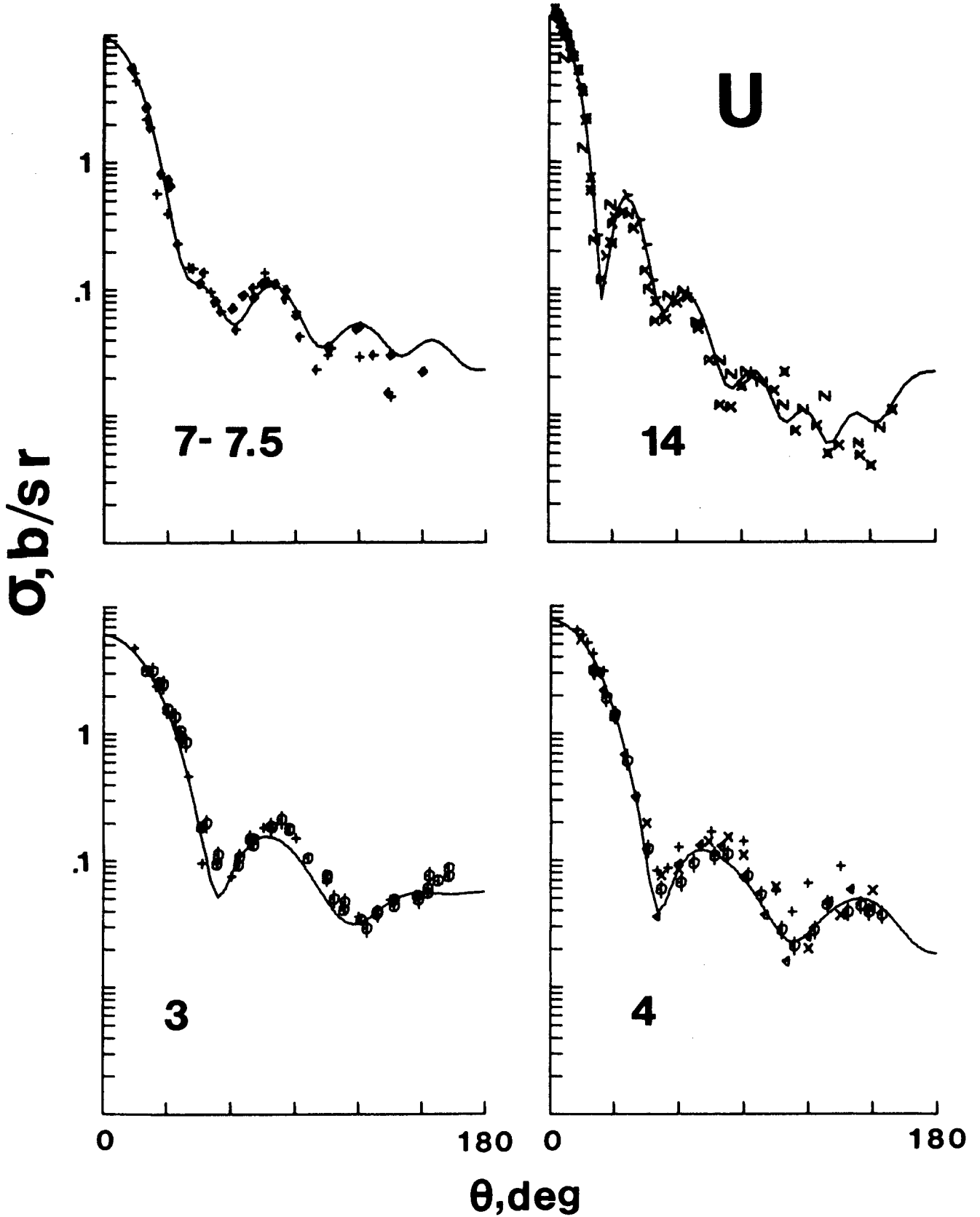


Fig. III-3. Comparisons of Measured and Evaluated Neutron Elastic Scattering Cross Sections at Higher Energies. Notation is as in Fig. III-2.



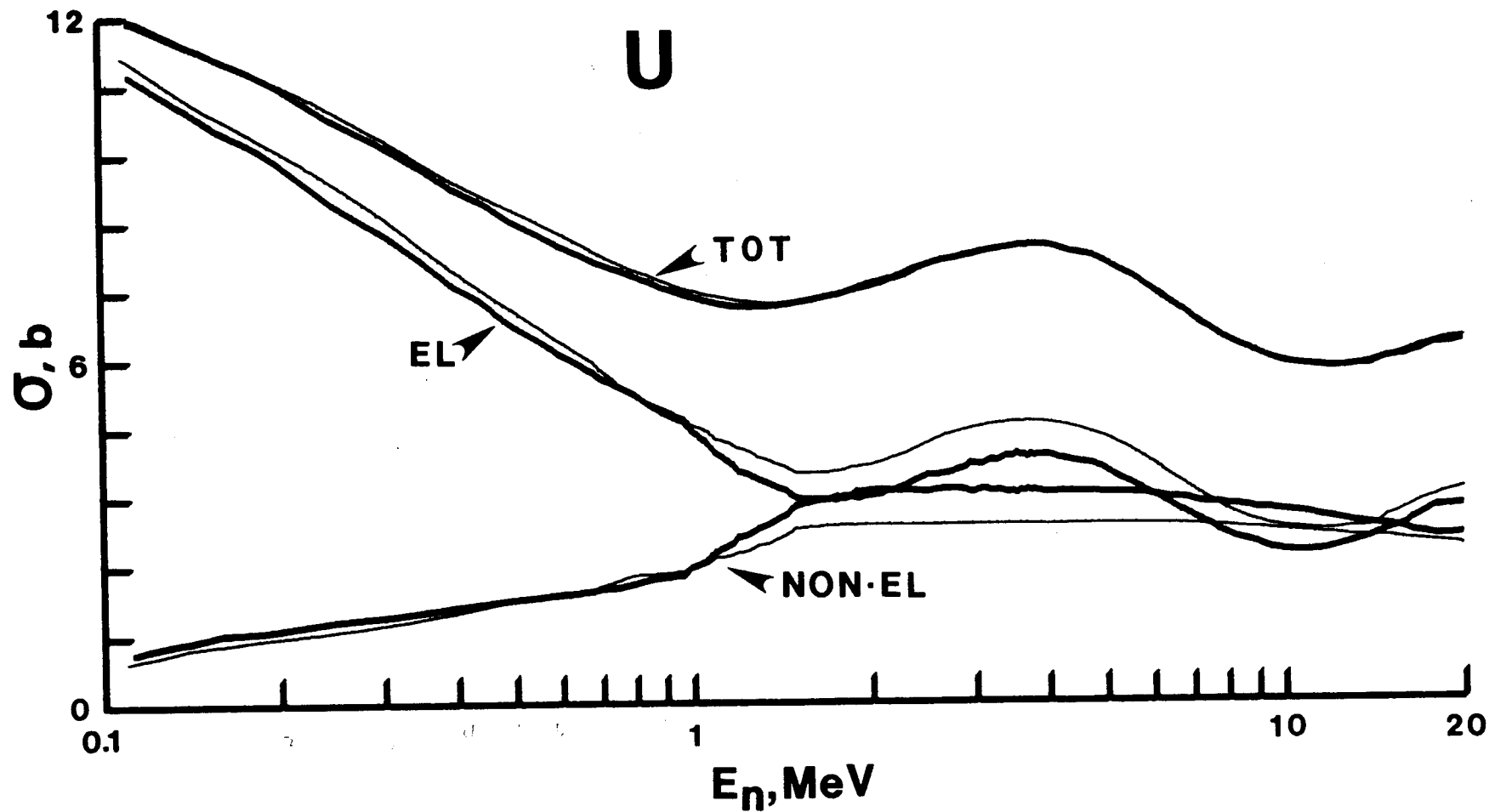


Fig. III-4. Comparison of Evaluated Neutron Total, Elastic-Scattering and Non-Elastic Cross Sections as Given in the Present Evaluation (heavy curves) and in ENDF/B-IV (lighter curves).

IV. NEUTRON INELASTIC SCATTERING PROCESSES

Neutron inelastic scattering processes are treated as: the excitation of discrete and explicitly identified states, the excitation of a composite of contributions from a number of discrete states (not always clearly and explicitly identified), and as the excitation of a continuum of unresolved states. The respective reaction Q-values are given in Table IV-1. The cross sections for the excitation of states at energies of $\lesssim 1.0$ MeV are reasonably known and are individually represented in the evaluation. Excited structure above ≈ 1.0 -MeV becomes more complex and uncertain and the corresponding cross sections are generally observed as collective contributions from several states which were not well resolved in neutron-cross-section measurements [IV-1, IV-2]. This evaluation represents the cross sections for the excitation of states at energies of ~ 1.0 -2.5-MeV with 10 discrete cross sections selected to be as representative of the measured cross sections as possible. This approximation is sufficient for most applications, avoids an undue proliferation of excitation functions (which could well overflow the prescribed format) and is representative of the available experimental information. States with excitations in the range 2.5-4.0 MeV are represented by a simple ladder model with the level density increasing with energy. This approximation is physically reasonable but not explicitly verified by experiment. It has the practical advantage of blending the discrete excitation functions into the continuum without a discontinuity that can have an adverse effect in some applications. The continuum representation extends upward from 2.5 MeV and thus overlaps and blends with the discrete excitation functions. Throughout, the non-elastic cross section (defined above) is a constraint. The inelastic

evaluation was a two-pass procedure. The first draft was derived from microscopic measured and calculated values and combined with the other components to form a complete draft file. This draft was then tested using ENDF critical benchmarks and other ENDF-IV files where necessary. The inelastic cross sections were then slightly adjusted to obtain an improved agreement between calculated and measured benchmark results. These adjustments were rigidly confined to the previously estimated uncertainties in the inelastic components and to those of the above non-elastic cross sections. This file was not allowed to deviate from a consistency with the microscopic data base.

A. Inelastic Neutron-Excitation of the Ground-state Rotational Band

This portion of the evaluation deals with the excitation of the 2+ (45 keV) 4+ (148 keV) and 6+ (308 keV) states. The latter contribution is very small thus the 8+ and higher-order states of this band are explicitly excluded though they may make very small contributions to some of the other measured discrete excitation cross sections. The evaluation is based on a correlated application of theory and experiment as defined in Ref. IV-3. The experimental data base was constructed from Refs. IV-3 through IV-14.

The prominent inelastic component of this band is due to the excitation of the 2+ (45-keV) state. The evaluation for this group is compared with the data base and the evaluation of ENDF/B-IV in Figs. IV-1 and IV-2. With a few exceptions, as discussed in Refs. IV-3 and IV-6, the evaluation is consistent with the data base to the maximum measured energy of 3.0-MeV. This consistency is reasonably quantified by an uncertainty band of +7.5 and -5.0% relative to the evaluation. In the important lower energy region the evaluation trends towards the lower "acceptable" experimental limit. There is no experimental

information above ~ 3.0 -MeV, thus the evaluation relies entirely on the model of Ref. IV-3 in this region. This results in larger uncertainties but probably not more than $\pm 20\%$ from ~ 2.5 to 5.0 MeV and above. The present evaluation is considerably different from that of ENDF/B-IV at both low and high energies as illustrated in Figs. IV-1 and IV-2.

The evaluated cross sections for the excitation of the 4+ (148 keV) are compared with that of ENDF/B-IV and the experimental results in Figs. IV-3 and IV-4. The evaluation is consistent within $\sim \pm 7\%$ with the majority of the experimental information and again there is a large difference between the present evaluation and that of ENDF/B-IV at higher energies. The difference in this area (and for the 45 keV state, above) is largely due to the inclusion of direct-reaction cross sections in the present evaluation as supported by a number of newer measurements of Refs. IV-3, IV-6, IV-8 and IV-9 and calculation.

The calculated and measured excitations of the 6+ (308 keV) state are very small. The contributions of this state are included in the evaluation but will have little effect upon most applications. The present evaluation is somewhat different from that of ENDF/B-IV, as indicated by recent measurements [IV-10], but the uncertainties are large ($\sim \pm 20\%$) and thus the differences may not be significant.

In the derivation of the above evaluated cross sections, theoretical extrapolation and interpolation was carried out as described in Refs. IV-3 and IV-6. This was particularly necessary in the interpretation of measured differential scattering cross sections at few-MeV energies. At these energies the measured values can be very discrepant with one another and/or with theory at angles of less than approximately 50° . Such measurements are very difficult

and the results uncertain. Therefore, differential values measured at energies above approximately 1.0 MeV and scattering angles of less than approximately 45° were not generally accepted. Theory was used to derive the angle-integrated cross section values from measurements as necessary. Generally, the theoretically calculated results were nearly as consistent with the measured values as the latter were among themselves as illustrated in Fig. III-1.

The emitted-neutron angular distributions resulting from the excitation of the 45 keV state were deduced from measured values extrapolated theoretically to energies of approximately 2.5 MeV. At higher energies they were taken from theory. The same general procedure was used for obtaining the angular distributions of neutrons resulting from the excitation of the 148-keV state. For both of these states the theory indicates large anisotropies at high energies. Neutrons emitted as a result of the excitation of the 308-keV state were assumed to be isotropic. This is a very crude assumption, but it is probably satisfactory in view of the small magnitude of the corresponding cross sections.

B. K = 0 Octupole Band

The significant components of this band consist of contributions from 1- (680 keV), 3- (732 keV) and 5- (827 keV) states. The excitations of these states have been observed in direct neutron measurements [IV-4, IV-5, IV-7, IV-10, and IV-11] and studies of the $(n;n'\gamma)$ process [IV-2, IV-15]. At lower energies the neutron results for the 1- and 3- states are reasonably consistent, with deviations between experimental results of 10-20%. Above ~ 1.5 MeV the measured values are more uncertain, but still the cross sections are reasonably defined to ~ 2.5 MeV. The most detailed $(n;n'\gamma)$ results are from Ref. IV-2 and give a very good definition near threshold. However, they

become less reliable at higher energies as complex branching ratios are not well known, low energy transitions are unobserved and transitions mix contributions from several bands. Experimental knowledge of the 5- state is far less certain, but the excitation is clearly much less than for either the 1- to 3- states. This data base is outlined in Fig. IV-5.

The evaluations for the 1- and 3- states is based primarily upon neutron measurements from threshold to threshold plus ~ 2 MeV. Near threshold, additional guidance is obtained from the $(n;n',\gamma)$ results. Above ~ 2.5 MeV, the evaluations for these two states follow a theoretical estimate adjusted to agree with the measured emission spectra at 14 MeV [IV-16]. A similar approach was followed for the 5- state except that theory suggests a somewhat different behavior near threshold than the experimental data do and the former was taken for the evaluation as the cross sections are small and measured values relatively uncertain. The evaluated results are compared with the data base and the ENDF/B-IV evaluation in Fig. IV-5. The measured data for the 1- and 3- states is consistent with the evaluation to within $\pm \sim 10\%$ and to within $\pm \sim 25\%$ for the 5- state to several MeV above threshold. Above 2-3 MeV the uncertainty of the evaluation is larger, but the cross sections are small and their magnitudes are at least qualitatively indicated by the 14 MeV measurements of Ref. IV-16. For the two prominent cross sections (1- and 3-) the present evaluation is similar to ENDF/B-IV below ~ 2.5 MeV with larger contributions at higher energies. The present evaluation for the 5- state is somewhat larger than that given in ENDF/B-IV but the difference is probably not significant in most applications.

Near thresholds the above processes were assumed to be due to compound-nucleus reactions with isotropic neutron emission. The results of Kammerdiener [IV-16] suggest large anisotropies at an incident energy of 14 MeV. The evaluation constructs the angular distributions of neutrons emitted via excitation of the 1- and 3- states by smoothly interpolating between these two reference energies. The cross sections for the excitation of the 5- state are relatively small so, for simplicity, the neutron emission was assumed to be isotropic for this state.

C. Excitation of States at $E_x \gtrsim 1.0$ MeV

At these excitation energies the evaluation combines discrete excitation cross sections into composite groups made up of contributions from a number of states. The group structure is selected as a compromise between the resolutions of the various experimental measurements, the definition needed for applications and the finite limitation of the format structure.

The first level of this sequence corresponds to an average excitation of 965 keV. Structure studies [IV-1, IV-2] indicate that this group is a composite of contributions from: β -band (0+ , 927; 2+, 966 keV), γ -band (0+, 997 keV), and Octupole-band (1-, 931; 2-, 950; 3-, 997 keV) states, at least. ($n;n',\gamma$) measurements are troubled with uncertain branching ratios, particularly those involving low-energy transitions between bands. Thus, they were used only for qualitative guidance. Cross sections obtained from neutron measurements are confined to Refs. IV-4, IV-5 and IV-10. The results of Ref. IV-5 probably did not include all components and thus, may be too small. The evaluation compromises between the results of Refs. IV-4 and IV-10 as shown in Fig. IV-6. The uncertainties are large but restricted by the overall

non-elastic cross section to 10-15% at energies of $\lesssim 2.0$ MeV. Here, and throughout this sequence, the excitation functions are given a long high-energy tail. The magnitudes of these tails are adjusted to give agreement with the broader-resolution measurements of Kammerdienerer at 14 MeV [IV-16]. Throughout the sequence, the angular distribution of emitted neutrons is assumed isotropic near threshold and forward-peaked at higher energies. The angular distributions are adjusted so as to extrapolate smoothly to the measured 14 MeV distributions of Ref. IV-16.

The next four groups correspond to excitations of 1048, 1170, 1250 and 1440 keV. These energies are taken from the observed results of Ref. IV-10. The $(n;n',\gamma)$ studies of Ref. IV-2 indicate that these groups consist of 3, 4, 7 and 8 components, respectively, and this may be an underestimate. Again, the cross sections derived from $(n;n',\gamma)$ measurements tend to be systematically lower than the results of the neutron measurements of Refs. IV-4 and IV-10. The latter are preferred due to ambiguities in the interpretation of the $(n;n',\gamma)$ results. The data base and the corresponding evaluations are shown in Fig. IV-7. The uncertainties in any one excitation function can be large but, again, the non-elastic cross section limit cumulative uncertainties from these four states to 5 to 15% at energies of a few MeV and below. The angular distributions and the high energy "tails" are defined as outlined above. At excitations of 1440 keV and above the primary data source is Ref. IV-10. These values for the higher energy excitations are the result of neutron emission measurements including a small contribution due to fission neutrons. The evaluation in this region is thus accordingly adjusted toward lower values. In addition, as noted below, the evaluation extends the

continuum component down to 2.5 MeV and this will compete with excitation cross sections having thresholds above this energy. The discrete evaluations are adjusted correspondingly.

The experimental evidence becomes fragmentary above 1440 keV and is based upon the emission measurements of Ref. IV-10. Groups are constructed from the measured values at E_x intervals of ~ 100 keV as illustrated in Fig. IV-8. Each of these groups certainly consists of many components. The experimental values are not very accurate but, using the reasonably known non-elastic cross section, an evaluation of group excitation functions is obtained. The uncertainty in any one of these groups may be large but, again, the cumulative uncertainty is estimated to be in the range 515%.

The remaining discrete inelastic scattering cross sections ($E_x \gtrsim 2.3$ MeV) have no direct basis in experiment. They are constructed from a simple ladder model with a qualitatively increasing level density with energy. The average level density of the ladder was selected as a compromise between the very high density of the physical reality and a reasonable working file limited to a finite number of levels. The relative shapes of these excitation functions are very similar and the magnitudes are selected to smoothly blend the discrete inelastic cross sections into the continuum while maintaining a consistency with the non-elastic cross sections. This avoids an abrupt change between the two representations that can have an adverse effect on many applications.

D. Excitation of the Continuum

The magnitude of the continuum inelastic cross section is defined by the non-elastic cross section and the remaining and independently-defined partial cross sections (e.g., fission, $(n;2n)$, etc.). The high-energy

(e.g., $\gtrsim 10$ MeV) behavior of the continuum cross sections and emission spectra is not well defined therefore the evaluation is guided by macroscopic "benchmark" trials as discussed in Section IX, below. The continuum inelastic scattering cross sections of the present evaluation are considerably smaller than those of ENDF/B-IV over wide energy ranges as illustrated in Fig. IV-9. In addition, the present evaluation extends the continuum component to higher energies than does ENDF/B-IV. These are significant differences in many applications as the inelastic continuum cross section contributes strongly to large energy transfers.

The continuum neutron-emission spectrum is assumed to be a Maxwellian distribution with the addition of a higher-energy component characteristic of pre-compound evaporation processes. The temperature parameters were determined from the measured data of Refs. IV-17, IV-18 and IV-19. These values are limited to the energy range ~ 2.5 -7.0 MeV and are perturbed by the fission neutron component. However, this is the energy range of prominent continuum cross sections and the fission and inelastic neutron temperatures are not grossly different. The magnitude of the pre-compound component was selected to give acceptable results for 14 MeV macroscopic "benchmark" tests as described in Section IX, below. The neutron emission from the continuum process was assumed to be isotropic. This is a crude approximation, but there is little alternative given the "acceptable" formats of the system. In addition to the continuum component, it should be noted that the treatment of the discrete excitation functions was chosen to account for many inelastic events initiated by high-energy neutrons (e.g., 14 MeV) resulting in a relatively small energy loss (i.e., $\lesssim 2.5$ MeV). This treatment also gives attention to the anisotropic emission of such neutrons.

The cumulative sum of the above inelastic-scattering components and the resulting total inelastic scattering cross section is illustrated in Fig. IV-10 together with the comparable total-inelastic-scattering cross section as given in ENDF/B-IV. The total inelastic scattering cross section of the present evaluation is much larger than that of ENDF/B-IV over wide energy ranges and, of course, consistent with the above non-elastic cross section. The differences in overall magnitudes can be deceptive in many applications as they alone do not define differences in the transfer matrix. Thus the present evaluation leads to smaller energy transfers than ENDF/B-IV at some incident energies and these may more than correct for the increase in the overall cross section in many applications. Some aspects of this effect are further discussed in Section IX below.

REFERENCES -- SECTION IV

- IV-1. Nuclear Data Sheets, A = 238; compiled by Y. A. Ellis (1970).
- IV-2. W. R. McMurray et al., Southern Universities Annual Report (to be published 1977). Preference is given to this structure reference.
- IV-3. A. Smith et al., Argonne National Laboratory Report, ANL/NDM-22 (1976); also submitted for publication.
- IV-4. E. Barnard et al., Nucl. Phys. 80, 46 (1966). (Herein noted as "I").
- IV-5. A. Smith, Nucl. Phys. 47, 633 (1963).
- IV-6. P. Guenther et al., Argonne National Laboratory Report, ANL/NDM-16 (1975).
- IV-7. L. Cranberg and J. Levin, Phys. Rev. 109, 2063 (1956).
- IV-8. G. Haouat et al., Proc. Inter. Conf. on the Interaction of Neutron with Nuclei, CONF-760715 (1976).

- IV-9. T. Marcella et al., Proc. Inter. Conf. on the Interaction of Neutron Nuclei, CONF-760715 (1976).
- IV-10. P. Guenther et al., private communication (1977).
- IV-11. E. Barnard et al., Proc. Second Inter. Conf. on Nuclear Data for Reactors, Helsinki; IAEA Press (1970). (Herein noted as "II").
- IV-12. L. Stromberg and S. Schwartz, Nucl. Phys. 71, 511 (1965).
- IV-13. P. Guenther et al., Proc. Conf. on Nucl. Cross Sections and Tech., National Bureau of Standards Publication, NBS-428 (1975).
- IV-14. J. Egan et al., Proc. Conf. on Nucl. Cross Sections and Tech., National Bureau of Standards Publication, NBS-428 (1975).
- IV-15. W. Poenitz, Proc. Second Inter. Conf. on Nuclear Data for Reactors, Helsinki, IAEA Press (1970).
- IV-16. J. Kammerdiener, Lawrence Livermore Laboratory Report, UCRL-51232 (1972).
- IV-17. L. Cranberg and J. Levin, Phys. Rev. 109, 2063 (1958).
- IV-18. N. Fetisov, Atom. Energy 3, 211 (1957).
- IV-19. R. Batchelor and J. Towle, Nucl. Phys. 65, 236 (1965).

TABLE IV-1. Q-Values of Discrete Inelastic
Scattering Processes of
This Evaluation

Group No.	Reaction Q-Value (MeV)
1	-0.045
2	-0.148
3	-0.308
4	-0.680
5	-0.732
6	-0.827
7	-0.965
8	-1.048
9	-1.170
10	-1.250
11	-1.440
12	-1.590
13	-1.750
14	-1.850
15	-1.950
16	-2.150
17	-2.300
18	-2.390
19	-2.493
20	-2.940
21	-3.189
22	-3.388
23	-3.538
24	-3.637
25	-3.737
26	-3.837
27	-3.909
Continuum	-2.489

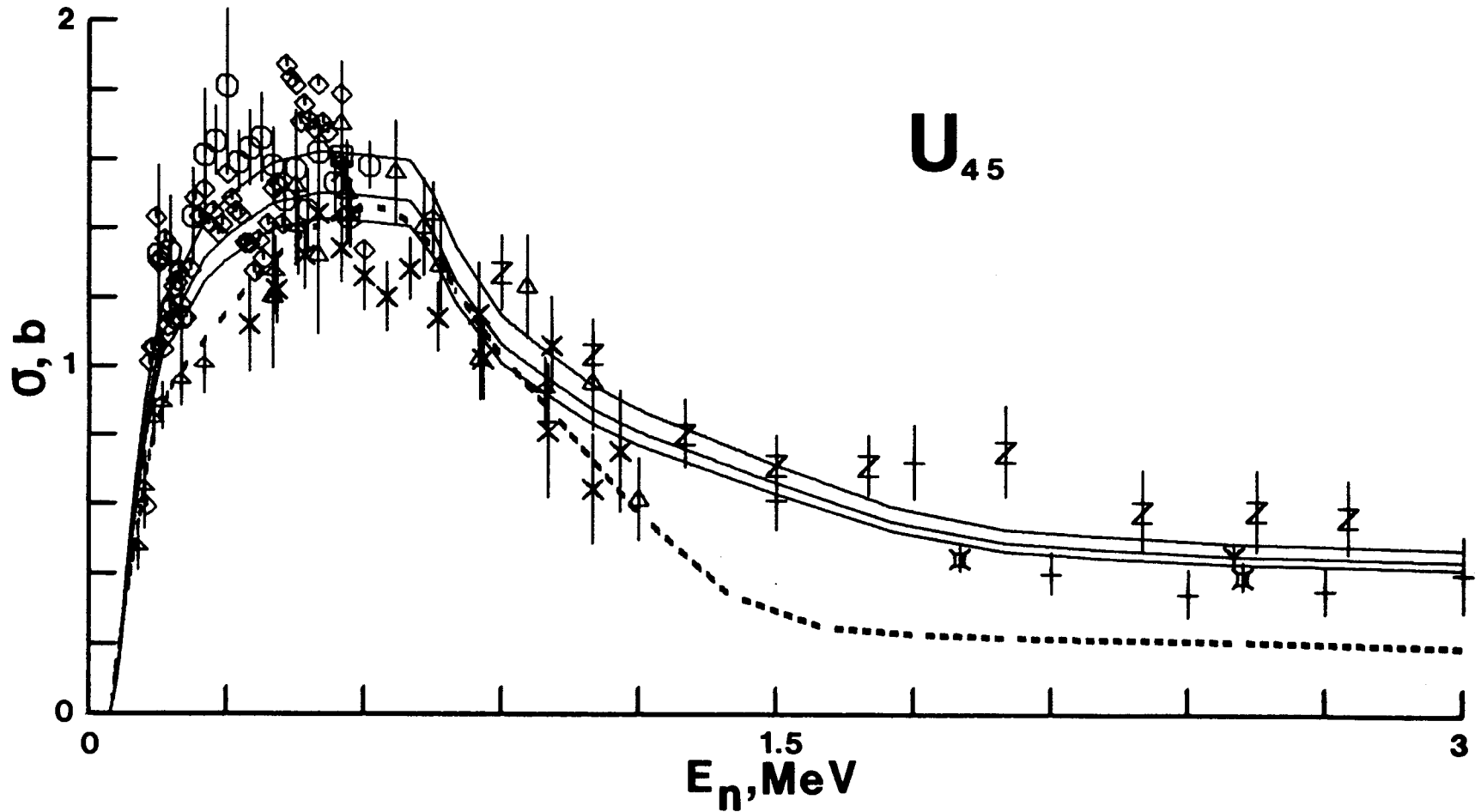
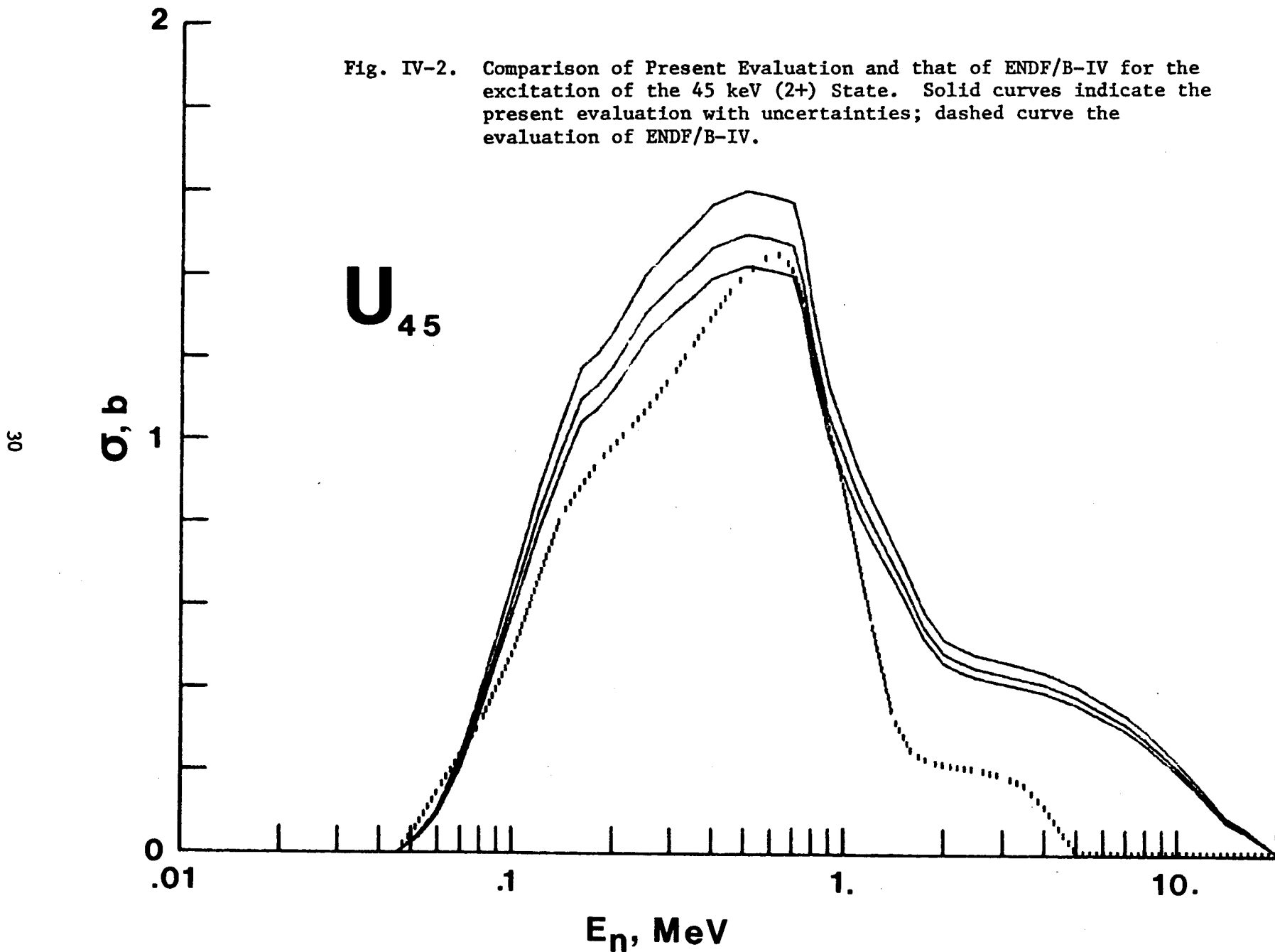


Fig. IV-1. Cross Sections for the Excitation of the 45 keV (2+) State. Measured values are indicated by data points as outlined in the text. Solid curves indicate present evaluation with \pm uncertainty limits. Dashed curve is from ENDF/B-IV.

Fig. IV-2. Comparison of Present Evaluation and that of ENDF/B-IV for the excitation of the 45 keV (2+) State. Solid curves indicate the present evaluation with uncertainties; dashed curve the evaluation of ENDF/B-IV.



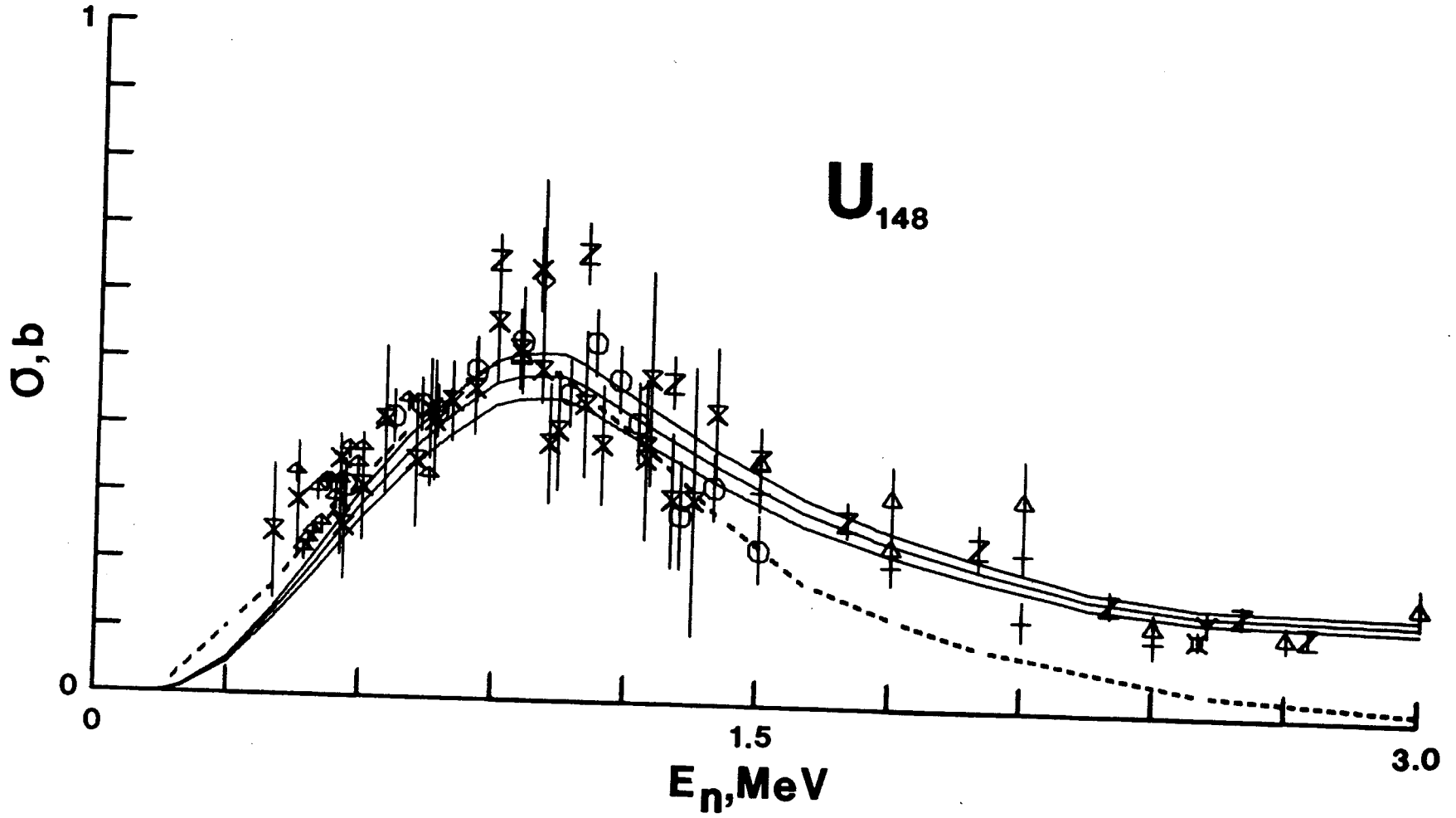
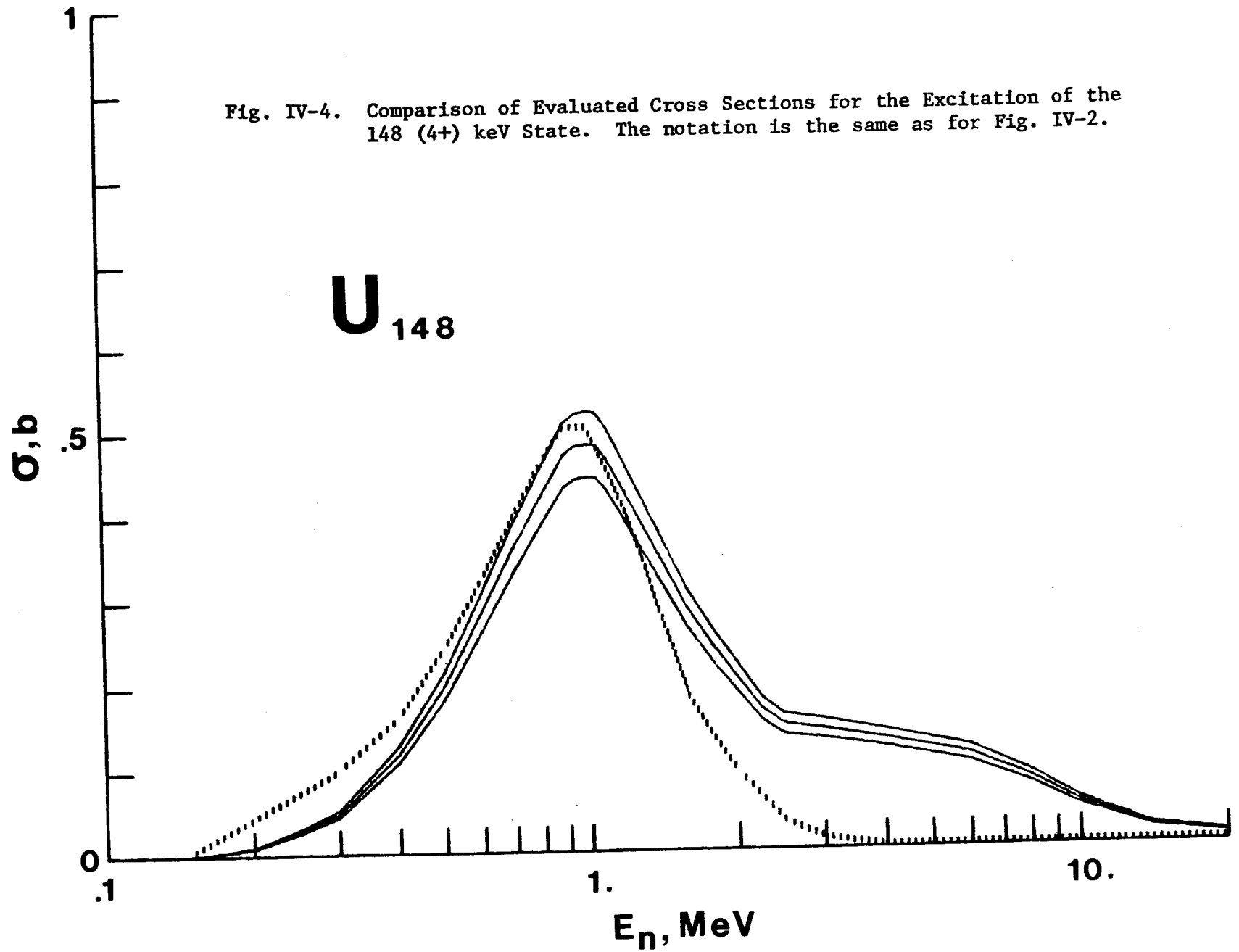


Fig. IV-3. Cross Sections for the Excitation of the ^{148}U (4+) keV State. Notation is the same as that of Fig. IV-1.

Fig. IV-4. Comparison of Evaluated Cross Sections for the Excitation of the 148 (4+) keV State. The notation is the same as for Fig. IV-2.



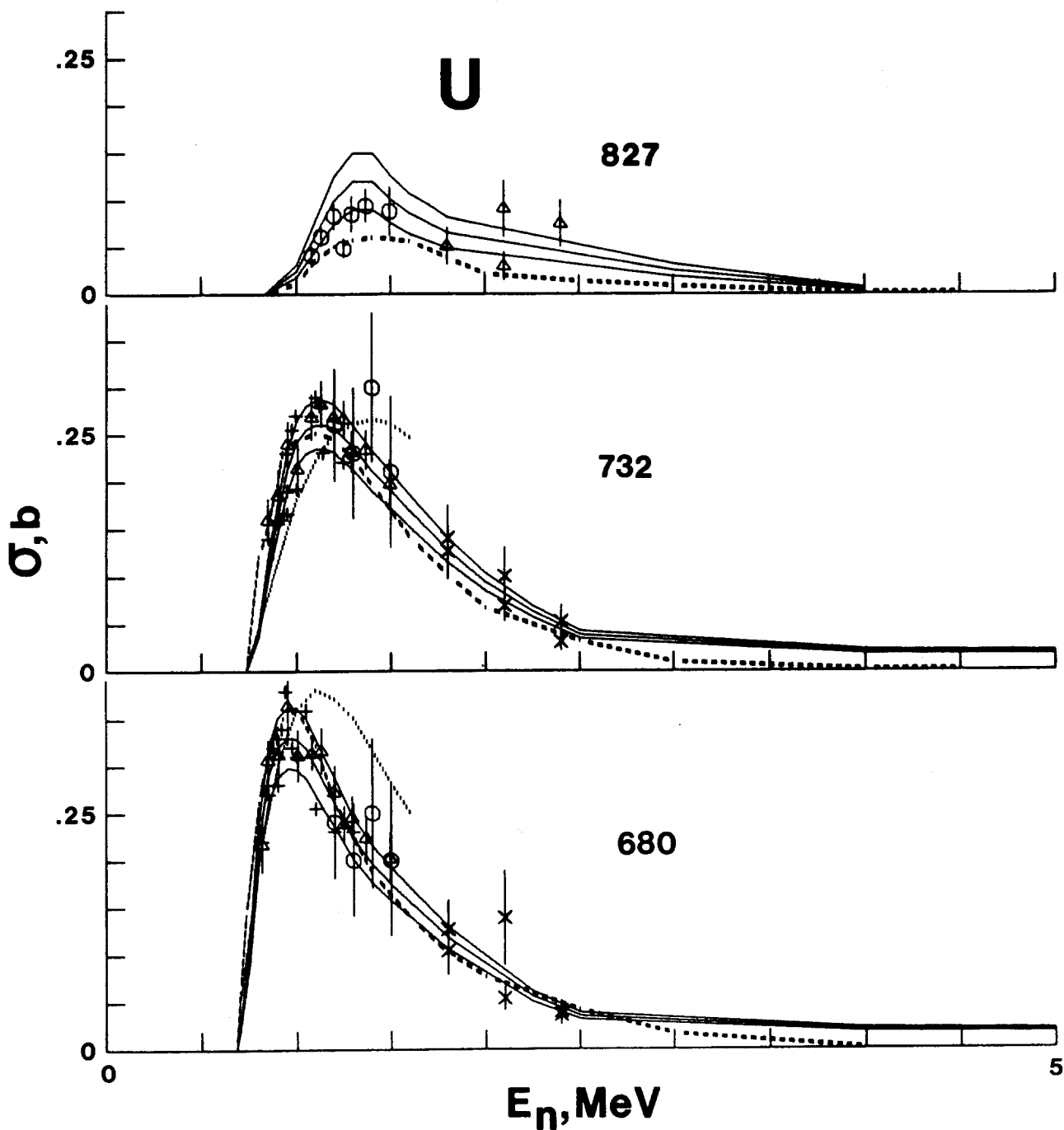


Fig. IV-5. Measured and Evaluated Cross Sections for the Excitation of the 680, 732 and 827 keV States. The notation is identical to that of Fig. IV-1 with the addition of results of $(n;n',\gamma)$ measurements indicated by dotted curves.

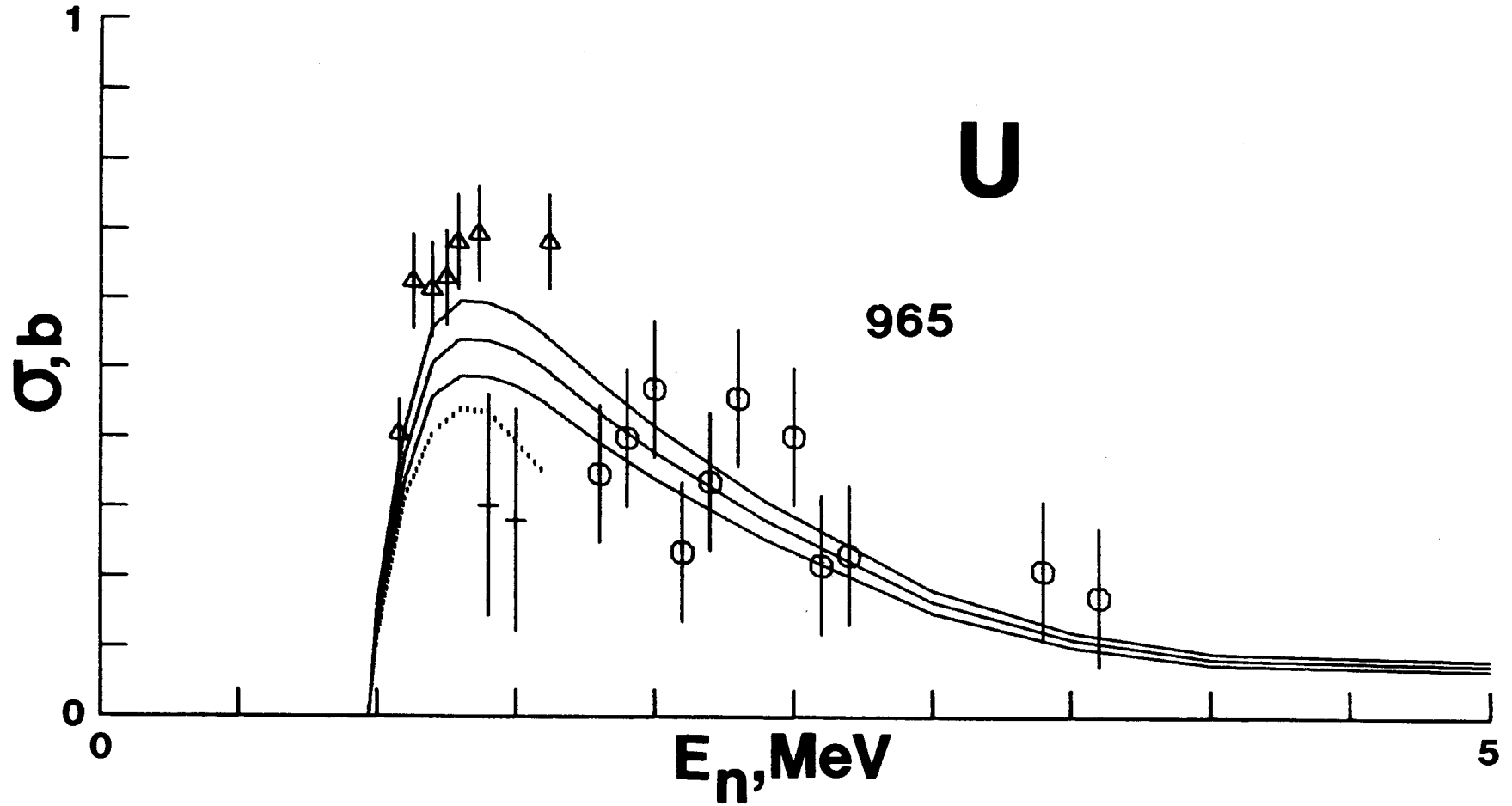


Fig. IV-6. Measured and Evaluated Cross Sections for the Excitation of the 965 keV State. The notation is the same as for Fig. IV-5.

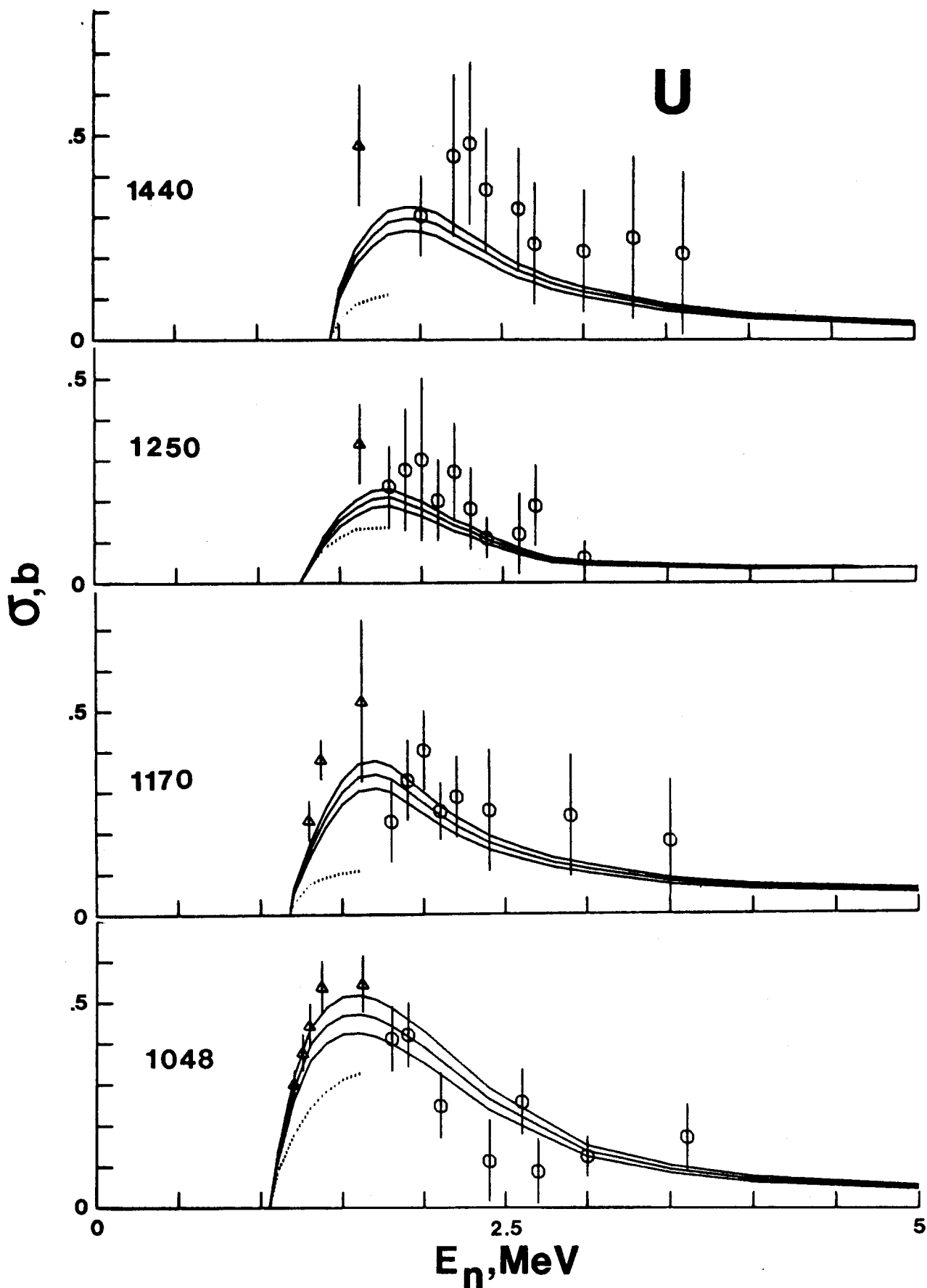


Fig. IV-7. Measured and Evaluated Cross Sections for the Excitation of 1048, 1170, 1250 and 1440 keV States. The notation is the same as for Fig. IV-5. 35

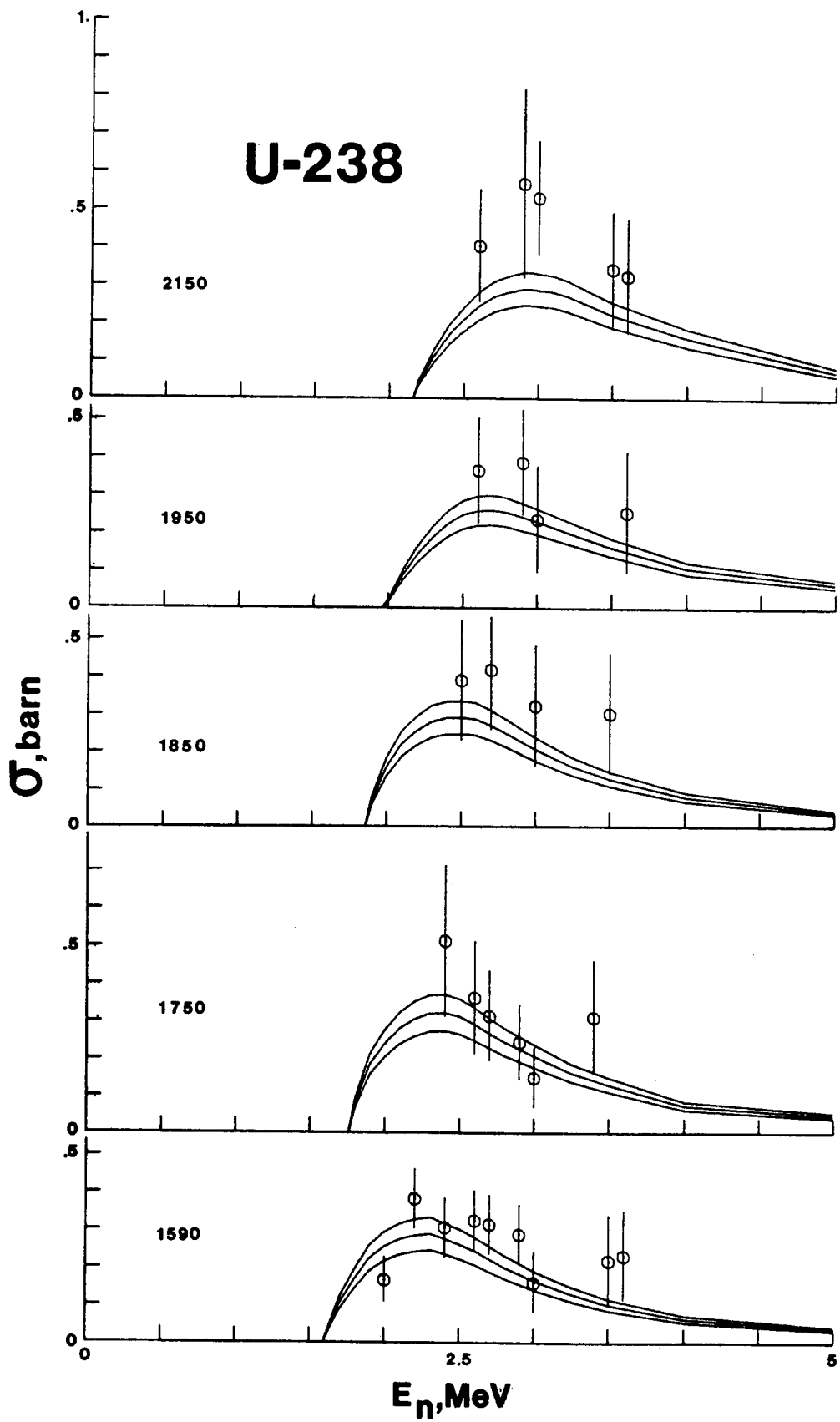


Fig. IV-8. Measured and Evaluated Cross Sections for the Excitation of 1590, 1750, 1850, 1950 and 2150 keV States. Notation is the same as for Fig. IV-5.

Fig. IV-9. Comparison of Evaluated Continuum Inelastic Scattering Cross Sections. The present evaluation with associated uncertainty band is indicated by solid curves. The ENDF/B-IV evaluation is noted by the dashed curve.

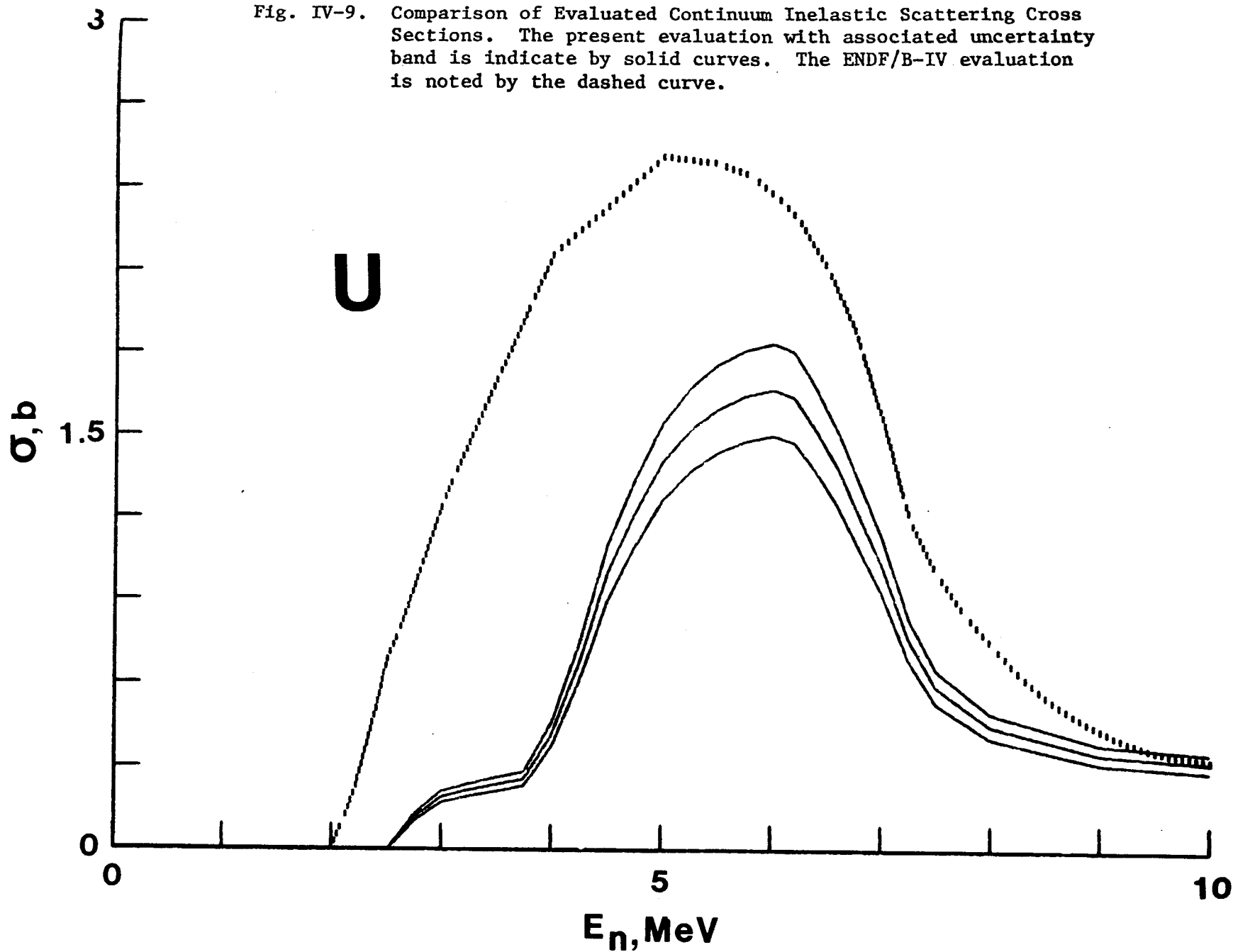
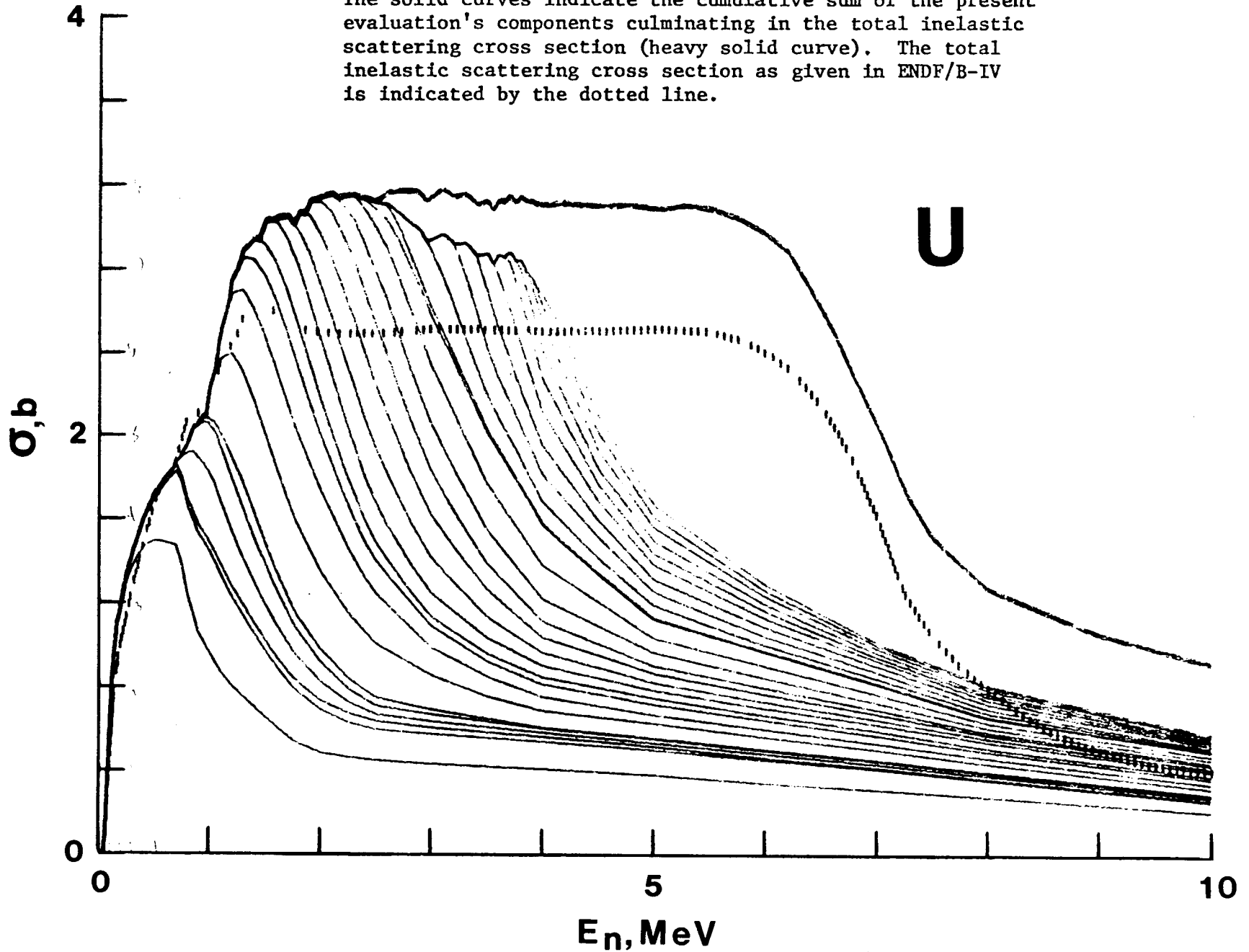


Fig. IV-10. Comparison of Evaluated Inelastic Scattering Cross Sections. The solid curves indicate the cumulative sum of the present evaluation's components culminating in the total inelastic scattering cross section (heavy solid curve). The total inelastic scattering cross section as given in ENDF/B-IV is indicated by the dotted line.



V. FISSION PROCESSES

A. General Procedures

Most of the existing ^{238}U (n;f) data sets were measured relative to ^{235}U (n;f), (U8/U5). However, some data are available which were measured relative to H(n,n) or absolutely determined by using associated particle techniques. As a first step, a separate evaluation of the ratio and the absolute data sets was carried out. The evaluated U8/U5 data set was converted to ^{238}U cross sections using ENDF/B-V values for ^{235}U , assuming a 2% uncertainty for the latter [V-1]. As a second and final step, a weighted average was formed between the two evaluated ^{238}U (n;f) sets. The resulting evaluated cross sections are shown in Fig. V-1. The procedures employed in the evaluation of the "absolute" ^{238}U (n;f) data and the U8/U5 ratio data have been described on several occasions [V-2, V-3 and V-4]. However, the final step of averaging the absolute ^{238}U and the (U8/U5) ^{238}U data is not consistent with the procedure advocated in Refs. V-2, V-3 and V-4. This deviation in the methods was necessary in order to remain consistent with evaluation techniques generally used for ENDF/B-V.

B. Input Data

Input data were obtained from comprehensive data files compiled for the 1976 ANL Fission Cross Section Meeting [V-4]. The use of the data is summarized in Tables V-1 and V-2. It should be noted that some data were excluded from the evaluation of the U8/U5 ratio because they were used in the ^{238}U evaluation or because they played a significant role in the evaluation of ^{235}U (ENDF/B-V). Input data sets were not altered.

C. Normalization

The normalization of the evaluated shape curves for ^{238}U and for the U8/U5 ratio is summarized in Tables V-3 and V-4. Only data above 2 MeV were utilized in order to avoid additional errors associated with energy-scale problems. Values for ^{238}U averaged over the fission-neutron spectrum were not used as in the evaluation of ^{235}U [V-3] due to the additional uncertainties associated with the energy-spectrum and cross-section energy scales. However, the spectrum-averaged values were calculated in order to compare with experimental values. A Maxwellian fission spectrum with an average energy (E) of 2.2 MeV was assumed, adjusted by a factor of 0.97 as suggested by Grundl [V-9]. The spectrum averaged ^{238}U results are:

This evaluation	0.334 b
Evaluation based on ^{238}U absolute values.	0.326 b
Evaluation based on U8/U5* ^{235}U (ENDF/B-V) values. . .	0.337 b

These values are to be compared with the experimental values of:

Abramov [V-10]	0.347 ± 0.006 b
Heaton [V-11].	0.3193 ± 0.009 b
Weight average	0.339 ± 0.012 b

The difference between the weighted experimental average and the present suggested ENDF/B-V is 1.5%. Due to the relatively large uncertainty of the spectrum-averaged values, their inclusion in the evaluation would have a small impact. It should be noted that energy-scale uncertainties of ~ 15 keV near threshold have a minor effect on the spectrum-averaged result (i.e. 0.3%). However, a 0.1-MeV shift in the average-fission-spectrum energy changes the spectrum-averaged value by 3.6%.

D. Partial Fission Cross Sections

Present ENDF/B practice dictates the inclusion of partial fission cross sections; e.g., (n;f), (n;n',f), (n;2n',f), etc. These are provided for in the full file of Pennington et al. [V-12]. However, the construction of these components is highly speculative and the primary file described in this document takes the simpler option of a single fission cross section and associated emission spectrum. The partial components for the full file of Ref. V-12 were obtained by setting a constant cross section value from the fission-cross-section minimum just prior to the onset of the next fission threshold and extending it to the maximum 20 MeV energy. This procedure follows ENDF/B-IV practice but is controversial. Calculations, some physical considerations, and the observed plateaus suggest cross sections varying only slowly with energy. However, the delayed neutron yield and, possibly, the fragment angular distributions suggest that the cross section with the highest primary neutron emission is dominant.

The energy-spectrum of the emitted fission-neutrons for the present file was calculated from the model of Howerton et al. [V-13]. The version of Ref. V-12 uses an energy-dependent watt spectrum derived using a semi-empirical interpretation of the total fission-neutron spectrum. In the method of Howerton et al. [V-13] the multiple-chance fission processes were dealt with by estimating the fractions for each fission mode then combining the resultant spectra at each incident neutron energy.

E. Observations and Comparisons of Experimental and Evaluated Data

Comparison of the "absolute" $^{238}\text{U}(n;f)$ and the $U8/U5 \cdot ^{235}\text{U}$ (ENDF/B-V) results in Fig. V-1 shows that a consistent-data-set fit would have lowered the recommended ^{235}U cross section (of ENDF/B-V) between 2 and 13 MeV. This

is supported by the ^{235}U data by Barton et al. [V-5] and recent data by Szabo and Marquette [V-6] above 3.0 MeV. Alternatively, the difference between the two sets shown in Fig. V-1 could also be resolved by lowering the U8/U5 ratio values in the 2-13 MeV range. This solution would be supported by the ratio measurements by Stein et al. [V-7] and recent data by Cance and Grenier [V-8]. Some of the differences between the two sets in the range 6-10 MeV could be due to energy-scale differences between ^{235}U , U8/U5 and ^{238}U measurements. The ^{235}U cross section does change by approximately a factor of 2 over a 2 MeV interval in the 5-7 MeV region.

A number of sets of experimental data are compared with the present evaluation in Figs. V-2 to V-8. Figure V-9 compares the present evaluation with that of ENDF/B-IV. There are differences between the two evaluations that are more evident in Fig. V-10 which shows the deviation of ENDF/B-IV from the present evaluation. In the important region above threshold the present evaluation differs from that of ENDF/B-IV by 3-4% over wide energy ranges and the differences can be both positive and negative.

F. Cross Section Uncertainties

Estimates of the uncertainties associated with the present evaluation are available on a point-by-point basis from the authors. Some illustrative guidelines are given in Table V-5.

G. Nu-Bar Prompt

Measurements of this quantity made since 1964 are reported in Refs. V-14 to V-17. The measurements were renormalized to a value of 3.73 for the spontaneous fission nu-bar of ^{252}Cf . The evaluated data for energies less than

6 MeV are as described in Ref. V-18. For incident neutron energies greater than 6 MeV the adopted values are based on the measurements of Ref. V-15. These nu-bar values are specific to this evaluation and not those of Ref. V-12. The latter file employs a different and new evaluation of nu-bar normalized to a ^{252}Cf spontaneous-fission nu-bar of 3.75.

H. Nu-Bar Delayed

A review of the experimental data for this quantity through April 1974 is reported in Ref. V-19. Additional measurements were reported in Ref. V-20. The values adopted for this evaluation are based on the experimental data. Again, this delayed nu-bar file is specific to the present evaluation and not that employed in Ref V-12.

REFERENCES -- SECTION V

- V-1. R. M. Bhat, Proc. of NEANDC/NEACRP Special Meeting on Fast Fission Cross Sections of U-233, U-235, U-238 and Pu-239, Argonne National Laboratory Report, ANL-76-90 (1976), page 307, also; R. Peelle, private communication (1976).
- V-2. W. Poenitz, Proc. Conf. on Neut. Stds. and Flux Normalization, AEC Symposium Series 23, p. 331 (1971).
- V-3. W. Poenitz, Memorandum to CSEWG, private communication (1975).
- V-4. W. Poenitz and P. Guenther, Argonne National Laboratory Report, ANL-76-90, 154 (1976).
- V-5. D. Barton et al., see Ref. V-21, p. 173.
- V-6. I. Szabo and G. Marquette, see Ref. V-21, p. 208.
- V-7. W. Stein et al., Proc. Conf. on Nucl. Cross Sections and Technology, Washington, Vol. 1, p. 627 (1968).
- V-8. M. Cance and G. Grenier, see Ref. V-21, p. 141.
- V-9. J. Grundl and C. Eisenhower, National Bureau of Standards Publication, 425, p. 250 (1975).

- V-10. Abramov et al., Proc. of Kiev Conf. (1973).
- V-11. H. Heaton II et al., see Ref. V-21, p. 333.
- V-12. E. Pennington, W. Poenitz and A. Smith, Trans. Am. Nucl. Soc. 26, 591 (1977).
- V-13. R. J. Howerton et al., The LLL Evaluated Nuclear Data Library (ENDL): Evaluation Techniques, Reaction Index, and Descriptions of Individual Evaluations, UCRL-50400, Vol. 15, Part A, p. 36, Lawrence Livermore Laboratory (1975).
- V-14. M. V. Savin et al., At. Energy 32, 408 (1972).
- V-15. M. Soleilhac et al., J. Nucl. Energy 23, 257 (1969).
- V-16. D. S. Mather, P. Fieldhouse and A. Moat, Nucl. Phys. 66, 149 (1965).
- V-17. I. Asplund-Nilsson, H. Conde and N. Starfelt, Nucl. Sci. Eng. 20, 257 (1964).
- V-18. R. J. Howerton, Nucl. Sci. Eng. 62, 438 (1977).
- V-19. S. A. Cox, Delayed Neutron Data - Review and Evaluation, Argonne National Laboratory, ANL/NDM-5 (1974).
- V-20. J. W. Meadows, The Delayed Neutron Yield of ^{238}U and ^{241}Pu , Argonne National Laboratory, ANL/NDM-18 (1976).
- V-21. W. Poenitz and A. Smith, Editors, Proc. of NEANDC/NEACRP Specialists Meeting on Fast Fission Cross Sections, Argonne National Laboratory Report, ANL-76-90 and supplement (1976).

TABLE V-1. Data-Use Summary for ^{238}U Fission
Cross-Section Evaluation

Data Set ^a	Use	
	Shape	Normalization
Vorotnikov	X	
Netter	X	X
Leugers	X	
Smith	X	X
Adams	X	
Emma	X	X
Pankratov	X	X
Kuks		X
Mongialio		X
Uttley		X
Flerov		X
Moat		X
Allen		X

TABLE V-2. Data-Use Summary for U8/U5 Ratio Evaluation

Data Set ^a	Use	
	Shape	Normalization
Grundl	X	
Poenitz		X
Meadows	X	X
Behrens	X	X
Cance	X	X
Stein	X	X
Lamphere	X	X
White	X	X
Fursov	X	X
Nordborg	X	X
Smirenkin		X
Moat		X
Adams	X	
Jarvis		X
Iyer		X
Berenzin		X
Hall		X
Bretcher		X
Z-Group		X
Chadwick		X
Nyer		X
Difilippo	X	
Coates	X	

^aExplicit references to the data sets of this table and of Tables V-2, 3, 4, and 5 are given in ANL-76-90 (see Ref. V-21). The supplement of that report also contains large graphical presentations of these data sets.

TABLE V-3. Factors for Normalizing U8/U5 Ratio Values to 0.432 at 2.5 MeV

Data Set	Factor
Poenitz	1.0078 ± 0.0186
Meadows	1.0047 ± 0.0141
Behrens	0.9989 ± 0.0117
Cance	0.9615 ± 0.0295
Stein	0.9668 ± 0.0250
Lamphere	1.0367 ± 0.1000
White	1.0019 ± 0.0200
Fursov	0.9741 ± 0.0250
Nordborg	0.9987 ± 0.0257
Smirenkin	1.0417 ± 0.1000
Moat	0.9759 ± 0.0452
Jarvis	0.9837 ± 0.0151
Iyer	0.9992 ± 0.1007
Berenzin	0.8781 ± 0.0652
Hall	0.9447 ± 0.1000
Bretcher	0.8946 ± 0.1000
Chadwick	0.7114 ± 0.1000
Nyer	0.9612 ± 0.0497
Average 1st Approximation	0.9910
3rd Approximation	0.9915 ± 0.0014

TABLE V-4. Factors for Arbitrarily Normalizing the ^{238}U Cross-Section Shape to 0.55 at 2.5 MeV

Data Set	Factor
Kuks	1.0092 ± 0.0364
Smith	0.9231 ± 0.0468
Netter	0.9726 ± 0.1000
Mongialio	1.0529 ± 0.1000
Emma	0.8942 ± 0.0500
Uttley	0.9439 ± 0.0263
Flerov	0.8867 ± 0.0442
Pankratov	0.9701 ± 0.1000
Moat	0.9464 ± 0.0177
Allen	0.8504 ± 0.0494
Average	0.9408 ± 0.0040

TABLE V-5. Illustrative Examples of Evaluated
U-238 Fission Cross Sections

E(MeV)	σ (b)	$\Delta\sigma$ (b)
.3000E-00	.1181E-03	.1051E-04
.4000E-00	.2506E-03	.2799E-04
.5000E-00	.3703E-03	.3613E-04
.6000E-00	.8365E-03	.9794E-04
.7000E-00	.1670E-02	.1852E-03
.8000E-00	.4352E-02	.3624E-03
.9000E-00	.1354E-01	.1045E-02
.1000E+01	.1703E-01	.1362E-02
.1200E+01	.4227E-01	.2581E-02
.1400E+01	.1870E-00	.1389E-01
.1600E+01	.4149E-00	.5641E-02
.2000E+01	.5226E-00	.7099E-02
.2500E+01	.5386E-00	.1559E-01
.3000E+01	.5237E-00	.1303E-01
.4000E+01	.5537E-00	.1309E-01
.5000E+01	.5419E-00	.1432E-01
.6000E+01	.6188E-00	.2411E-01 3.9%
.8000E+01	.1021E+01	.3302E-01 3.2%
.1000E+02	.1003E+01	.2931E-01 2.9%
.1200E+02	.1005E+01	.3691E-01
.1400E+02	.1126E+01	.4832E-01 4.3%
.2000E+02	.1461E+01	.1246E-00 8.5%

Fig. V-1. Present Evaluated Fission Cross Sections. \square = values obtained from ratio relative to ^{235}U fission of ENDF/B-V, \circ = values obtained from absolute ^{238}U measurements and solid line the weighted average of these two subsets.

48

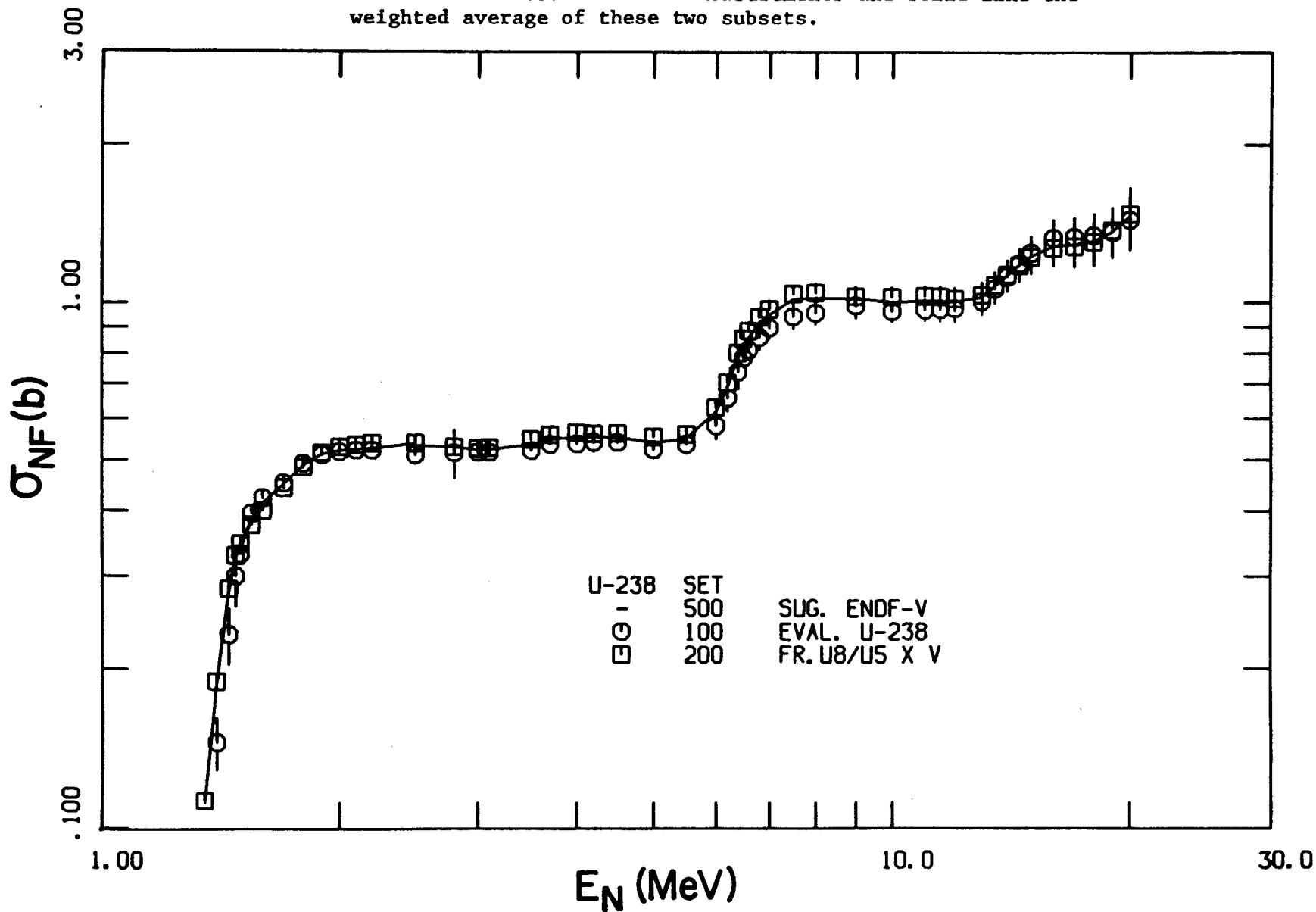


Fig. V-2. Comparison of Present Evaluation and with Recent ^{238}U Fission-Cross-Section Results. Measured values are obtained relative to $\text{H}(n;n)$ and by using associated particle techniques. Data values given in Ref. V-21 and similarly for all subsequent fission-cross-section figures.

67

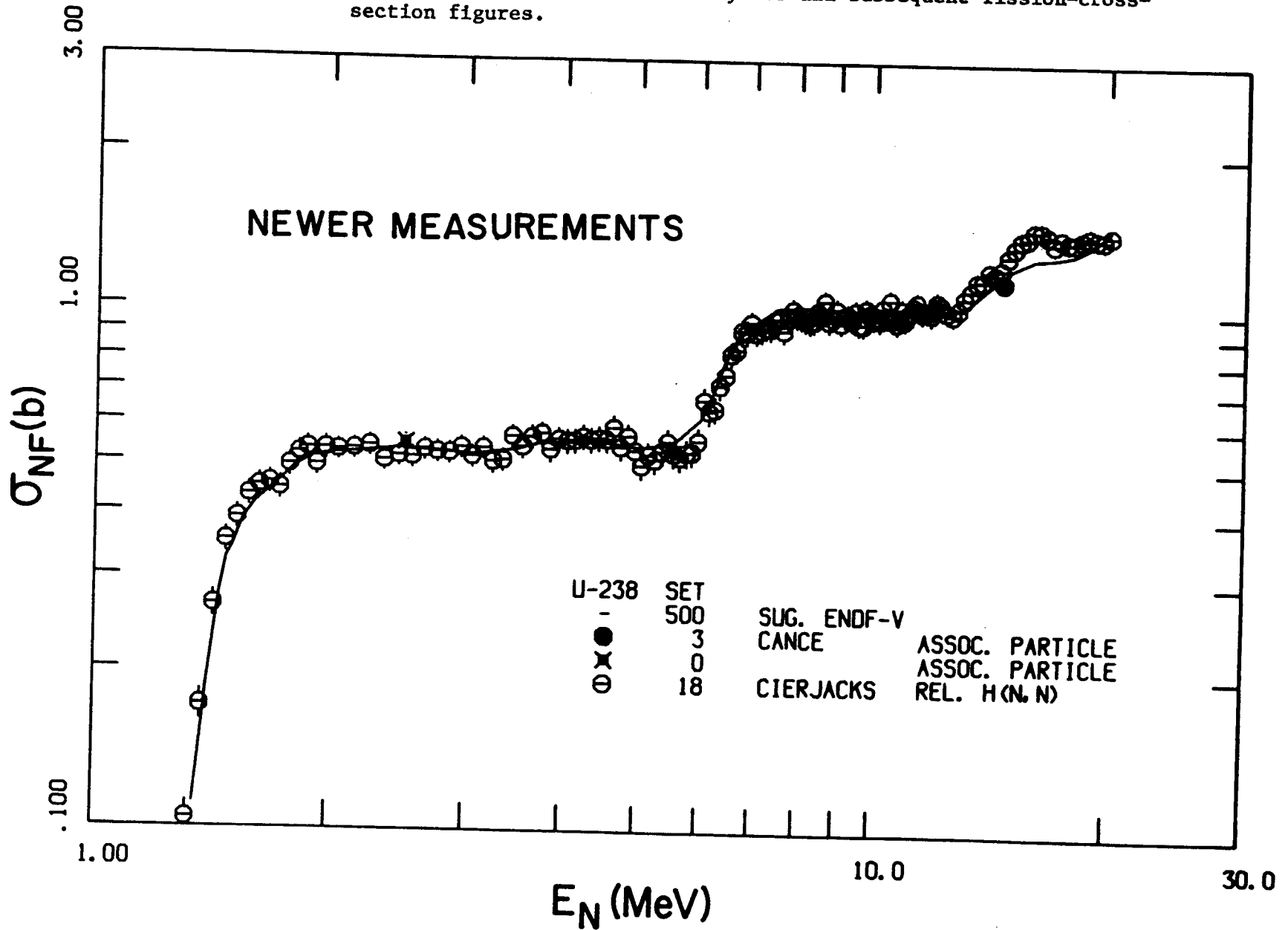


Fig. V-3. Comparison of Present Evaluation with Values Measured Relative to ^{235}U (ENDF/B-V).

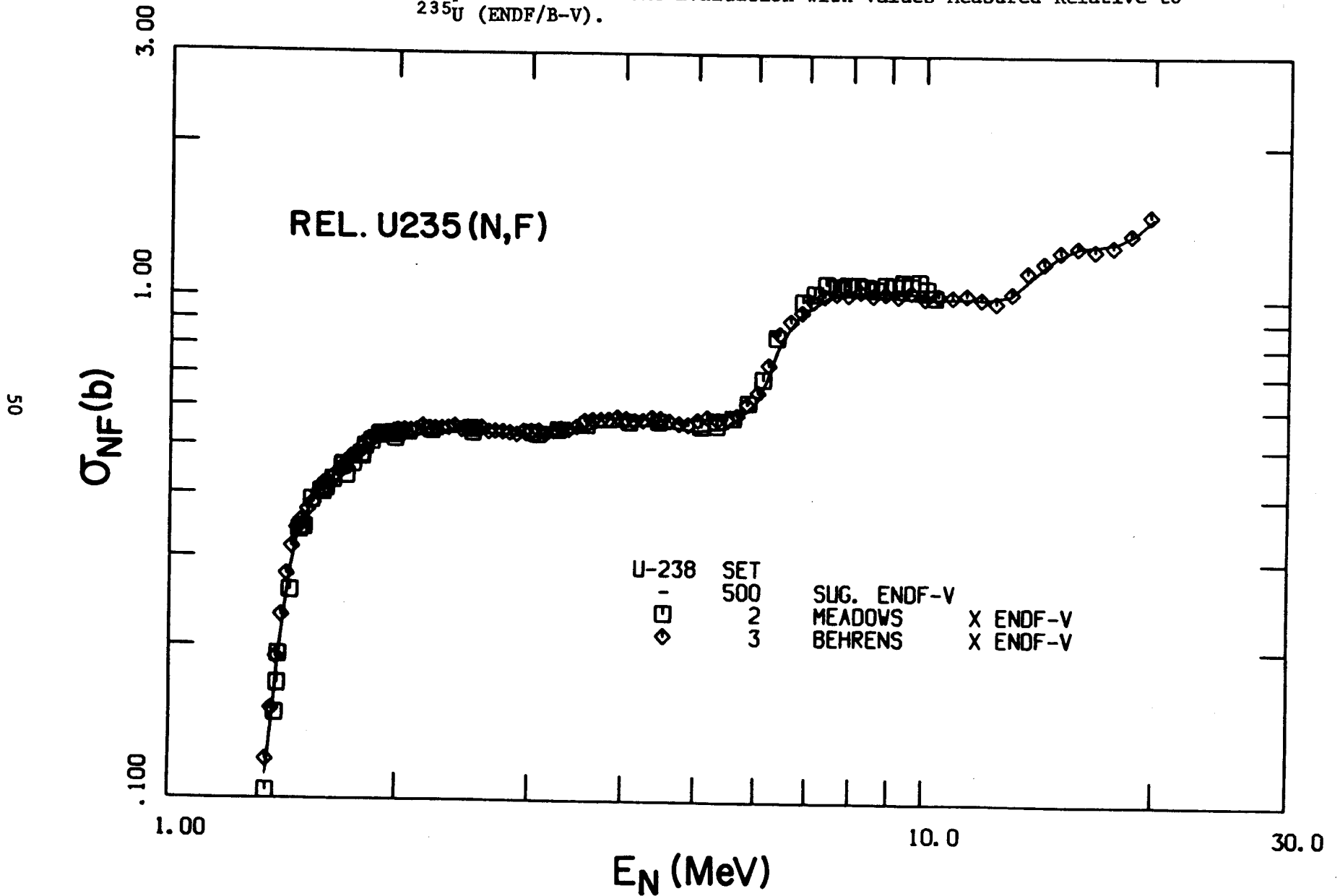


Fig. V-4. Comparison of Present Evaluation with Older Values Measured Relative to the H(n;n) Cross Section or Calibrated Long Counters.

51

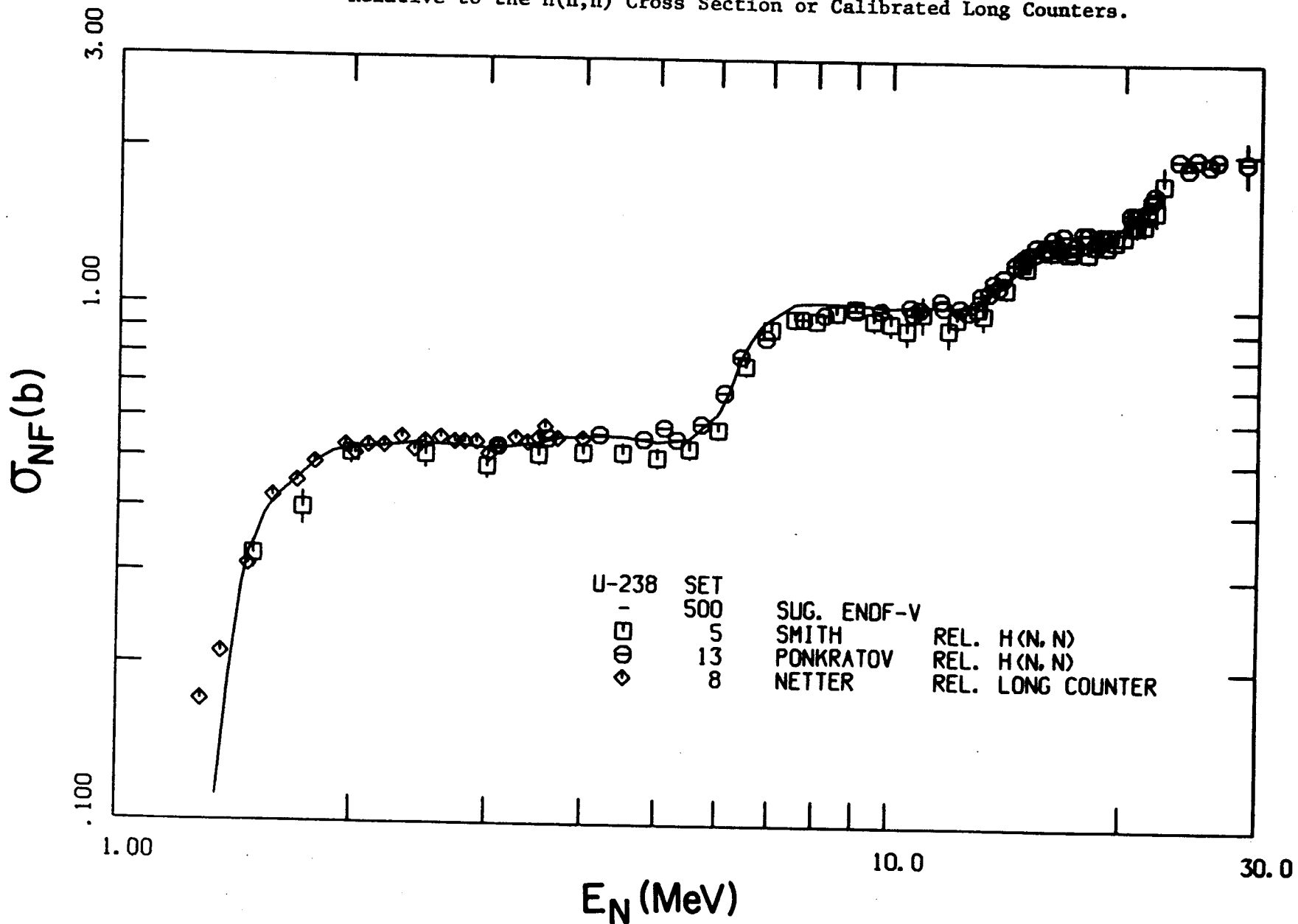


Fig. V-5. Comparison of Present Evaluation with Measured Ratio Values Normalized to ENDF/B-V ^{235}U Fission.

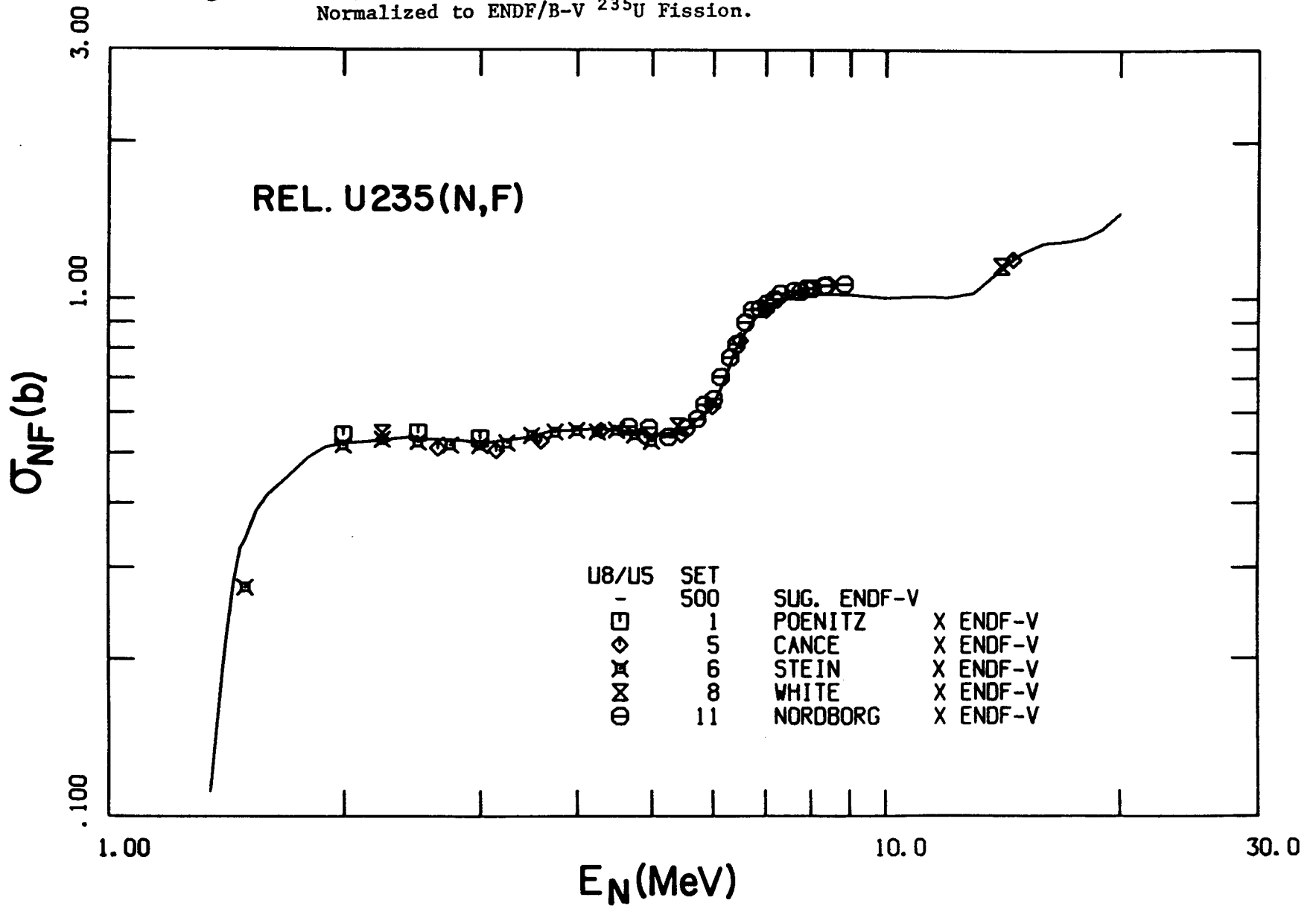


Fig. V-6. Comparison of this Evaluation in the Threshold Region with Measured Ratios Normalized to ^{235}U (ENDF/B-V).

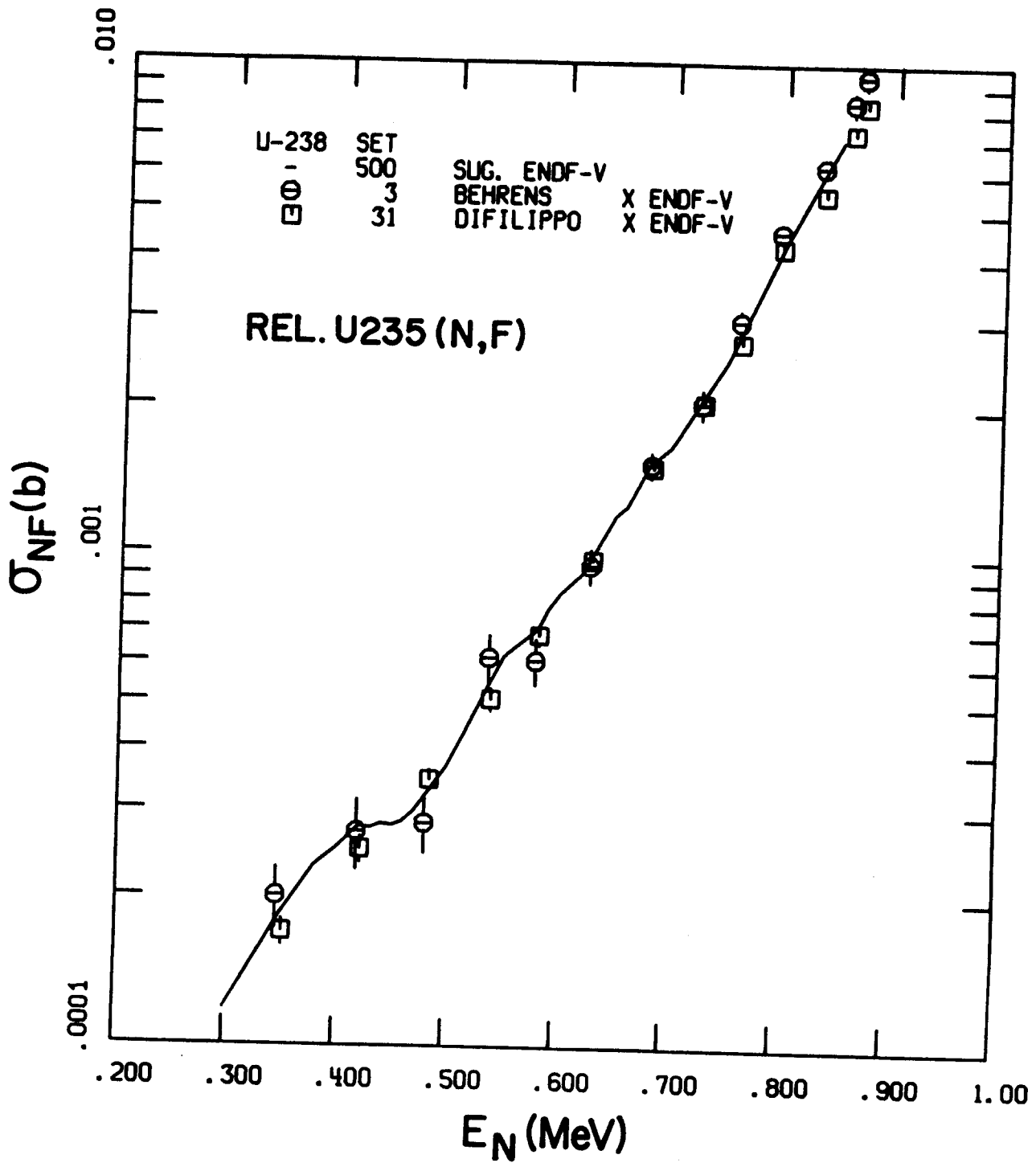
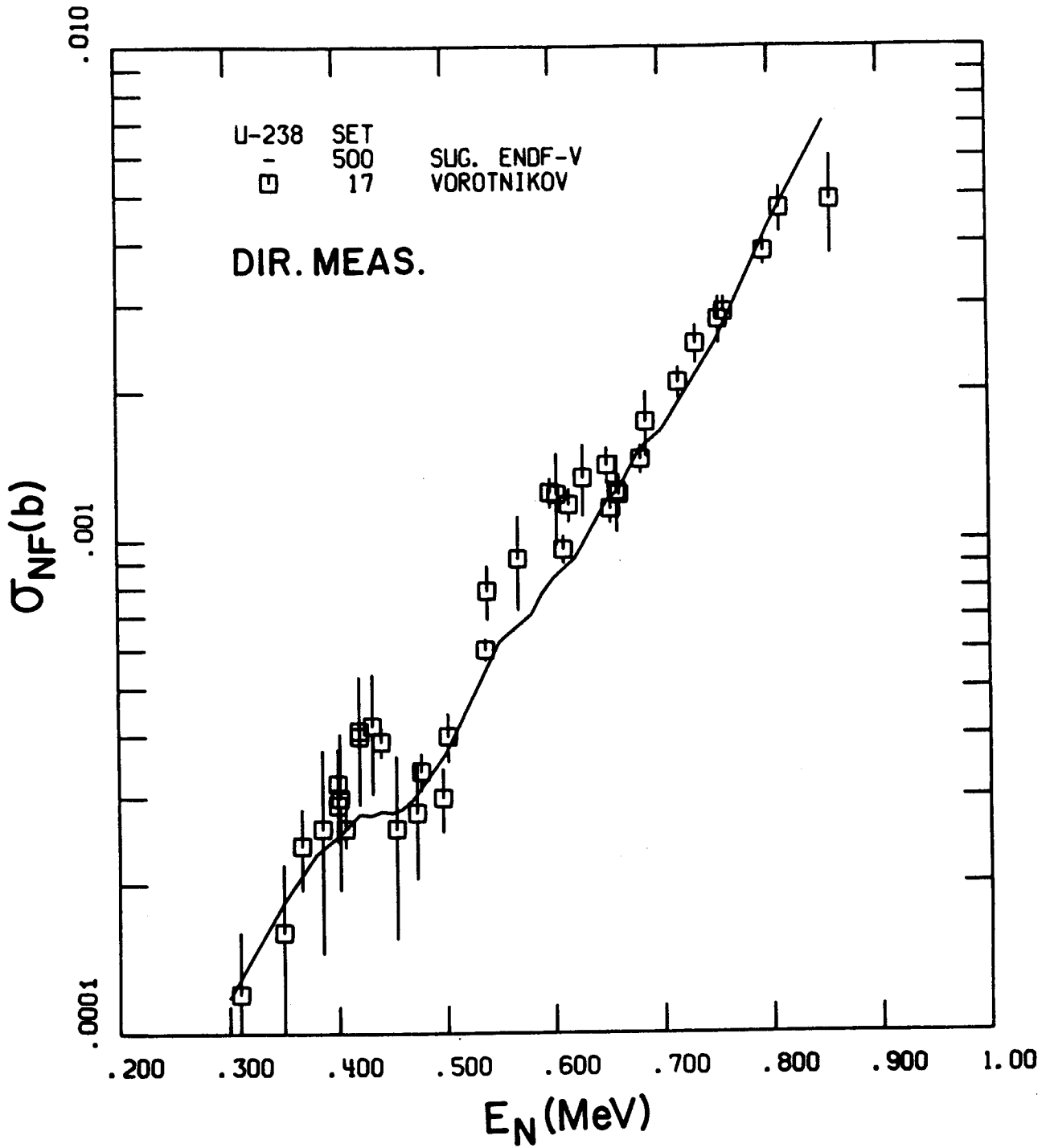


Fig. V-7. Comparison of this Evaluation in Threshold Region with Directly Measured Values.



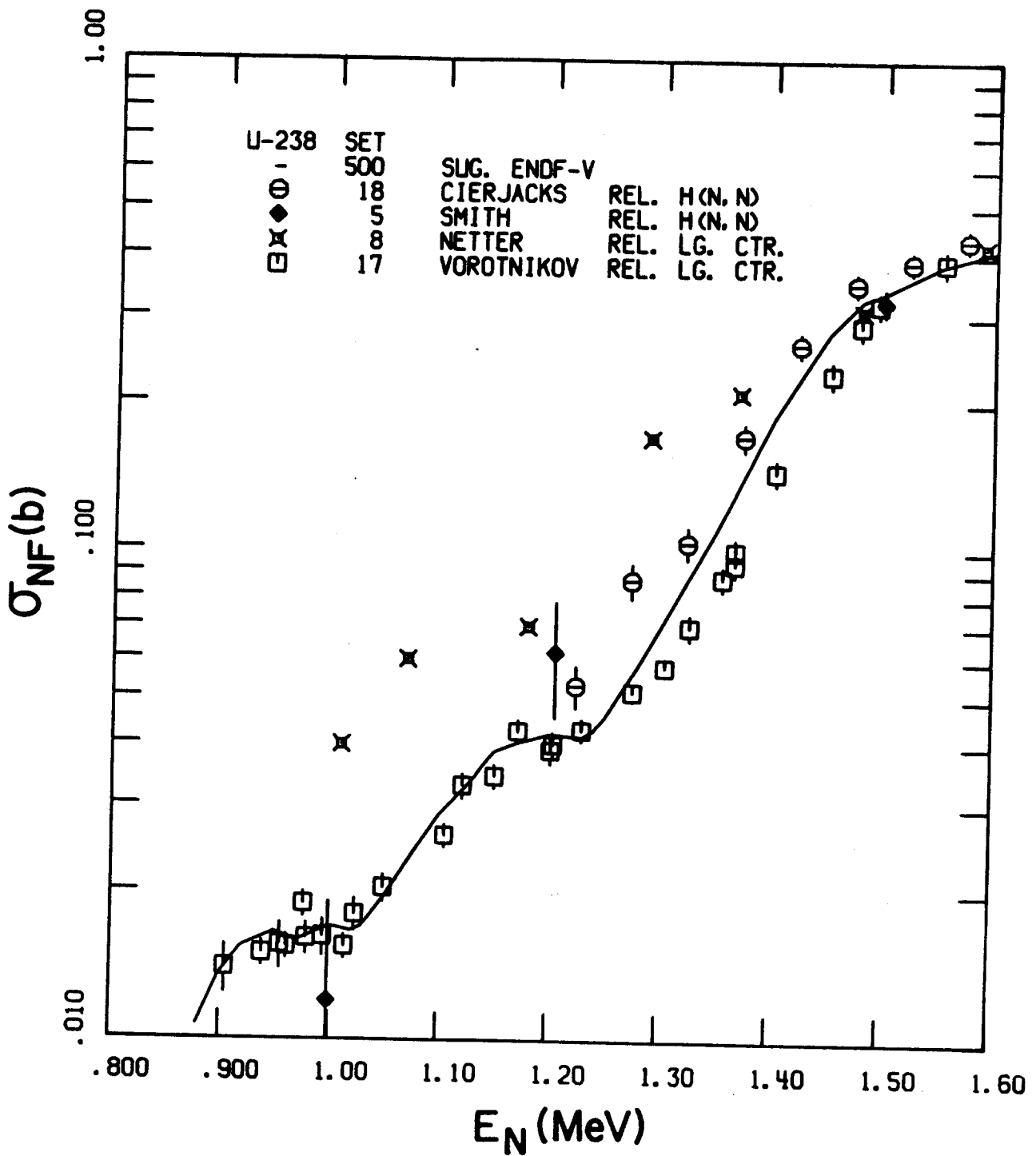


Fig. V-8. Comparison of this Evaluation in Threshold Region with Values Measured Relative to H(n;n) or Calibrated Long Counters.

Fig. V-9. Comparison of the Present ^{238}U Fission Cross-Section Evaluation with that of ENDF/B-IV.

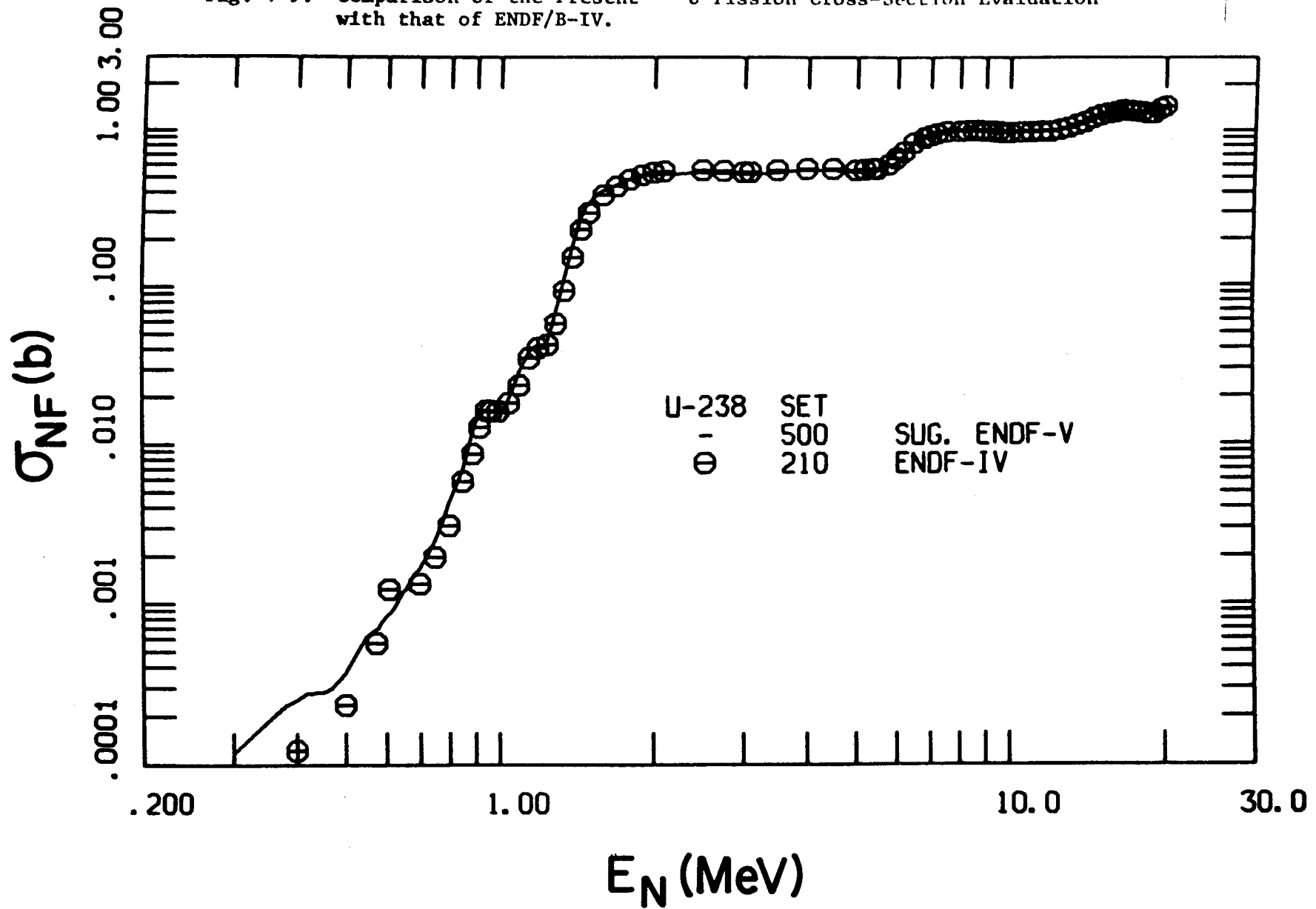
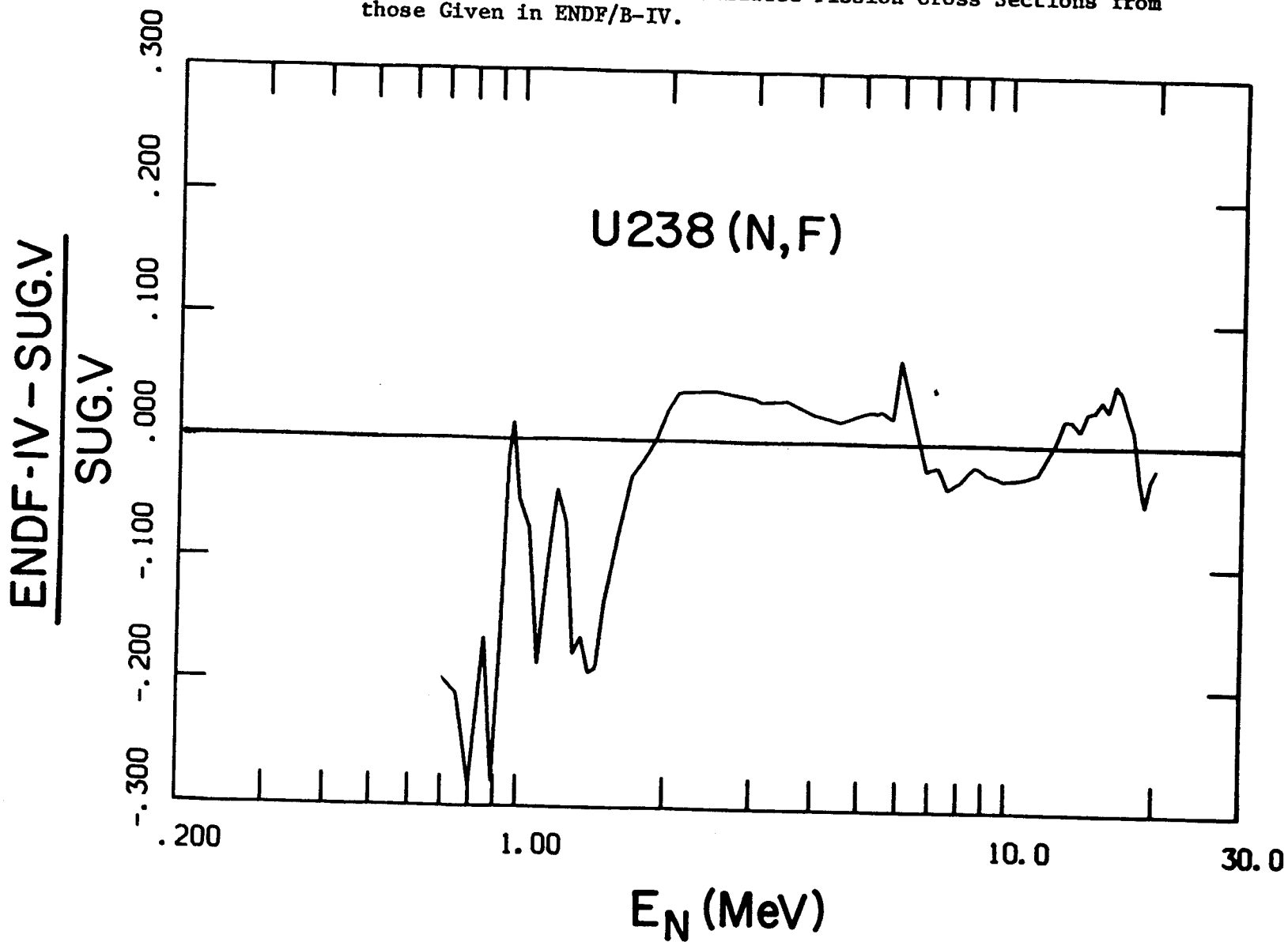


Fig. V-10. Deviation of the Present Evaluated Fission Cross Sections from those Given in ENDF/B-IV.



VI. NEUTRON RADIATIVE CAPTURE

A. General Procedures and Conclusions

The evaluation of ^{238}U (n, γ) cross sections followed the same procedure as that of ^{238}U (n,f), described above. In the first step the following quantities were evaluated:

1. ^{238}U (n, γ) absolute and/or rel. to H(n,n)
2. ^{238}U (n, γ)/ ^{10}B (n, α)
3. ^{238}U (n, γ)/ ^{235}U (n,f)
4. ^{238}U (n, γ)/ ^{197}Au (n, γ)

The ratios of steps 2-4 were multiplied by the prior evaluated standard data for ^{10}B (n, α), ^{235}U (n,f) and ^{197}Au (n, γ). For both, ^{235}U (n,f) and ^{197}Au (n, γ), an extrapolation to energies below 200 keV was required. The ^{197}Au (n, γ) values were taken from ENDF/B-IV which is not significantly different from version V at higher energies. The "estimated" ^{235}U (n,f) cross sections of Ref. VI-1 were used below 200 keV. They are representative of recent values. The ^{10}B (n, α) values were taken from Ref. VI-2. The final ^{238}U cross section was constructed from the four evaluated components. An alternate procedure of point-by-point weighted-average calculation resulted in insignificantly different results. The above cited evaluation technique was applied between 20 and 1700 keV. While the present evaluation is limited to energies above the first inelastic threshold the evaluated energy-averaged cross section was determined at lower energies in order to provide values for unresolved resonance parameters. At higher energies (e.g., >5 MeV) the evaluation takes into consideration the extensive multiple-scattering perturbations that may

distort many of the measured values. In the higher-energy (e.g., >2 MeV) region the existing data base is sparse and, consequently, the evaluation is relatively uncertain but this is not of much consequence in many applications.

Figures VI-1 and VI-2 compare the composite evaluation with the components obtained from the above four independent steps. These independent results agree, within their respective uncertainties, with the composite evaluated result. However, the uncertainties are relatively large reflecting those associated with the various measurements and the rather poor agreement of even the newer measured values. This applies to data points within individual data sets as well as between different data sets based on the same or different reference cross sections.

Figures VI-3 and VI-4 compare the present evaluation with that of ENDF/B-IV. There are differences in the important region below ≈ 1.0 MeV. They are both positive and negative and as large as 10%.

B. Data Base and Associated Remarks

1. Input data sets used for absolute $^{238}\text{U}(n;\gamma)$ values (including data rel. to $\text{H}(n;n)$) are as follows:
 - a. Pearlstein and Moxon [VI-3] -- Shape and absolute data. The substantial scatter of data points exceeds the quoted uncertainties by up to five standard-deviation.
 - b. Menlove and Poenitz [IV-4] -- Shape and absolute data. The ^7Be value was used to normalize the shape data. The U8/Au ratio measurement was used in the evaluation of that quantity.
 - c. Ryves et al. [VI-5] -- Shape and absolute data. The difference between these data and those of Set d is 10-20% in the 150-250 keV range and exceeds cumulative quoted uncertainties.

- d. Le Rigoleur [VI-6] -- Shape and absolute data. The finality of these data is uncertain.
 - e. Belanova [VI-7] -- Absolute shell transmission value. Several experiments are reported and several interpretations exist.
 - f. Miessner and Arai [VI-8] -- Absolute value. Effective absorption cross section is measured at 30 keV.
 - g. Macklin and Lyon [VI-9] -- Absolute data for Sb-Be and D₂O sources.
 - h. Staviskii et al. [VI-10] -- Absolute absorption cross section for Sb-Be source.
 - i. Fricke et al. [VI-11] -- Shape data only.
 - j. Hanna and Rose [VI-37] -- Absolute and shape data.
 - k. Panitkin and Sherman [VI-21] -- Absolute at 30 keV.
 - l. Davletchin et al. [VI-38].
2. Input data sets for the $^{238}\text{U}(n,\gamma)/^{10}\text{B}(n,\alpha)$ ratio.
- a. Fricke et al. [VI-11] -- Absolute and shape data. Data only up to 80 keV.
 - b. De Saussure et al. [VI-12] -- Absolute and shape data.
 - c. Rimawi and Chrien [VI-13] -- Absolute value with Fe-filtered beam.
 - d. Yamamura et al. [VI-14] -- Absolute value with Fe-filtered beam.
 - e. Moxon et al. [VI-15] -- There are a series of experiments. Corrected data for the later ones were quoted by Sowerby et al. (AERE-R-7273). Only the last quoted set should be considered

valid data (private communication by M. C. Sowerby, Sept. 1975). These data were measured relative to $^{10}\text{B}(n;\alpha,\gamma)$ using $^{10}\text{B}(n;\alpha)$ as a reference. The data were evaluated together with the $^{238}\text{U}(n;\gamma)/^{10}\text{B}(n;\alpha)$ ratio data.

- f. Tolstikov et al. [VI-16] -- Shape and absolute data. Original graph shows four points above 100 keV; CSISRS quotes only two.
 - g. Block et al. [VI-17] -- Shape and absolute data.
 - h. Stavisskii et al. [VI-18] -- Shape and absolute data. Several sets reported.
3. Input data for the $^{238}\text{U}(n;\gamma)/^{235}\text{U}(n;f)$ ratio.
- a. Poenitz [VI-19] -- Absolute and shape data. 30 keV value.
 - b. Lindner and Naple [VI-20] -- Absolute and shape data.
 - c. Panitkin et al. [VI-21] -- Shape only.
 - d. Weston et al. [VI-22] -- Absolute values of $^{238}\text{U}(n;\gamma)/^{235}\text{U}$ (abs.), converted with α .
 - e. Diven et al. [VI-23] -- Absolute and shape data.
 - f. Barry et al. [VI-24] -- Absolute and shape data. Data are often referred to as relative to $\text{H}(n;n)$. However, actually the measurement was in sandwich-geometry using fission chambers by White. Thus, these data were converted to ratios using White's $^{235}\text{U}(n;f)$ results and evaluated as ratio data.
 - g. Spencer and Kaeppler [VI-25] -- Shape data.
 - h. Linenberger and Miskel [VI-26] -- Shape and absolute data.
4. Input data for the $^{238}\text{U}(n;\gamma)/^{197}\text{Au}(n;\gamma)$ ratio.
- a. Poenitz [VI-27] -- Shape and absolute values.
 - b. Brzoski et al. [VI-28] -- Absolute value at 400 keV.

- c. Menlove and Poenitz [VI-29] -- Absolute value at 30 keV (see above).
 - d. Gibbons et al. [VI-30] -- Absolute values. Obtained by eliminating $\text{In}(n;\gamma)$ and $^{10}\text{B}(n;\alpha,\gamma)$ reference values.
 - e. Spencer and Kaeppler [VI-25] -- Shape data only.
 - f. Bilpuch et al. [VI-31] -- Shape data only. Obtained by eliminating $^{10}\text{B}(n;\alpha)$ and $\text{H}(n,n)$ and long counter reference values.
 - g. Berqvist [VI-32] -- Absolute and shape data. Obtained by eliminating the $\text{Ag}(n,\gamma)$ reference cross section.
5. Data considered above 2 MeV.
- a. Panitkin [VI-2].
 - b. Lindenberger and Miskel [VI-26]
 - c. Barry [VI-24].
 - d. Lindner and Nagle [VI-20].
 - e. Drake [VI-33].
 - f. Perkin [VI-34].
6. Data not utilized.
- a. Macklin [VI-35] -- Independent absolute-reference $\text{Ta}(n;\gamma)$ values are not available. The author did not consider these data to be final (private communication 1968),
 - b. Leipunski [VI-36] -- Unclear reference.

Some of the above experimental values are compared with the present evaluation in Figs. VI-5 to VI-12.

C. Uncertainties

A detailed statement of uncertainties is available from the authors. Illustrative values throughout the energy range are given in Table VI-1.

REFERENCES -- SECTION VI

- VI-1. W. Poenitz and A. Smith, Argonne National Laboratory, ANL-76-90 (1976).
- VI-2. G. Hale, Los Alamos Scientific Laboratory, private communication (1976).
- VI-3. S. Pearlstein and M. Moxon, UKUDC(E) Report, 172U, Vol. 8, p. 2 (1976) and private communication.
- VI-4. H. Menlove and W. Poenitz, Nucl. Sci Eng. 33, 24 (1968).
- VI-5. T. Ryves et al., J. Nucl. Energy 27, 519 (1973).
- VI-6. C. LeRigoleur et al., National Bureau of Standards Publication, NBS-425, p. 802 (1975).
- VI-7. T. Belanova et al., Nucl. Sci. Eng. 35, 395 (1969).
- VI-8. A. Miessner and E. Arai, Nucl. Sci. Eng. 8, 428 (1966).
- VI-9. R. Macklin and W. Lyon, Phys. Rev. 107, 504 and 114, 1619 (1959).
- VI-10. Yu. Ya. Stavisskii et al., Atom. Energy 20, 431 (1966).
- VI-11. M. Fricke et al., Proc. of Conf. on Nucl. Data for Reactors, Helsinki, IAEA Press, Vienna, Vol. 2, p. 265 (1970).
- VI-12. G. De Saussure et al., Nucl. Sci and Eng. 51, 385 (1973).
- VI-13. K. Rimawi and R. Chrien, National Bureau of Standards Publication, NBS-425 (1975).
- VI-14. N. Yamomura et al., National Bureau of Standards Publication, NBS-425, p. 0-2(1975).
- VI-15. M. Moxon et al., Atomic Energy Research Establishment Report, AERE-R-6064 (1974).
- VI-16. V. Tolstikow et al., Atom. Energy 15, 414 (1963).
- VI-17. R. Block et al., Transactions of the American Nuclear Society, Toronto Meeting (1976).
- VI-18. Yu. Ya. Stavisskii et al., Conf. On Nucl. Data for Reactors, Helsinki, IAEA Press, Vienna, Vol. 2, p. 667 (1970).
- VI-19. W. Poenitz, Nucl. Sci. Eng. 40, 383 (1970).

- VI-20. M. Lindner and R. Nagle, Lawrence Livermore Laboratory Report, UCRL-75838 (1974).
- VI-21. Yu. Panitkin and L. Sherman, INDC Report, INDC(CCP) 65/4 (1976).
- VI-22. L. Weston et al., EANDC Report, EANDC-33U (1963).
- VI-23. B. Diven et al., Phys. Rev. 120, 556 (1960).
- VI-24. J. Barry et al., J. Nucl. Energy AB18, 481 (1964).
- VI-25. R. Spencer and F. Kaeppler, National Bureau of Standards Publication, NBS-425, p. 620 (1975).
- VI-26. G. Linenberger and J. Miskel, Los Alamos Scientific Laboratory Report, LA-467 (1946).
- VI-27. W. Poenitz, Nucl. Sci. Eng. 57, 300 (1975).
- VI-28. J. Brzosko et al., Acta. Phys. Polonica B2, 489 (1971).
- VI-29. H. Menlove and W. Poenitz, Nucl. Sci. Eng. 33, 24 (1968).
- VI-30. J. Gibbons et al., Phys. Rev. 122, 182 (1961).
- VI-31. E. Bilpunch et al., Ann. Phys. 10, 455 (1960).
- VI-32. I. Bergqvist, Arkiv. Fys. 23, 425 (1962).
- VI-33. D. Drake et al., Phys. Lett. 36B, 557 (1971).
- VI-34. J. Perkin et al., Proc. Phys. Soc. 72, 505 (1958).
- VI-35. R. Macklin, Oak Ridge National Laboratory, private communication (1969).
- VI-36. A. Leipunski et al., Second Conf. on Atoms for Peace, Geneva, Vol. 15, p. 50 (1958).
- VI-37. R. Hanna and B. Rose, J. Nucl. Energy 8, 197 (1959).
- VI-38. A. Davletchin et al., Conf. on Neutron Physics, Kiev (1975).

TABLE VI-1. Illustrative Evaluated (n; γ) Cross Sections of U-238

E(MeV)	σ (b)	$\Delta\sigma$ (b)
.2000E-01	.4954E-00	.4246E-01
.3000E-01	.4526E-00	.1287E-01
.4000E-01	.3993E-00	.1261E-01
.6000E-01	.2989E-00	.1252E-01
.8000E-01	.2264E-00	.1072E-01
.1000E-00	.1977E-00	.1021E-01
.2000E-00	.1288E-00	.3180E-02
.4000E-00	.1068E-00	.3199E-02
.6000E-00	.1147E-00	.3100E-02
.8000E-00	.1221E-00	.4905E-02
.1000E+01	.1215E-00	.6558E-02

Fig. VI-1. The Present Evaluated (n; γ) cross sections (solid line) Compared with the Components Based Upon $^{238}\text{U}(n;\gamma)/^{235}\text{U}(n,f)$ and $^{238}\text{U}(n;\gamma)/^{10}\text{B}(n;\alpha)$ Ratio Values.

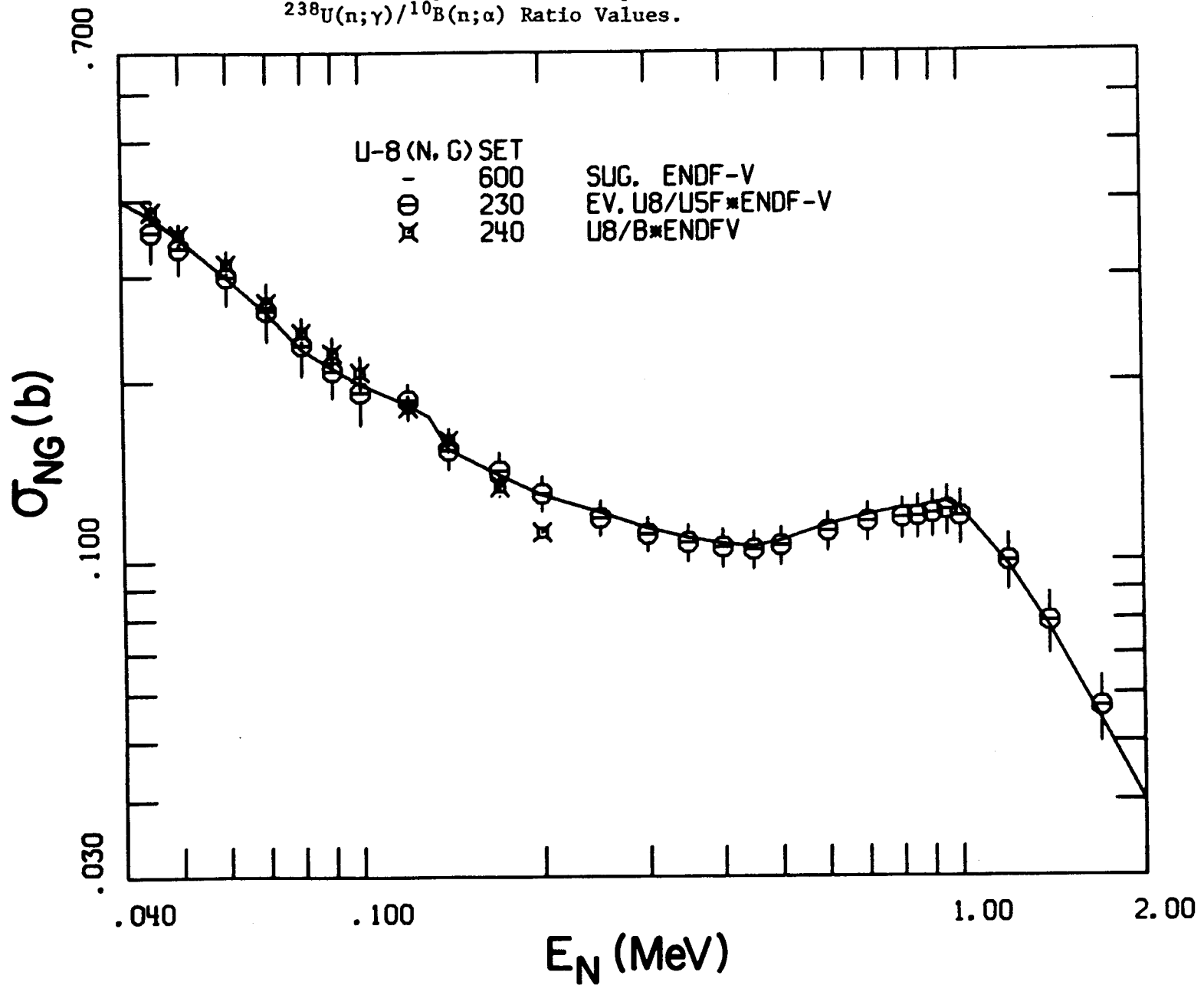


Fig VI-2. The Present (n; γ) Evaluation Compared with the Components Based Upon Absolute Measurements and Measurements of the $^{238}\text{U}(n;\gamma)/^{197}\text{Au}(n;\gamma)$ Ratio.

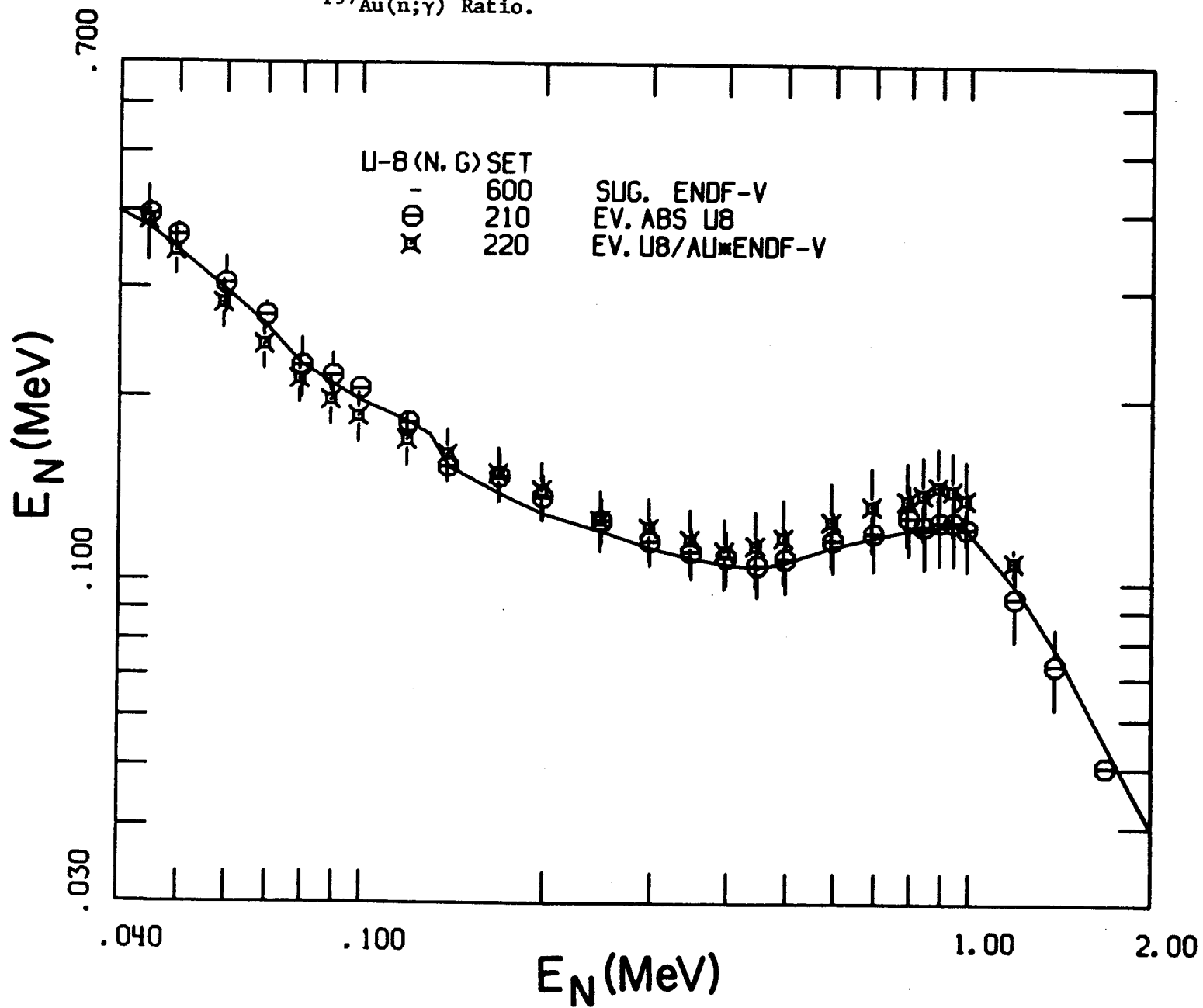


Fig. VI-3. Comparison of the Present $^{238}\text{U}(n,\gamma)$ Evaluation (solid curve) with that of ENDF/B-IV (data points).

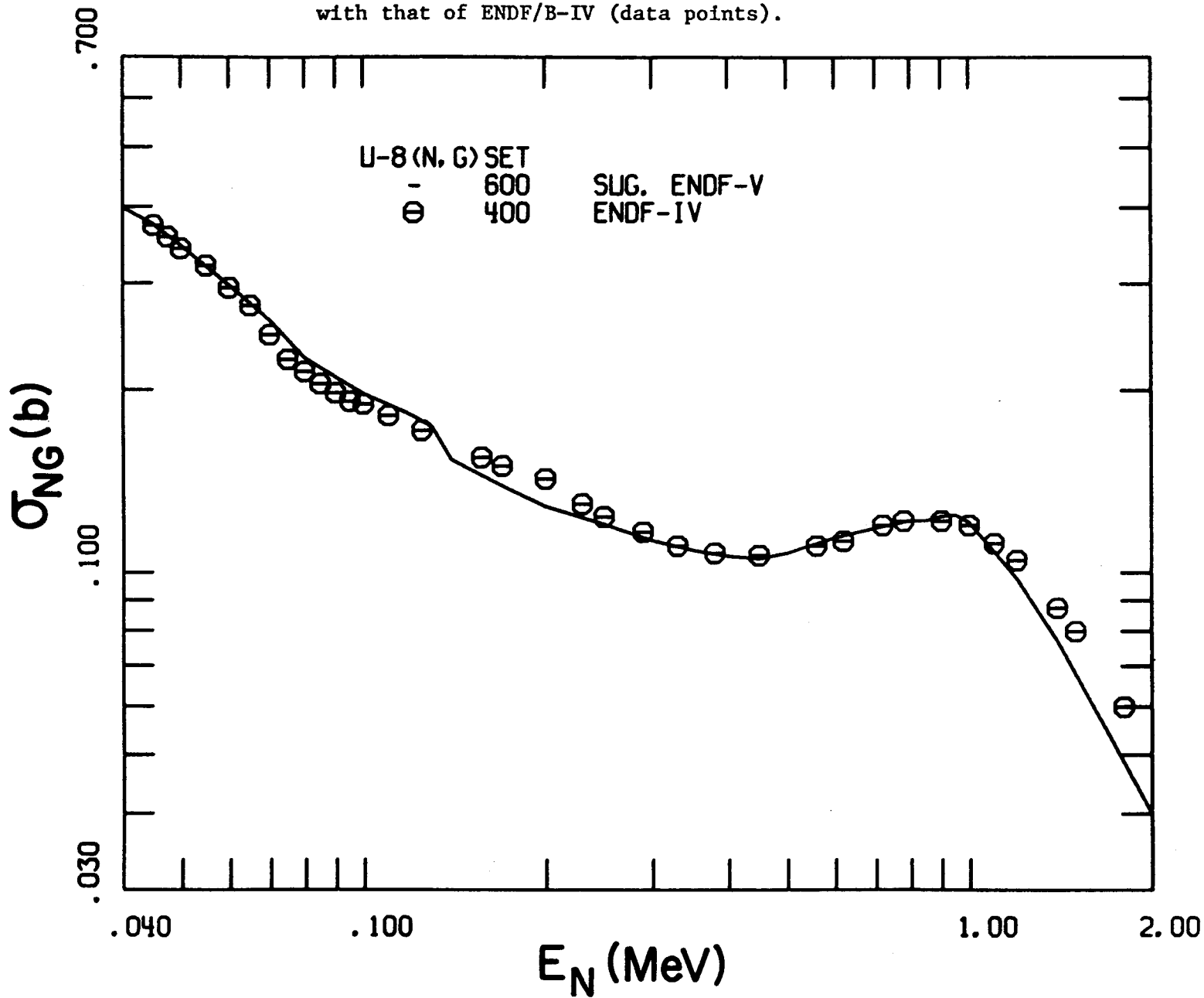


Fig. VI-4. Fractional-Energy-Dependent Difference of the ENDF/B-IV $^{238}\text{U}(n;\gamma)$ Evaluation from the Present Evaluation (i.e., (IV-Present/Present)).

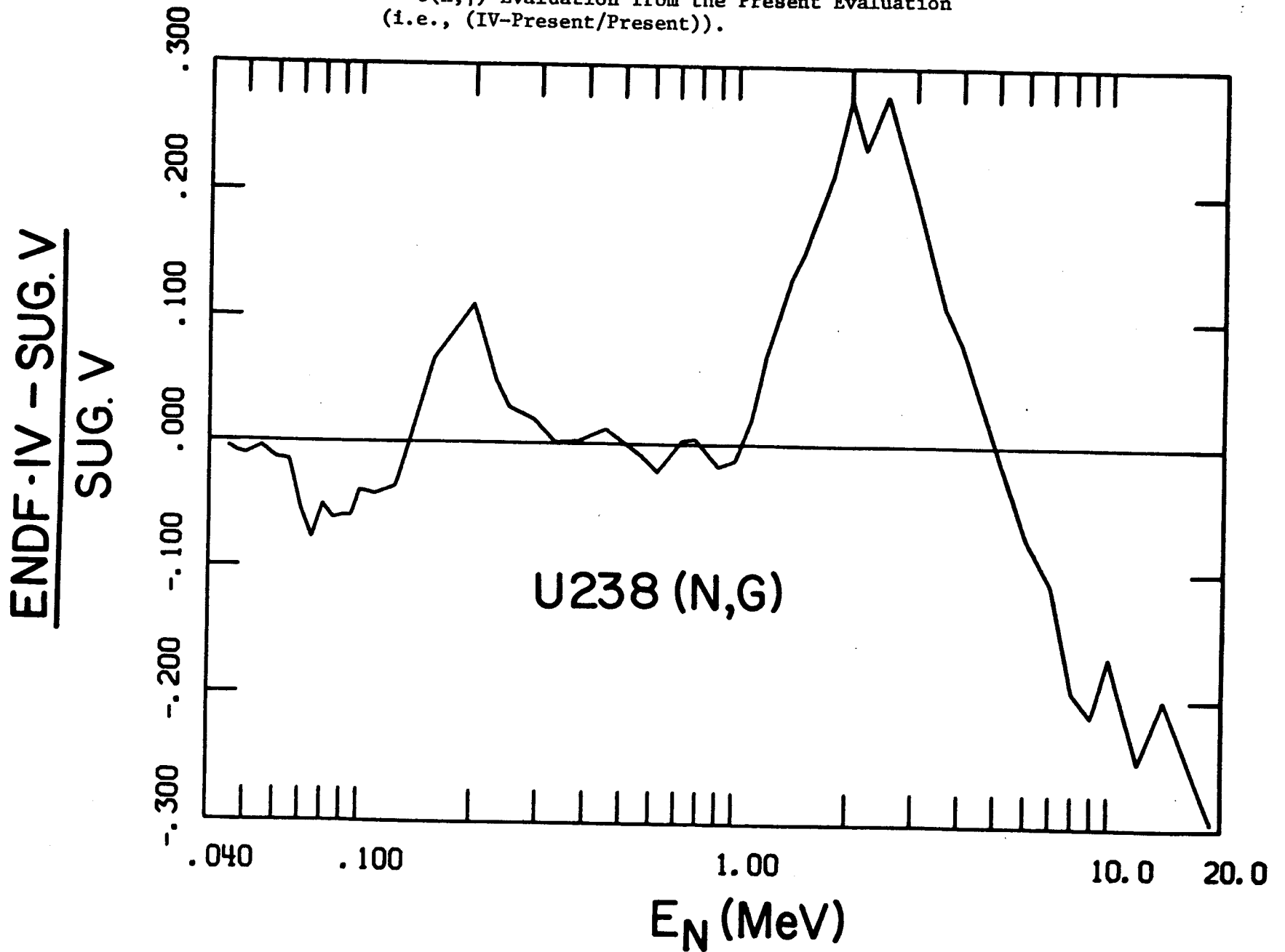


Fig. VI-5. Comparisons of the Present Evaluated $^{238}\text{U}(n,\gamma)$ Cross Sections (solid line) with Measured Values (data points). The measured values are outlined in the text and taken from Refs. VI-3 to VI-36.

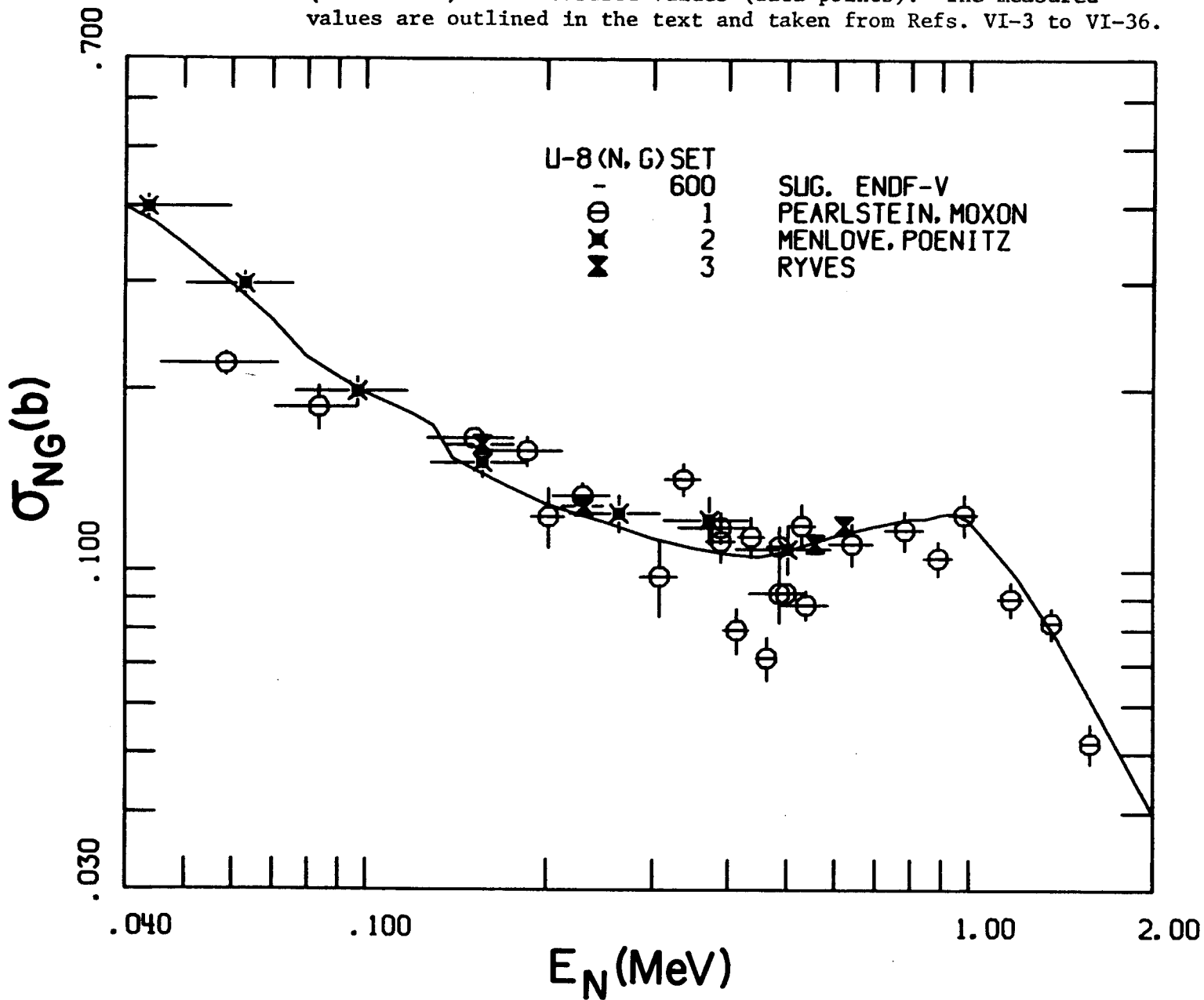


Fig. VI-6. Comparisons of the Present Evaluated $^{238}\text{U}(n,\gamma)$ Cross Sections (solid line) with Measured Values (data points). The measured values are outlined in the text and taken from Refs. VI-3 to VI-36.

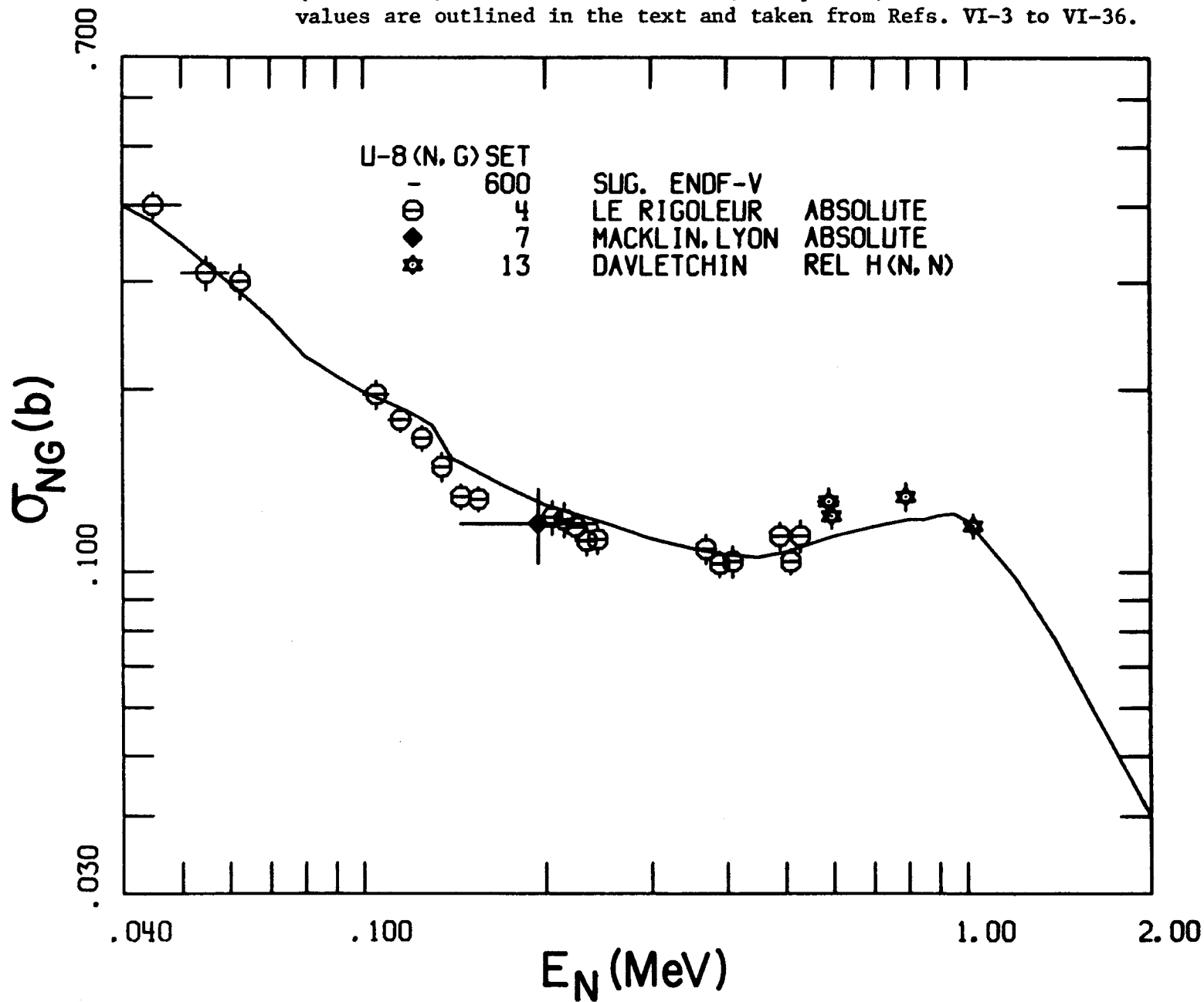


Fig. VI-7. Comparisons of the Present Evaluated $^{238}\text{U}(n,\gamma)$ Cross Sections (solid line) with Measured Values (data points). The measured values are outlined in the text and taken from Refs. VI-3 to VI-36.

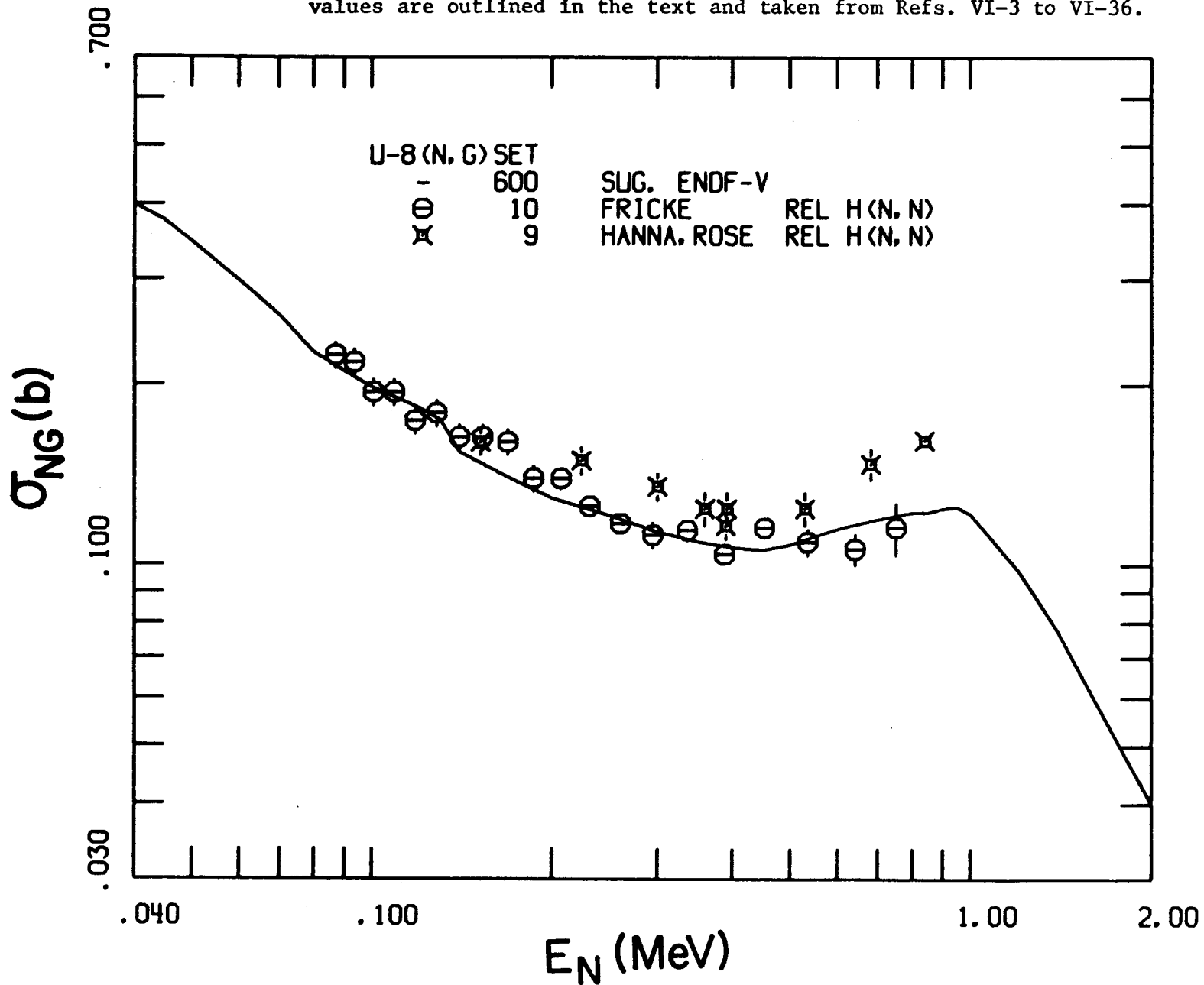


Fig. VI-8. Comparisons of the Present Evaluated $^{238}\text{U}(n,\gamma)$ Cross Sections (solid line) with Measured Values (data points). The measured values are outlined in the text and taken from Refs. VI-3 to VI-36.

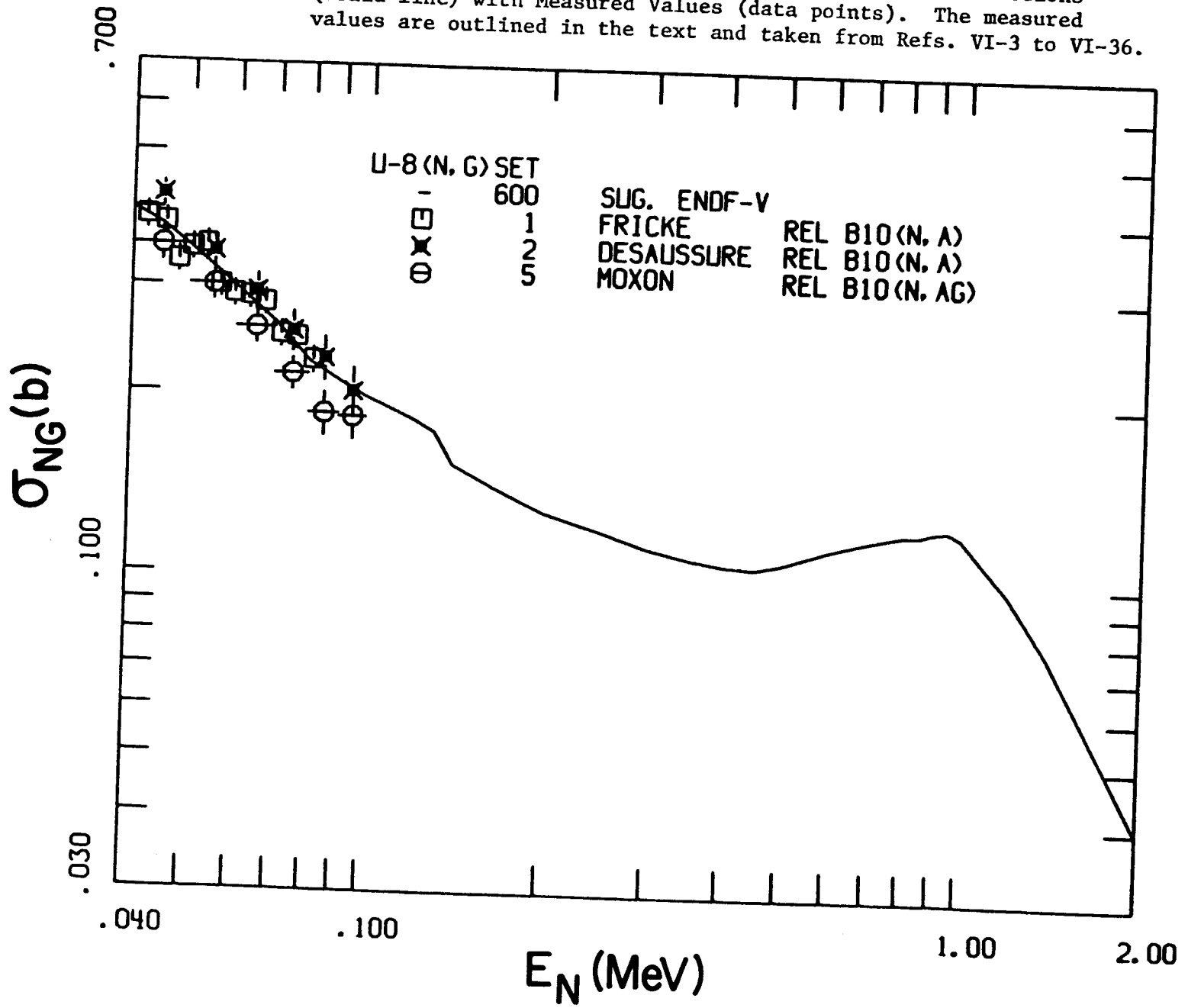


Fig. VI-9. Comparisons of the Present Evaluated $^{238}\text{U}(n,\gamma)$ Cross Sections (solid line) with Measured Values (data points). The measured values are outlined in the text and taken from Refs. VI-3 to VI-36.

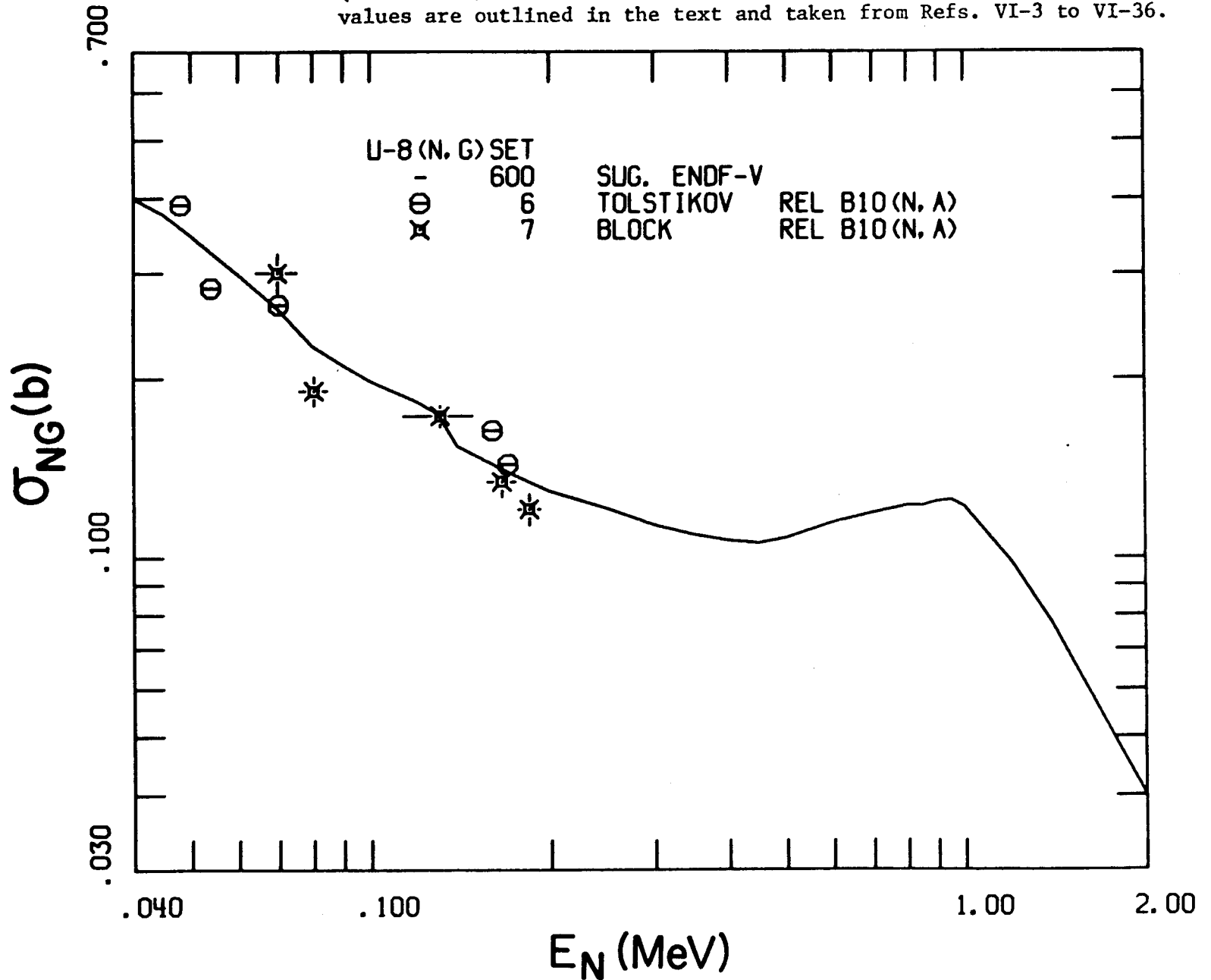


Fig. VI-10..Comparisons of the Present Evaluated $^{238}\text{U}(n,\gamma)$ Cross Sections (solid line) with Measured Values (data points). The measured values are outlined in the text and taken from Refs. VI-3 to VI-36.

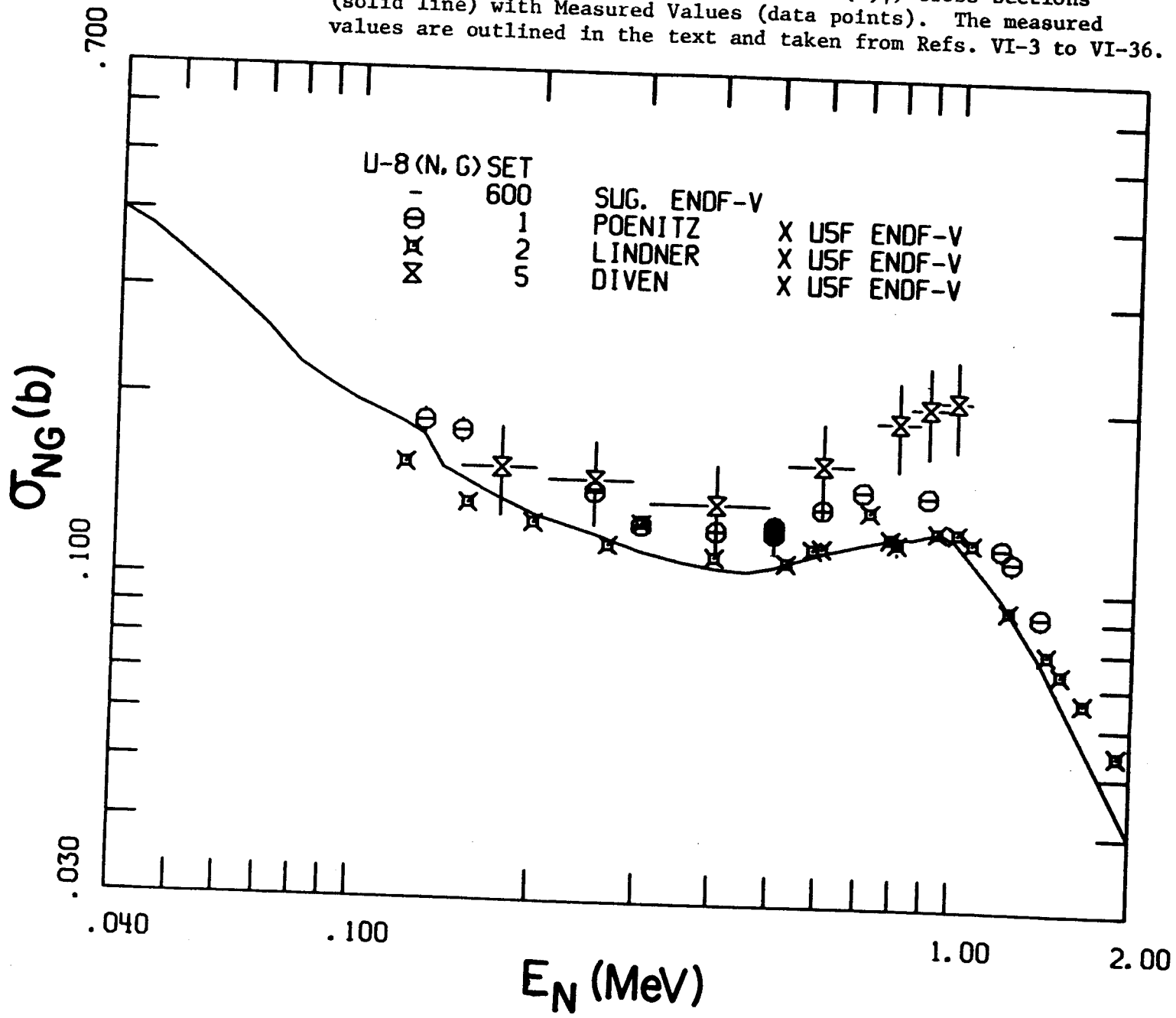


Fig. VI-11. Comparisons of the Present Evaluated $^{238}\text{U}(n,\gamma)$ Cross Sections (solid line) with Measured Values (data points). The measured values are outlined in the text and taken from Refs. VI-3 to VI-36.

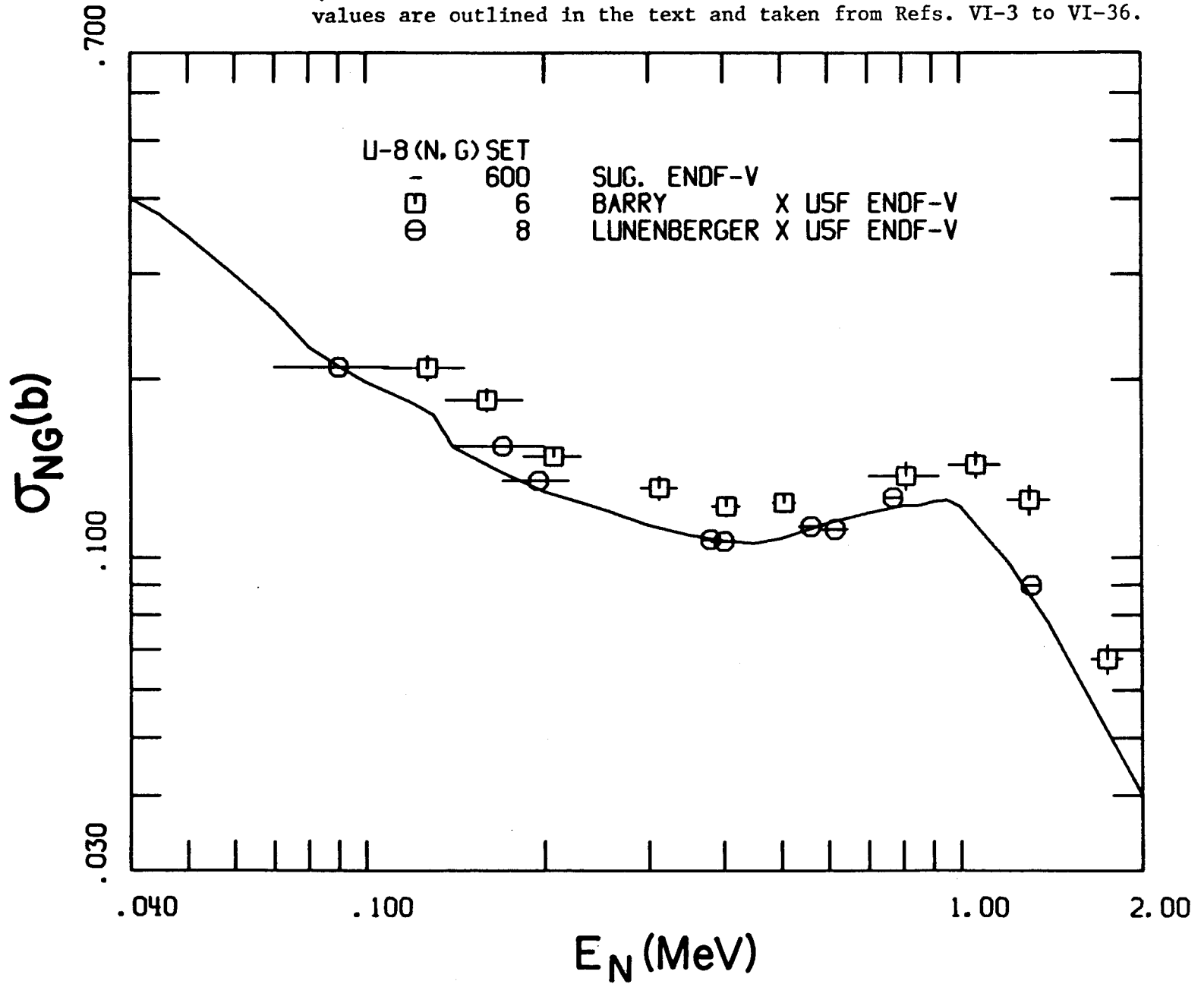
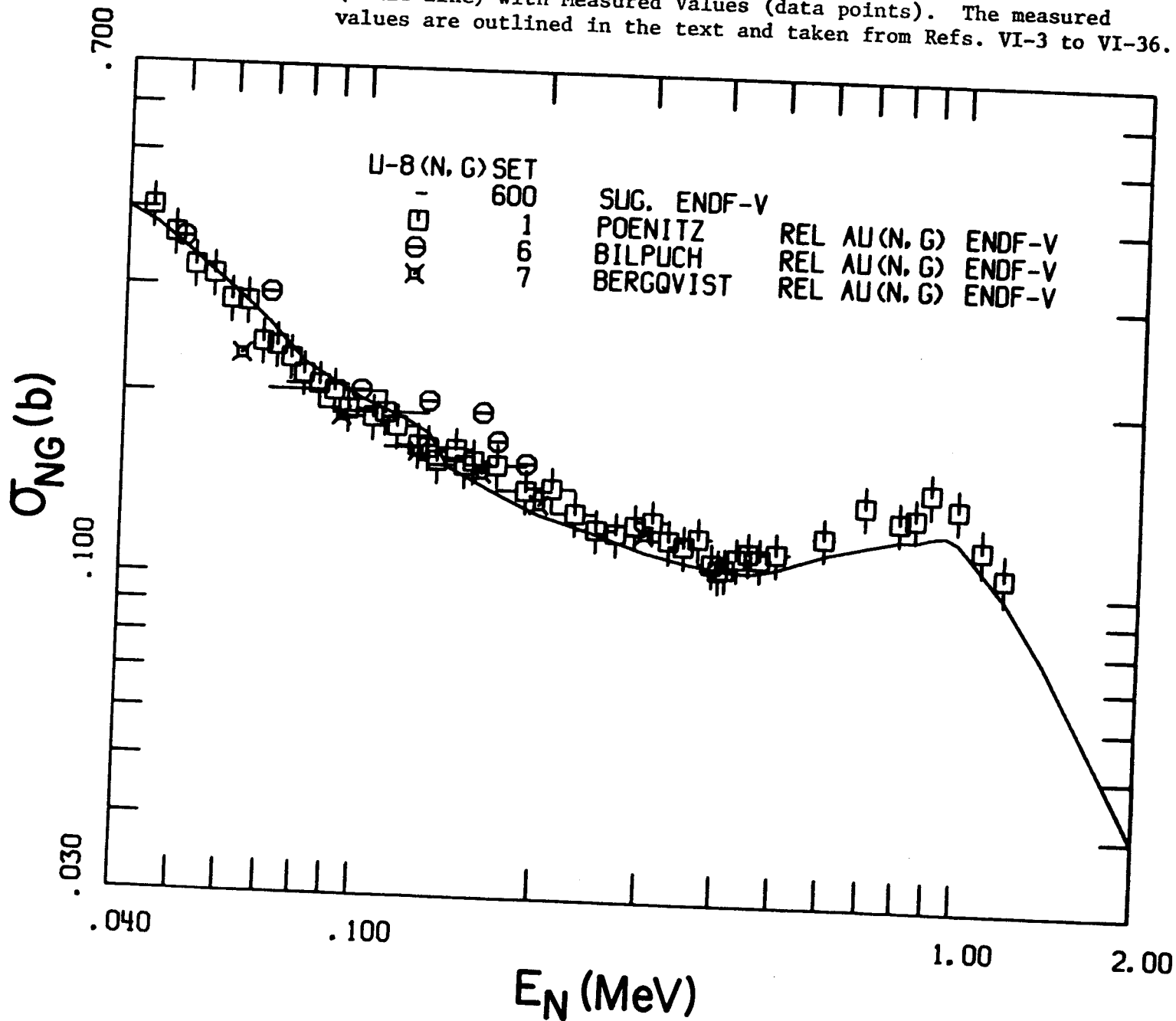


Fig. VI-12. Comparisons of the Present Evaluated $^{238}\text{U}(n,\gamma)$ Cross Sections (solid line) with Measured Values (data points). The measured values are outlined in the text and taken from Refs. VI-3 to VI-36.



VII. (n;2n') AND (n;3n') PROCESSES (Q = -6.044 AND -11.269 MeV, RESPECTIVELY)

The (n;2n') evaluated cross sections were constructed from the data base of Refs. VII-1 to VII-12. The data is not always reported in detail but, where possible, the measured values were referenced to the cross sections of this file (e.g., where relevant to ^{238}U fission) and of the ENDF/B-V reference-standard file. These renormalizations changed some of the experimental values by significant amounts, usually downward. The evaluation is compared with the data base and that of ENDF/B-IV in Fig. VII-1. The present evaluation is lower than that of ENDF/B-IV in magnitude over wide energy intervals by approximately 10%. There also is a difference at higher energies, e.g., above approximately 16 MeV. The high-energy portion of the present evaluation is supported by the recent preliminary results of Ackermann et al. [VII-12]. The uncertainties in the present evaluation are estimated to be less than 10% in regions of relatively large cross section as illustrated in Fig. VII-1. The associated neutron emission spectra were constructed from the statistical interpretation of Segev et al., [VII-13] with the addition of a "harder" spectral component representing pre-statistical-equilibrium processes. The angular distributions were assumed to be isotropic.

The (n;3n') evaluation followed procedures essentially identical to those employed in the (n;2n') evaluation, above. However, the data base (VII-2, VII-4, VII-10, VII-14 and VII-15) was far less definitive, as illustrated in Fig. VII-2, and thus the evaluation is more uncertain. The present evaluation is a little lower than that of ENDF/B-IV, but the difference may not be significant in view of the uncertainties involved in the evaluation. Again, the method of Segev et al., [VII-13] was used to generate the emitted-neutron spectra and the neutron emission was assumed to be isotropic.

REFERENCES -- SECTION VII

- VII-1. J. Phillips, Atomic Energy Research Establishment Report, AERE-NP/R-2033 (1956).
- VII-2. D. Mather and L. Pain, Atomic Weapons Research Establishment Report, AWRE-O-47/69 (1969).
- VII-3. G. Antronov et al., Atom. Energy 5, 456 (1958).
- VII-4. D. Mather et al., Atomic Weapons Research Establishment Report, AWRE-O-72/72 (1972).
- VII-5. Graves et al., as quoted in Ref. VII-8.
- VII-6. R. Batchelor and J. Towle, Nucl. Phys. 65, 236 (1965).
- VII-7. J. Landrum et al., Phys. Rev. 68, 1938 (1973).
- VII-8. J. Knight et al., Phys. Rev. 112, 359 (1958).
- VII-9. J. Perkin and R. Coleman, J. Nucl. Energy 14, 69 (1961).
- VII-10. J. Frehaut, National Bureau of Standards Publication, NBS-425 (1975).
- VII-11. A. Daroczy et al., Proc. of Kiev Conf. (1971).
- VII-12. A. Ackermann et al., NEANDC Report, NEANDC(E)-161U (1974).
- VII-13. M. Segev et al., private communication (1976) see also; Trans. Am. Nucl. Soc. 22, 679 (1975).
- VII-14. K. Allen et al., J. Nucl. Energy 14, 100 (1961).
- VII-15. P. White, J. Nucl. Energy 16, 261 (1962).

Fig. VII-1. Comparison of Measured and Evaluated $^{238}\text{U}(n;2n')$ Cross Sections. Measured values are indicated by data points as cited in the text. Solid curves indicate the present evaluation and ± 10 percent variations. Dashed curve is from ENDF/B-IV.

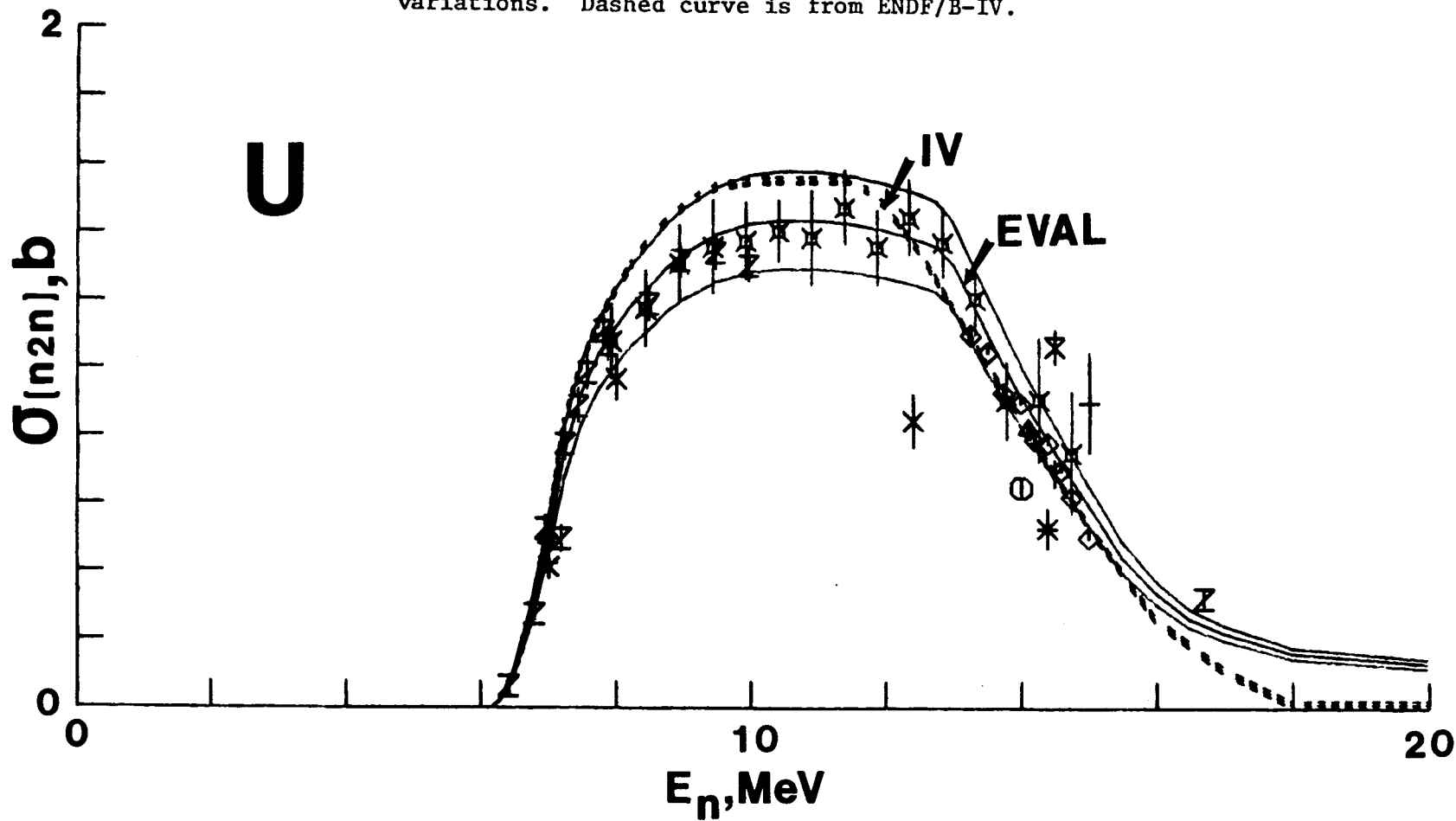
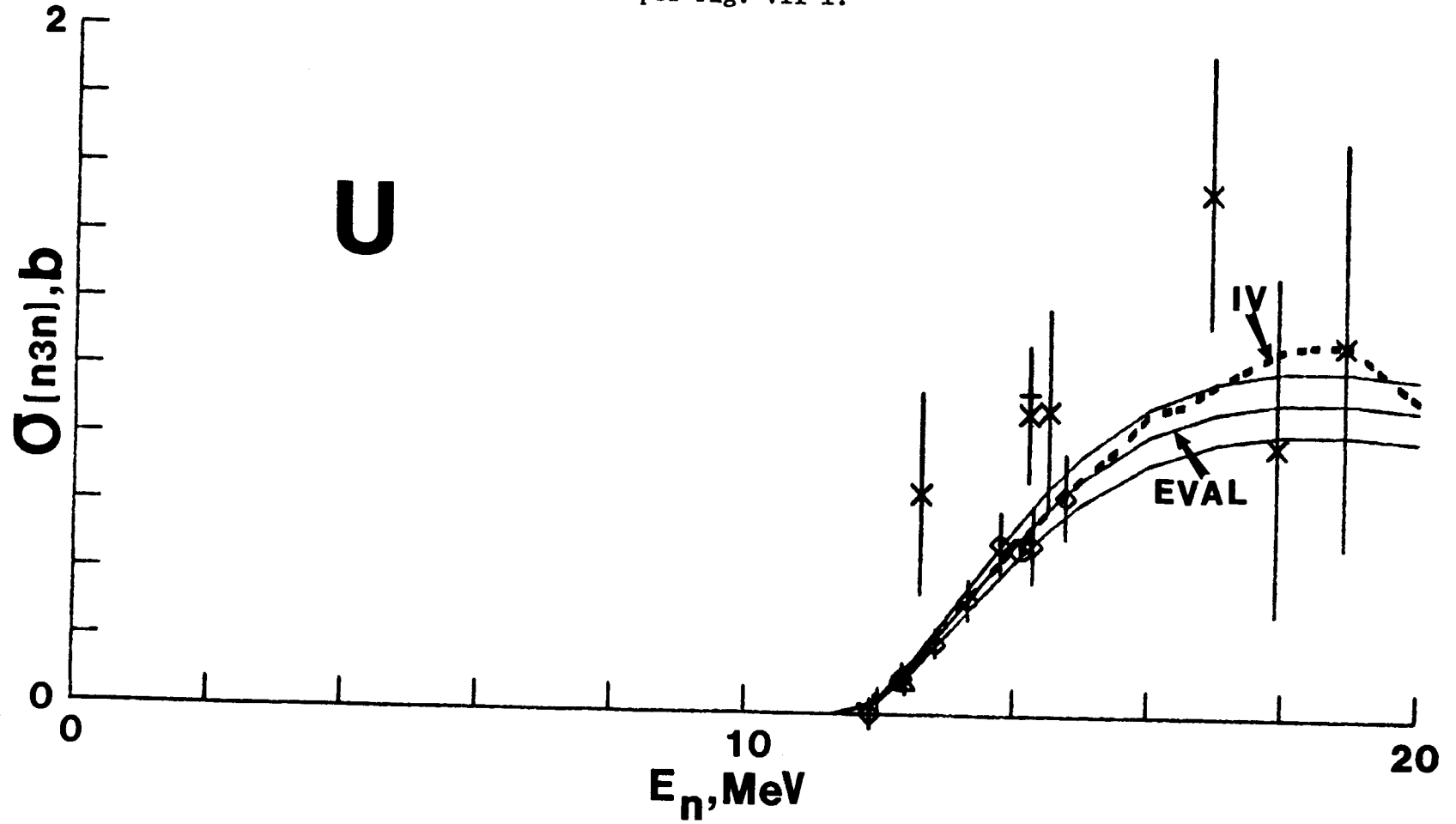


Fig. VII-2. Comparison of Measured and Evaluated $^{238}\text{U}(n;3n')$ Cross Sections. Notation is as per Fig. VII-1.



VIII. PHOTON PRODUCTION PROCESSES

A. General Procedures

Photon production cross sections and spectra are presented in two incident-neutron-energy ranges with the division at 0.05 MeV.

B. Photon Production for $E_n < 0.05$ MeV

For the lower range, the photon production is presented as multiplicities and spectra for the capture and fission reactions.

While no subthreshold fission cross section is presented in this evaluation, the data for photon production from the fission process in the low energy range are included in anticipation of a nonzero subthreshold fission cross section being added. The photon multiplicity that should be applied to the fission cross section was obtained by assuming 6.2 MeV of photon energy from fission and dividing this value by the average measured photon energy from the fission of ^{235}U as reported in Ref. VIII-1.

The capture gamma-ray spectrum for ^{238}U has been accurately measured only at thermal neutron energies [VIII-2]. Some measurements have also been made in the low eV and low keV region [VIII-3]. The latter measurements, however, were made only at resonance re-energies, and have several obvious difficulties: (1) they disagree in spectral shape and in normalization with the very accurate thermal measurement of Ref. VIII-2; (2) they extend only down to 1 MeV photon energy and their integrated spectral intensities suggest that the intensity for photon energies less than 1 MeV is very small; (3) even with the lower photon energy cutoff at 1 MeV, some of the spectra violate energy conservation by as much as 30%. For the above reasons, the data of Ref. VIII-3 were not used.

C. Photon Production for $E_n \geq 0.05$ MeV

Measurements of photon production from 1.09 to 14.8 MeV are reported in Ref. VIII-4. Lind and Day measured cross sections for production of nine specific photons for incident neutron energies from 0.6 to 1.7 MeV [VIII-5]. In this evaluation the measured data were used for checking calculated values obtained by using the R-Parameter formalism of Perkins, Haight and Howerton reported in Ref. VIII-6. The calculated values were in reasonable agreement with experiment and were used because the method of calculation insures conservation of energy on the average. This is an important point when using the evaluated data file for linked neutronic-photonic calculations.

REFERENCES -- SECTION VIII

- VIII-1. R. W. Peele and F. C. Maienschein, Phys. Rev. C3, 373 (1971).
- VIII-2. E. T. Journey, private communication (1971).
- VIII-3. J. John and V. J. Orphan, Gamma-Rays from Resonant Capture of Neutrons in ^{238}U , Gulf Radiation Technology Report, GA-10186 (1970).
- VIII-4. P. S. Buchanan, Texas Nuclear Corp. Report, ORO-2791-32 (1971).
- VIII-5. D. A. Lind and R. B. Day, Ann. Phys. 12, 485 (1961).
- VIII-6. S. T. Perkins, R. C. Haight and R. J. Howerton, Nucl. Sci. Eng. 57, 1 (1975).

IX. SOME INTEGRAL TESTS

Some initial tests employed integrals of the microscopic inelastic scattering file. The average energy loss per inelastic-scattering event was calculated as a function of incident energy. Results obtained with the present evaluation were generally lower than those obtained with ENDF/B-IV; by large amounts in the few MeV incident-energy range (e.g., 40% at 5 MeV). This was due to changes in the discrete inelastic neutron excitation cross sections and the large reduction in the continuum component. The latter is particularly sensitive as that type of process results in large energy transfers. The product $\overline{\sigma E}$ due to inelastic scattering was calculated as a function of energy using the present evaluation and that of ENDF/B-IV. Below 1.5 MeV the two results were similar. At higher energies there were differences both positive and negative, particularly above about 4.0 MeV. The implication of these differences will depend upon the application. For an example, the quantity:

$$\overline{\sigma} \equiv \frac{\int_0^{\infty} E_{\text{loss}} * \sigma_{\text{inel}} * \text{FLUX}(E) * dE}{\int_0^{\infty} \text{FLUX}(E) * dE}$$

was calculated over a representative GCFR spectrum (i.e., FLUX) using the present evaluation and ENDF/B-IV. The comparative results were:

$$\overline{\sigma} \text{ (present evaluation) } = 2.682, \text{ b}$$

$$\overline{\sigma} \text{ (ENDF/B-IV) } = 2.801, \text{ b}$$

Thus the present evaluation implies a harder spectrum than obtained using ENDF/B-IV in this illustrative fast-reactor type despite the overall larger inelastic-scattering cross sections of the present evaluation.

Macroscopic tests of the higher energy portion of the file employed critical spheres of ^{233}U , ^{235}U and ^{239}Pu with ^{238}U tampers of varying thicknesses up to about 20 cm [IX-1]. k_{eff} was calculated using 175 group cross sections and the TARTNP Monte Carlo code [IX-2]. The ^{238}U cross sections were those of the present evaluation extended to lower energies (below 45 keV) using ENDF/B-IV. These spheres are characterized by relatively hard spectra and not sensitive to this low energy extrapolation. Other cross sections requisite to the calculations (e.g., those of ^{233}U , ^{235}U and ^{239}Pu) were taken from the ENDL library [IX-3]. The resulting calculated k_{eff} values are summarized in Table IX-1 and compared with similar values obtained with the ENDL file alone (including ENDL ^{238}U). Generally, the present evaluation leads to results marginally better than those obtained with the ENDL library alone but the "improvement" is within the uncertainty of the calculations. Both files overpredict average k_{eff} by 0.2-0.46% and both values are within the estimated systematic uncertainties of the calculational model. These results suggest that the present evaluation is as suitable for the criticality calculation of clean-spherical criticals with ^{238}U blankets as those now in common use and imply that the higher-energy portions of the present evaluation are realistic.

The suitability of the evaluation for Controlled Thermonuclear Reactor design was examined by comparing measured and calculated neutron spectra emitted from varying thicknesses of ^{238}U spherical shells pulsed with 13.2 to 14.8 MeV neutron sources at their centers. The preliminary version of the file was initially used with no precompound processes in either (n;n') or (n;2n') reactions. As a consequence, the calculated emergent spectra was not

in particularly good agreement with that observed experimentally. The precompound process was then introduced into the file in an iterative manner so as to improve the agreement between measured and calculated emergent spectra. As finally adjusted, the file was reasonably successful in describing the measured emission spectra and the precompound components of $(n;n')$ and $(n;2n')$ processes were essentially those of the ENDL library [IX-3]. For example, emergent spectra were calculated for two spheres, one with a thickness of ~ 0.7 mfp (3.63 cm) and the other with a thickness of ~ 2.8 mfp (10.91 cm). Comparisons of measured and calculated results at two angles (relative to the incident deuteron beam) for each sphere are shown in Figs. IX-1, IX-2, IX-3 and IX-4. Table IX-2 presents comparisons of calculated and experimental integrals for each of the four cases shown in Figs. IX-1 through IX-4. The three integrals given for each case are the elastic peak (which includes any transmitted neutrons); the energy region from the elastic peak to 2 MeV; and the total energy range from the incident neutron energy to 2 MeV.

A draft of the present evaluation was combined with the lower-energy- and fission-process portions of the proposed ENDF/B-V file as constructed by Pennington et al., [XI-4] to form a complete draft file. Pennington [IX-4] then used this draft to calculate the criticality of ZPR-6-7 assemblies. The group cross sections were obtained using MC²-2 [IX-5]. k_{eff} was calculated with the present draft and with ENDF/B-IV. All other necessary cross section were taken from ENDF/B-IV. The initial results indicated that the calculated k_{eff} obtained with the draft was slightly smaller than given by ENDF/B-IV and the latter is already smaller than measured values. The

transfer matrix was examined in the context of estimated uncertainties in the microscopic inelastic scattering cross sections and adjustments of the microscopic values made in a manner that would improve the macroscopic result while, at the same time, being consistent with uncertainties in the microscopic inelastic-scattering cross sections and the non-elastic cross section. The latter is a very stringent restriction and the adjustments nowhere resulted in changes in the non-elastic cross section of more than 6% and generally much less. The adjustment tolerance in the inelastic scattering cross sections at low energies (e.g., below 1.0 MeV) were not large and primarily in the various threshold regions where there are no direct microscopic measurements, (e.g., below 150 keV for the 45 keV state). Above about 1.5 MeV knowledge of the microscopic inelastic scattering cross sections is uncertain and adjustments of 10% can be tolerated providing a general consistency with the non-elastic cross section is maintained. Other high energy reactions of the present evaluation were not adjusted. The calculations were then repeated with the adjusted file with the results summarized in Table IX-3 through four developmental versions. The present file leads to k_{eff} values very similar to those obtained with ENDF/B-IV. Further significant adjustments of the microscopic inelastic scattering cross sections probably would be difficult to accept in the context of measured cross section values. Furthermore, the calculations to this point had to employ the ENDF/B-IV data file for all cross sections other than those of ^{238}U and portions of these other cross-section files are known to be in error in ways that will increase the calculated k_{eff} (e.g., total cross section of iron). Thus further adjustments based upon such a distorted data base may even be

deceptive. There are, of course, other macroscopic parameters that are sensitive to the data, e.g., central worths. These have not been examined in the context of the present evaluation. Such more comprehensive tests should await the availability of the complete draft ENDF/B-V system.

It is interesting to compare the broad-group cross sections applicable to ZPR-6-7 as obtained with this evaluation with those of ENDF/B-IV as shown in Tables IX-3 and IX-4. The present inelastic cross sections are much larger but the energy transfer can be less. The present radiative capture cross sections are marginally smaller than those of ENDF/B-IV over much of the energy range. The fission cross sections are similar.

REFERENCES -- SECTION IX

- IX-1. V. Hampel, private communication (1970). To be published in a compendium by B. Koponen, Lawrence Livermore Laboratory (1978).
- IX-2. E. F. Plechaty and J. R. Kimlinger, TARTNP: A Coupled Neutron-Photon Monte Carlo Transport Code, Lawrence Livermore Laboratory Report, UCRL-50400, Vol. 14 (1976).
- IX-3. R. J. Howerton et al., The LLL Evaluated Nuclear Data Library (ENDL): Evaluation Techniques, Reaction Index, and Descriptions of Individual Evaluations, Lawrence Livermore Laboratory Report, UCRL-50400, Vol. 15, Part A (1975), Part B (1976), Part C (1976), Part D in press (1977), Part E to be published (1978).
- IX-4. E. Pennington, W. Poenitz and A. Smith, Trans. Am. Nucl. Soc. 26, 591 (1977).
- IX-5. H. Henryson II et al., Argonne National Laboratory Report, ANL-8144 (1976).
- IX-6. C. Wong et al., Livermore Pulsed Sphere Program: Program Summary through July 1971, Lawrence Livermore Laboratory Report, UCRL-51144, Rev. 1 (1972).

TABLE IX-1. Spherical Crits; U Reflected

Core	Reflector Thickness (cm)	k_{eff} -ANL	k_{eff} -ENDL
U-233	2.30	0.998 ± .003	0.998 ± .003
U-233	5.31	1.007 ± .003	1.005 ± .003
U-233	19.91	0.997 ± .003	1.002 ± .003
U-235	1.76	1.005 ± .003	1.004 ± .003
U-235	4.47	1.008 ± .003	1.009 ± .003
U-235	9.96	1.008 ± .003	1.004 ± .003
U-235	18.01	0.996 ± .003	1.005 ± .003
Pu-239	1.93	0.995 ± .003	1.003 ± .003
Pu-239	4.13	1.004 ± .003	1.008 ± .003
Pu-239	6.74	0.997 ± .003	1.007 ± .003
Pu-239	19.60	1.009 ± .003	1.006 ± .003
		Ave. = 1.0022	1.0046

^a"ANL" denotes results obtained with draft ANL U-238 file and all other cross sections from ENDL. "ENDL" results obtained with the ENDL file alone.

^bQuoted uncertainties are statistical. Beyond this there may be systematic uncertainties associated with the calculational model of ≤ 0.007 .

^cAll calculations by R. Howerton (LLL) using the 175 group TART Monte Carlo code.

TABLE IX-2. Comparisons of Experimental and Calculated Integrals

Angle	<u>Elastic Peak</u>			<u>11.8 MeV to 2 MeV</u>			<u>Incident Energy to 2 MeV</u>		
	Calc	Exp	C/E	Calc	Exp	C/E	Calc	Exp	C/E
<u>0.7 mfp Sphere</u>									
30°	.648	.649	.998	.272	.311	.875	.920	.960	.958
120°	.722	.704	1.026	.313	.336	.932	1.035	1.040	.995
<u>2.8 mfp Sphere</u>									
30°	.229	.235	.974	.342	.342	1.000	.571	.577	.990
120°	.254	.273	.930	.389	.403	.965	.643	.676	.951

TABLE IX-3. k_{eff} of ZPR-6-7 and ZPR-6-6A as Calculated with Various Versions and Files of ^{238}U Evaluated Data^a

Version-File	k_{eff}	
	ZPR-6-7	ZPR-6-6A
ENDF/B-IV	0.96713	0.97891
ENDF/B-V, Version 1	0.96303	0.97745
ENDF/B-V, Version 2 Adjusted $\sigma_{inel.}$	0.96782	-
ENDF/B-V, Version 3 Adjusted $\sigma_{inel.}$ Plus Other Changes, Primarily Prompt and Delayed Nu-bar	0.96696	0.97851
ENDF/B-V, Version 4 Modifications of Version 3 Extended to Include ENDF/B-V Unresolved Resonance Parameters	0.96694	0.97832

^aThese results should be corrected by +0.0184(6-7) and +0.0086(6-6A) to account for heterogeneity and transport effects as set forth by CSEWG benchmark procedures.

TABLE IX-4. Comparison of ENDF/B-V and ENDF/B-IV ^{238}U Cross Sections for ZPR-6-7

Group ^a	ENDF/B-V				ENDF/B-IV			
	σ_{inel} (barn)	$\bar{E}_{f,\text{inel}}$ ^b (MeV)	$\sigma_{n\gamma}$ (barn)	σ_{nF} (barn)	σ_{inel} (barn)	$\bar{E}_{f,\text{inel}}$ ^b (MeV)	$\sigma_{n\gamma}$ (barn)	σ_{nF} (barn)
1	2.005	3.903	0.0047	0.9013	1.515	1.226	0.0041	0.8928
2	3.088	2.181	0.0103	0.5553	2.498	1.151	0.0106	0.5673
3	3.140	1.423	0.0239	0.5311	2.499	1.203	0.0292	0.5497
4	3.045	0.930	0.0564	0.4109	2.549	0.770	0.0666	0.3948
5	2.384	0.700	0.1110	0.0293	2.281	0.662	0.1128	0.0261
6	1.818	0.573	0.1153	0.0014	1.828	0.564	0.1146	0.0012
7	1.561	0.340	0.1087	0.0002	1.435	0.338	0.1095	0.0001
8	1.295	0.201	0.1229		1.105	0.198	0.1297	0.0001
9	0.976	0.110	0.1587		0.795	0.109	0.1623	
10	0.442	0.0460	0.2215		0.370	0.0453	0.2094	
11	0.0598	0.0160	0.3306		0.0803	0.0155	0.3274	
Avg.	1.005	0.621			0.889	0.520		

^aAll groups have half-lethargy widths starting at 10 MeV.

^bThe final energy is computed using the midpoint energies of the sink groups.

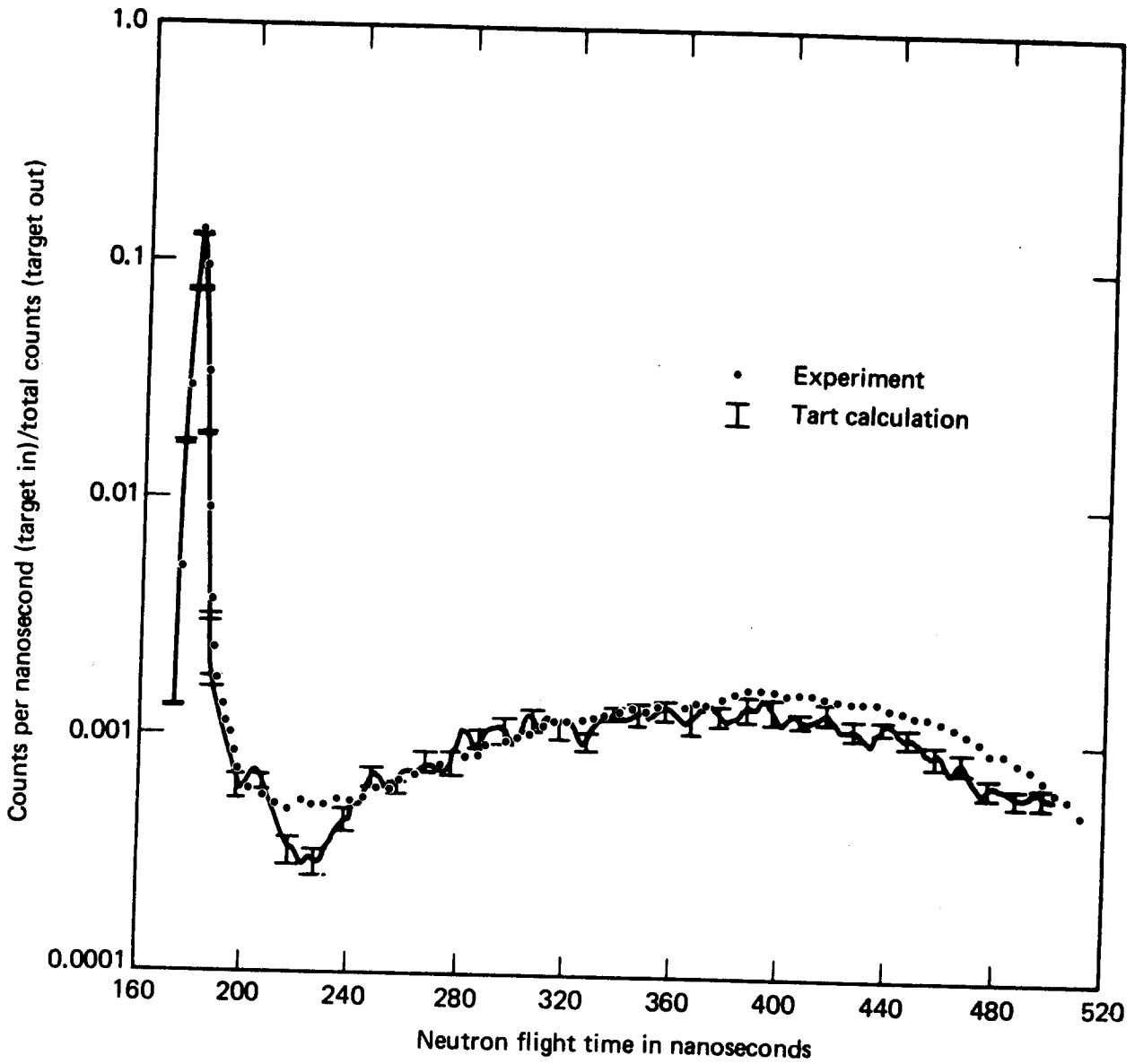


Fig. IX-1. Comparison of measured and calculated emergent neutron spectra for a nominal 14 MeV pulsed sphere with thickness 0.7 mfp (3.63 cm) (see Ref. IX-6) at an observation angle of 26° as described in the text.

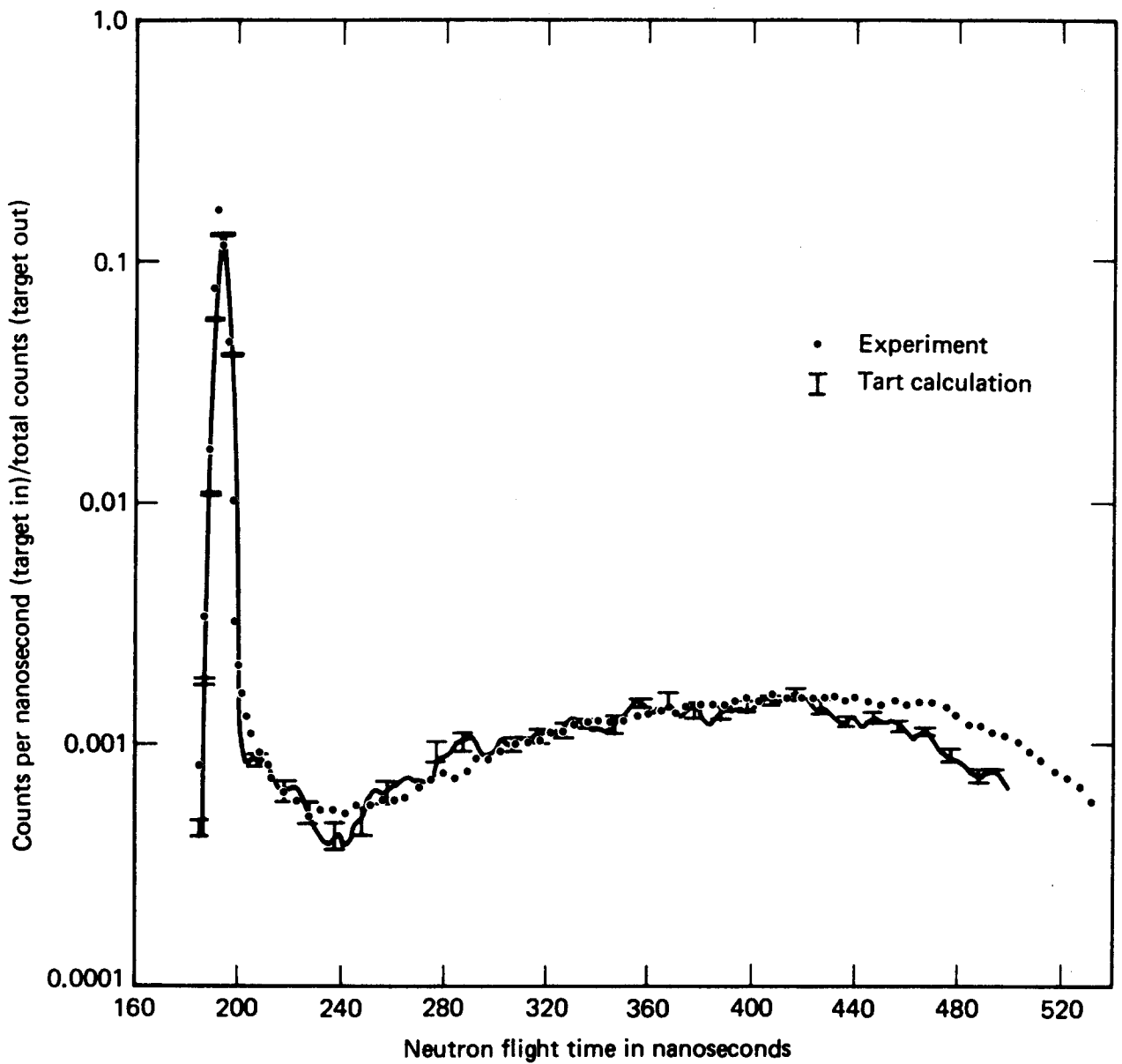


Fig. IX-2. Comparison of measured and calculated emergent neutron spectra for a nominal 14 MeV pulsed sphere (see Ref. IX-6) with thickness 0.7 mfp (3.63 cm) at an observation angle of 120° as described in the text.

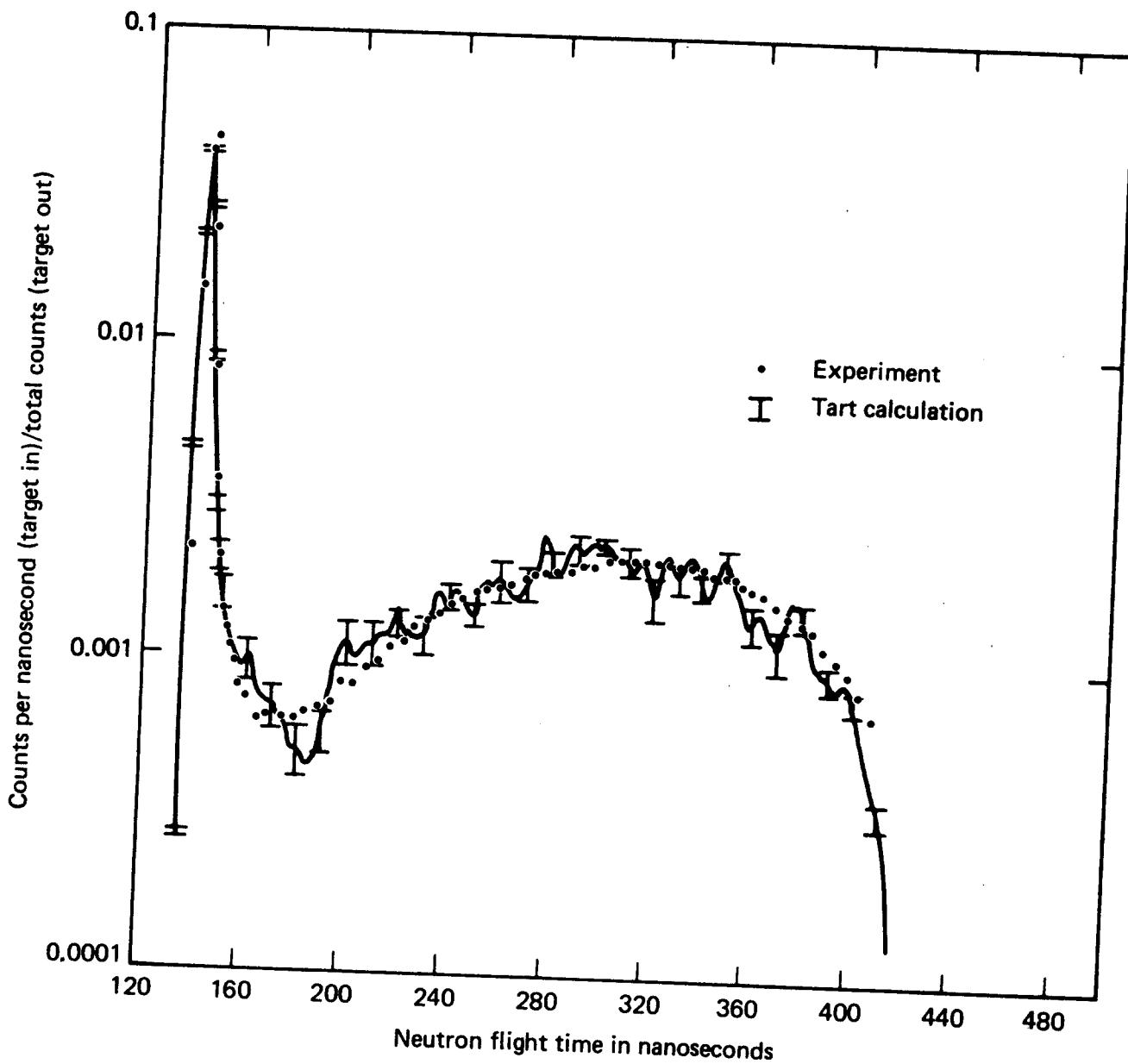


Fig. IX-3. Comparison of measured and calculated emergent neutron spectra for a nominal 14 MeV pulsed sphere with thickness 2.8 mfp (10.91 cm) (see Ref. IX-6) at an observation angle of 26° as described in the text.

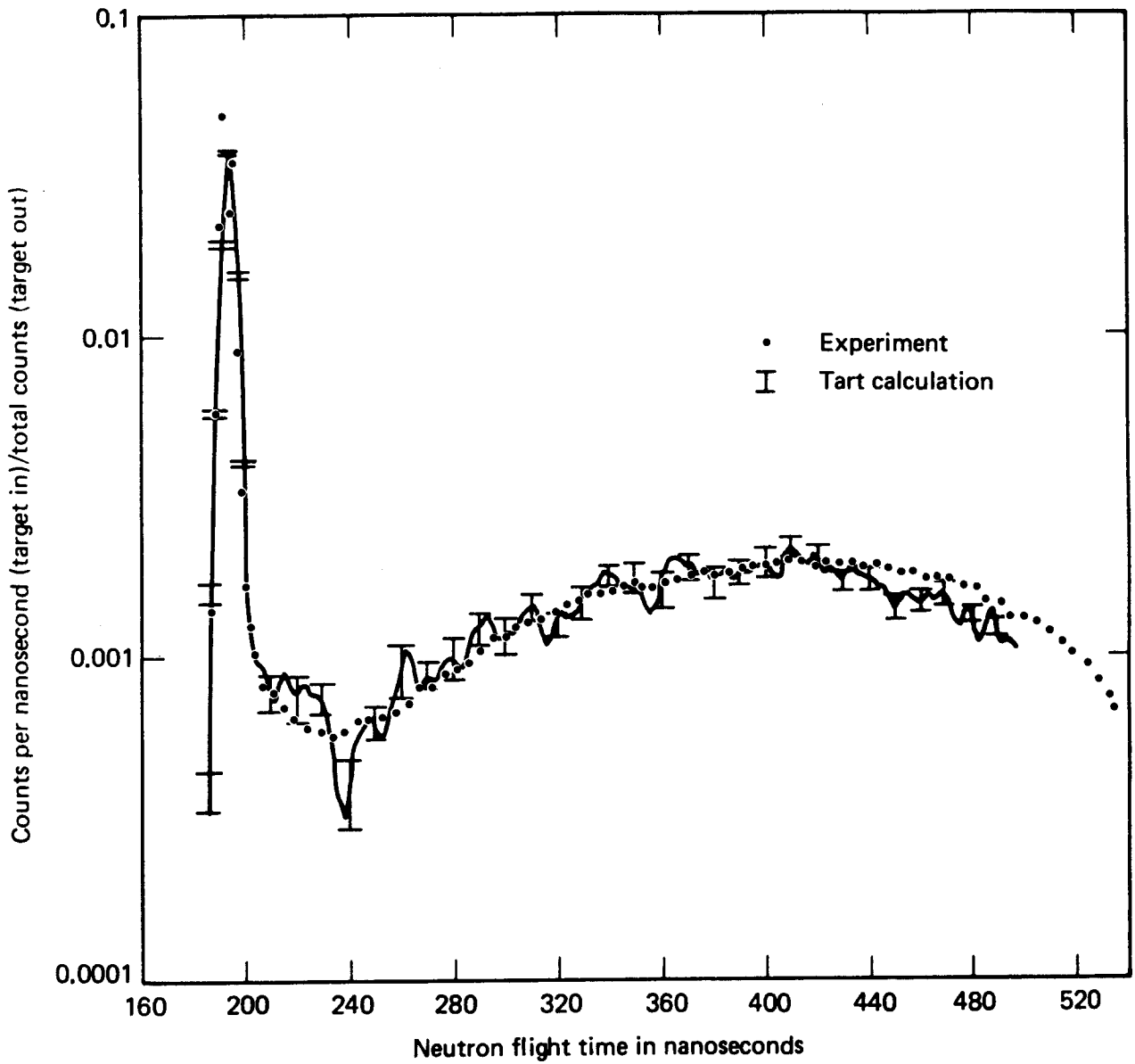


Fig. LX-4. Comparison of measured and calculated emergent neutron spectra for a nominal 14 MeV pulsed sphere (see Ref. IX-6) with thickness 2.8 mfp (10.91 cm) at an observation angle of 120° as described in the text.

X. SUMMARY COMMENT

The present ^{238}U evaluation differs significantly from that of ENDF/B-IV. While the neutron total cross sections given by the two files are very similar, the elastic scattering cross sections are considerably different, particularly above 1.0 MeV. This difference implies a large increase in the non-elastic cross section as given in the present evaluation relative to that of ENDF/B-IV and thus a similar increase in the total- inelastic-scattering cross section. However, the components of the inelastic scattering cross sections of the present file are distributed in such a manner that the energy transfer per inelastic event at incident energies in the MeV range is considerably less than given by ENDF/B-IV in many applications. The fission cross sections of the two files are qualitatively similar but there are quantitative differences of up to 4% in important energy regions and the differences exceed 30% in the threshold region. There are also differences in the radiative capture cross section ranging up to 10% in the important few hundred keV region. The present (n;2n') cross sections are smaller than those of ENDF/B-IV in the region of large magnitudes and larger at higher energies where the (n;2n') cross sections are relatively small. Excepting the total cross section, the differences between the two files very frequently exceed the accuracies requested for the precise prediction of the neutronic behavior of many fission-reactor systems.

Preliminary benchmark tests of the present file indicate good performance at high energies. Criticality calculations using bare metal spheres with varying ^{238}U tampers generally give very good results. Tests of the file at fast-power-reactor energies were encouraging. Calculated criticality of ZPR-benchmark critical assemblies was at least as good as that obtained with ENDF/B-IV despite the fact that these tests required the use of

ENDF/B-IV values for a wide variety of other materials abundant in typical ZPR assemblies. Some of these files are in question. More definitive tests of the fast-reactor capability of the present evaluation must await the completion of the full ENDF/B-V system which will, hopefully, improve the cross sections of the other components of the typical ZPR assembly.